FREQUENCY RESPONSE MECHANISM IN LOW CARBON POWER SYSTEM

Ph. D. Thesis

VIVEK PRAKASH
2015REE9007

DEPARTMENT OF ELECTRICAL ENGINEERING
MALAVIYA NATIONAL INSTITUTE OF TECHNOLOGY JAIPUR
JAIPUR (INDIA)
NOVEMBER, 2019

FREQUENCY RESPONSE MECHANISM IN LOW CARBON POWER SYSTEM

Submitted in

fulfillment of the requirements for the degree of

DOCTOR OF PHILOSOPHY

by

VIVEK PRAKASH

(2015REE9007)

Under the Supervision of

PROF. H. P. TIWARI **DR. ROHIT BHAKAR**

DEPARTMENT OF ELECTRICAL ENGINEERING

MALAVIYA NATIONAL INSTITUTE OF TECHNOLOGY JAIPUR

NOVEMBER, 2019

DECLARATION

I, **Vivek Prakash**, declare that this thesis titled, **"Frequency Response Mechanism in Low Carbon Power System"** and the work presented in it, are my own. I confirm that:

- This work was done wholly or mainly while in candidature for a research degree at this university.
- Where any part of this thesis has previously been submitted for a degree or any other qualification at this university or any other institution, this has been clearly stated.
- Where I have consulted the published work of others, this is always clearly attributed.
- Where I have quoted from the work of others, the source is always given. With the exception of such quotations, this thesis is entirely my own work.
- I have acknowledged all main sources of help.
- Where the thesis is based on work done by myself, jointly with others, I have made clear exactly what was done by others and what I have contributed myself.

Date:

Vivek Prakash
(2015REE9007)

Department of Electrical Engineering
MALAVIYA NATIONAL INSTITUTE OF TECHNOLOGY JAIPUR

CERTIFICATE

This is to certify that the thesis entitled **"Frequency Response Mechanism in Low Carbon Power System"** being submitted by **Vivek Prakash** (ID. No. 2015REE9007) is a bonafied research work carried out under my supervision and guidance in fulfillment of the requirement for the award of the degree of **Doctor of Philosophy** in the Department of Electrical Engineering, Malaviya National Institute of Technology Jaipur, India. The matter embodied in this thesis is original and has not been submitted to any other University or Institute for the award of any other degree.

(Prof. H. P. Tiwari)
Supervisor
Professor
Department of Electrical Engineering
MNIT Jaipur
Jaipur -302017, India

(Dr. Rohit Bhakar)
Supervisor
Associate Professor
Department of Electrical Engineering
MNIT Jaipur
Jaipur -302017, India

Place: Jaipur
Date:

ACKNOWLEDGEMENTS

It would not have been possible to write this thesis without the help and support of the kind people around me, to only some of whom it is possible to give particular mention here.

Foremost, I would like to express my deepest gratitude to my respected research supervisors, **Dr. Rohit Bhakar** and **Prof. (Dr.) H. P. Tiwari,** for their valuable guidance, scholarly inputs and consistent encouragement. This work is possible only because of the unconditional moral support provided by them. I had a great freedom to plan and execute my ideas in research without any pressure. This made me to identify my own strength and drawbacks, and particularly boosted my self-confidence.

I would like to specially thank **Dr. Rohit Bhakar** for giving me the opportunity to work with him, and introducing me to the world of research. I inspired from you about the true research and its value, which I feel at the end is very important for budding researchers like me. I always ended up with confidence and full of energy after the discussions with you. You gave me your full support whenever I had problems. Thank you again for your care and kindness.

I feel profound privilege to thank **Prof. Udaykumar R. Yaragatti**, Director M.N.I.T Jaipur for providing me an opportunity to work towards my Ph.D. degree and for excellent infrastructure facilities in the institute.

My heartily thanks goes to **Prof. Rajesh Kumar**, Head, Electrical Engineering Department for extending all the necessary support and providing a healthy research atmosphere in the department. I thank all the faculty members of the department for their continuous encouragement and moral support, which motivated me to strive for better.

I wish to express fruitful thanks to **Prof. Vikas Gupta**, **Dr. Prerna Jain** and **Dr. Deepti Saxena**, members of Departmental Research Evaluation Committee, for the inspiring discussions and fruitful suggestions that enhanced the quality of my research work.

I would also like to thank the technical and support staff of the department for their support and help, whenever I needed.

I cannot forget to thank my senior Ph.D. colleagues, **Dr. Kailash Chand Sharma, Dr. Parul Mathuria** and **Dr. Amita Sharma** for their cooperation and memorable association. It was an immense pleasure to work alongside with them.

My heartfelt thanks to **Mrs. Suman Sharma, Mr. Sandeep Chawda**, **Ms. Falti Teotia, Mr. Sreenu Sreekumar, Ms. Priyanka Kushwaha, Ms. Anjali Jain, Mr. Y. Sumanth** and **Ms. Meenakshi Khandelwal,** it was wonderful to share **Power Management Research Lab.** with you. The discussion I used to have with you on various topics provided a relaxing time from research. Apart from this, your advice during my struggling period with research was of great significance.

Special thanks to my present and ex colleagues with whom I have enjoyed my past three years, starting from **Ranjeet Kumar Jha**, **Satyendra Singh**, **Soumyadeep Ray**, **Bhatt Kunal Kumar**, **Rajvir Kaur**, **Akanksha Shukla**, **Dr. Pradeep Anjana, Dr. Nandkishore Gupta, Dileep Kumar**, **Saurabh Kumar**, **Ajay Kumar**, **Dev Kumar, Tanuj Rawat, Pranda Prasanta Gupta and Jayprakash Keshri**.

I would also like to thank my lifelong friends **Mr. K. K. Sharma, Vivek Nandan, Vikas Koundilya, Vishal Shrivastava, Rajeev Kumar, S. R. Vighnesh Iyer, Vijay Pratap and Vipul Mandal** for their friendship and unconditional moral support.

Finally, I would like to express profound gratitude to my family members for all they have undergone to bring me up to this stage. I wish to express gratitude to my parents, **Smt. Manorma Gupta** and **Late Sh. Manoj Kumar Gupta**, and my Father-in-Law, **Sh. P. K. Gupta** and Mother-in-Law, **Mrs. Sadhna Gupta** for their kind support, the confidence and the love they have shown to me. You are my greatest strength and I am blessed to be your son. I would like to thank my wife **Mrs. Swati Gupta** for her continuous support and belief on me. You always motivated me like true friend and helped me to do best in every situation. I also would like to thank my brother **Rahul Prakash** & beloved sisters **Sujata, Vijeta and Priyanka Prakash** for being a good friend and understanding me well during this tough situation.

At end of my thesis, it is a pleasant task to express my thanks to all those who contributed directly or indirectly in many ways to the success of this study and made an unforgettable experience for me.

Vivek Prakash

ABSTRACT

Renewable Energy Sources (RES) like wind & Photovoltaic (PV) generation are evolving as a clean, sustainable and cost-effective solution to meet increasing energy needs in future low carbon power systems. Wind/PV penetration in power systems is increasing due to various subsidies and support schemes from the governments, apart from technical improvements in generation systems. Large integration of uncertain wind/PV generation with the grid would displace conventional generation at a fast rate and impose uncertainties of wind speed, cloud transients, solar insolation, *etc*. Displacement of synchronous generation with these uncertain generation sources is likely to create several operational challenges for the grid operators, such as reduction in system inertia, generation-load imbalance, increase in frequency response requirement, and system operational risk. This necessitates a wider understanding of the system operational challenges arising out of large RES penetration in the grid, to create opportunities for reliable and secure system operation.

Frequency response is the inherent ability of the system or elements of the system to maintain generation-load balance at the time of frequency deviation. Based on the response delivery time frames, the frequency response is classified as Primary Frequency Response (PFR), secondary frequency response and tertiary frequency response. PFR is generally delivered completely within 20 seconds. It is implemented through governor controller assisted by the system's moment of inertia and frequency dependent load response. Secondary frequency response is delivered within few minutes and implemented by Automatic Generation Controller (AGC) often referred to as Load Frequency Controller. Tertiary frequency response is the manual control actions taken by the System Operator (SO) to bring back the frequency at nominal value and is delivered in minutes to hours.

Recent studies on frequency response assessment in interconnections worldwide indicate declining frequency response capability over the last decade. Some of the identified reasons include steam power plants working on sliding pressure operating mode; nuclear units working in blocked governor mode; low inertia in the new generator designs; lack of individual reserves available with utilities, *etc*. These reasons have prompted industry-wide efforts and forced SO to ensure adequate frequency response in future low carbon power system.

In this regard, the main focus of this thesis is to develop a mechanism for the assessment of system inertia and PFR adequacy in system operations under uncertain RES generation. Due to RES generation uncertainty, system operation like Unit Commitment (UC) becomes a challenging decision-making problem. Hence, this research concentrates on the development of efficacious algorithms for RES uncertainty characterization and its representation in decision-making problems like UC. The obtained UC decisions contribute in investigating important aspects of frequency response *viz.* estimation and prediction of system inertia condition, PFR requirement, the optimal combination of generators required for PFR adequacy, within a comprehensive framework.

The research work in this thesis begins with addressing wind/PV generation uncertainty modelling problem. Stochastic nature of wind/PV power can be modeled using the Auto-Regressive Integrated Moving Average (ARIMA) model. ARIMA is a benchmark model for modeling stochastic process like prediction of electricity prices, load and goods prices. It works on stationary time series data. Uncertainty modelling with ARIMA model requires a degree of differentiation and order of suitable model. Wind/PV power uncertainty is modelled by considering 1000 wind/PV power scenario generations. After scenario generation, backward reduction algorithm is utilized to obtain ten representative scenarios. It is observed that both generated and reduced scenarios vary around their mean value, with a 95 percent confidence interval.

Scenario-based stochastic approach model RES uncertainty precisely, but requires computationally demanding simulations. To handle the computational burden interval forecast technique is proposed in the literature. It is a robust technique, which requires less computational effort than the stochastic approach. In Interval forecast, uncertainty is modeled with three non-probabilistic scenarios (*i.e.* central forecast, upper bound & lower bound). Hence, it requires less computational time but produces conservative and thus expensive generation schedules. This is because of the constraints imposed on the feasibility of transitions, from lower to upper bound of wind/PV power interval, and vice versa, between any two consecutive time periods. Such extreme transitions have a low probability and could be replaced by less severe ramp constraints. The advantage and limitations of interval and scenario approaches are incorporated to develop a modified interval algorithm. In the proposed algorithm, uncertainty is modeled using upper and lower bounds, as in the interval formulation, but inter-hour ramp requirements are based on five artificial net load scenarios and hence accurately capture the expected wind/PV power output and reduce the computational burden.

Uncertainty in wind/PV generation forecast and its characterization in UC, requires large reserve capacity to maintain the generation load balance. The deterministic UC are widely used to schedule the reserves. However, these formulations did not consider probabilistic modeling and cost benefits of maintaining reserves. Scenario-based Stochastic UC (SUC) formulation is used to schedule operating reserves, while wind/PV power scenario generation technique is used to address the associated uncertainty. This technique considers probabilistic modeling and reduces the operating cost, however, obtaining a SUC solution is more challenging computationally as it considers a large number of scenarios. Scenario reduction technique is used to mitigate the computational burden. However, an insufficient number of scenarios usually leads to a less accurate solution and in turn, increases the operating cost.

In this context, a novel computationally fast Modified Interval UC (MIUC) computational framework is proposed with the objective to minimize the operation cost. Modified interval forecast algorithm is used to characterize the wind/PV power uncertainty. In addition to generation scheduling this work further contributes by PFR scheduling of generators. As PFR was inherently available with conventional generation, it's scheduling within UC received relatively little attention. Large wind/PV generation in existing power system increase the requirement of PFR services, as the existing wind/PV generators are weak in providing inertia and PFR. This necessitates optimal PFR schedules from UC. PFR scheduling is required to make frequency stable at an intermediate state, following the largest infeed loss.

To highlight the efficacy of the proposed MIUC model, a systematic comparative assessment with SUC is carried out, for computational, cost performance, PFR scheduling performance, the impact of frequency response parameter variation, and RES curtailment. Computationally fast solutions obtained through the proposed MIUC model, within acceptable time intervals, can strongly benefit system operations.

In addition to PFR scheduling under wind/PV uncertainty, estimation of system inertia is essential considering grid’s frequency security. System inertia is a key power system characteristic which provides instant support to the frequency, following contingencies like large infeed loss. There is a limited understanding of system behaviour to provide inertia & PFR with high renewable penetration. Currently, SOs hardly assess system inertia impact to calculate future PFR requirement, which is planned/procured for an expected worst-case contingency. As system inertia condition varies over a day’s time, fixed PFR estimation based on the worst-case scenario is not efficient. Hence, it is

imperative to predict system inertia condition for upcoming hours, considering the current operation status of all generators. Using this information, expected system inertia could be calculated for each hour.

In this regard, this research work contributes by proposing a novel exposition and methodology to predict system inertia condition over a day with incremental wind generation, following the largest infeed loss. ROCOF and frequency deviation are considered as a security criterion to obtain maximum wind penetration limit considering network codes. Impact of variation in frequency security parameters on operation cost and wind curtailment is assessed, to obtain suitable ROCOF setting for minimum wind curtailment. Results provide information of system inertia condition and PFR availability, along with maximum wind generation limit, without violating system security criteria. This would help SO in the assessment of required PFR to handle contingencies, like largest generation outage of the system.

Wind/PV integration lead to both diversifications of generation sources and an increase in overall cost due to the additional frequency response requirement. A recent analysis in the National Grid, United Kingdom reveals that PFR requirements are expected to increase significantly over the next 15 years. Scenario-based study is performed for different combinations of RES generation for computation of PFR requirements caused due to uncertainty. It is concluded that PFR requirements and impact of uncertainty is reduced with RES mix. Diversified RES mix provides smooth generation portfolio. Hence, generation predictability would increase and the probability of extremes values would decrease. This would result in a reduction in overall PFR requirements. Conventional and RES generation have an idiosyncratic effect on system frequency and there is limited understanding of PFR requirement with various generation mix characteristics.

In this context, finally, this thesis contributes by proposing a novel exposition of optimal generation mix with the objective to reduce operation cost, while maintaining systems' frequency response ability. Assessment of PFR adequacy with diversified generation mix is proposed and overall cost performance is analyzed for different cases. ROCOF setting and frequency deviation are considered as frequency security limit to obtain an optimal generation mix. Results obtained provide optimal generation output, PFR contribution from different generating units. Operation cost is reduced with the addition of wind and PV generation. However, the overall cost is increased because of the high investment cost of wind & PV unit. Optimal generation mix is obtained through step by step evaluation of system frequency security criteria.

In view of the growing penetration of wind/ PV power in interconnections globally, the research work presented in this thesis offers an innovative mechanism to mitigate system inertia and PFR challenges under uncertainty. This is an evolving research area for the industry and requires novel mechanisms to handle the same. The research proposed in this thesis offers solutions within acceptable operational time frames. This would help SO to handle inevitable contingencies like largest infeed loss. Moreover, the proposed model has the potential to offer solutions for the PFR ancillary service market clearing and dispatch in future low carbon systems.

Proposed research work could be extended to investigate synthetic inertia provision from wind turbines/PV to support the frequency response. In addition to this, inertia related market design, PFR contribution from technologies like interruptible load, energy storage, and the electric vehicle could be the future scope of the proposed work.

CONTENTS

LIST OF TABLES

LIST OF FIGURES

LIST OF SYMBOLS

The symbols used in the text have been defined at appropriate places, however for easy reference, the list of principle symbols is given below.

Symbol	Explanation
A. Indexes and sets	
t, T	Index and set of time interval.
i, I	Index and set of generator units.
b, B	Index and set of linear segments of generator cost curve.
j, J	Index and set of generator start-up costs.
G_{ng}	Generator set with disabled governor.
w, W	Index and set of wind farms.
pv, PV	Index and set of PV plants.
l, L	Index of transmission line, set of transmission lines.
s, S	Index of bus, set of buses.
n, N	Index of scenario set of scenarios.
r, R	Index of reserve, set of reserves.
B. Variables	
$G_{i,t}$	Output power of unit i in time interval t (MW).
$G_{b,i,t}$	Output power of segment b of generator i in time interval t (MW).
$S_{i,t}$	Combined start-up and shut down cost of generator i in time interval t ($).
LS_t	Load shed in time interval t (MW).
$Su_{i,t,j}$	Binary variable, start-up cost matrix (1 if generator i starts up during time t for cost segment j, 0 otherwise).
$\chi_{i,t}$	Binary variable, generator up/down status (1 if generator i is on during hour t, 0 otherwise).
$\chi_{i,t}^{up}, \chi_{i,t}^{dn}$	Binary variable, generator start-up/down status (1 if generator i starts up in time interval t, 0 otherwise).
$\Upsilon_{i,t}$	Binary variable, generator headroom availability status for PFR (1 if headroom is available for generator i in time t, 0 otherwise).
$W_{w,t}^{curt} / PV_{pv,t}^{curt}$	Wind, w & PV, pv power curtailment during hour t (MW).
$P_{i,t}^{nad} / P_{i,t}^{ss}$	PFR available from generator i at nadir /steady-state time t (MW).
$P_{i,t}$	Total PFR from generator i at time interval t (MW).
$\Delta f^{nadir} / \Delta f^{ss}$	Frequency deviation at nadir/steady state (Hz).
$\delta_{i,t}$	Generator i governor status at time t (1 if enabled, 0 otherwise).
$\theta_{s,t,n}$	Voltage angle at bus s, time interval t, scenario n (radian).
R_t^{ins}	Inefficient reserve at time t (MW).

C. System parameters and constants

LF_t	Forecasted load in time interval t (MW).
LN_t	Net Load at time interval t (MW).
$W_{t,w}^{av}$	Wind power available from wind farm w at time interval t (MW).
$PV_{t,pv}^{av}$	PV power available from pv at time interval t (MW).
Nl_i	No load cost of generator i ($).
$Cs_{i,b}$	Running cost of generator i , for b^{th} segment of the cost curve ($/MW).
TI_i^{md} / TI_i^{mu}	Minimum down/up time of generator i in initial time period (h).
TR_i^{md} / TR_i^{mu}	Minimum down/up time of generator i in remaining time period (h).
$G_i^{\max} / G_i^{\min}$	Generator i maximum/ minimum output (MW).
R_i^{up} / R_i^{dn}	Generator i ramp up/down limit (MW/h).
$Suc_{i,j}$	Generator i start-up cost of segment j ($).
$TO_{i,j}^{up} / TO_{i,j}^{lo}$	Generator i, upper/lower limit of segment j based on generator off time (h).
f_0	Nominal frequency (Hz).
ΔP	Infeed loss (MW).
LD	Load damping rate (1/Hz).
T^{de}	PFR delivery time (s).
$\Delta f^{\max}$	Maximum frequency deviation (Hz).
f^{ss}	Steady state frequency (Hz).
H_i / H_i^L	Inertia constant of generator/ Lost generator i (s).
Δf^{db}	Governor's frequency dead band (Hz).
H^{eqload}	Equivalent load inertia (s).
t^{ss} / t^{nadir}	Time to reach steady-state/ nadir frequency (s).
f^{nadir}	Nadir frequency (Hz).
$f^{\min}$	Lower limit of permissible system frequency (Hz).
$P^C / P^{Cnad} / P^{Css}$	PFR capacity requirement, overall / at nadir/ at steady-state (MW).
H^{sys} / H^{req}	System Inertia/Inertia requirement (MWs).
$G_i^{db} / G_i^{db\max}$	Governor dead band/ maximum allowed dead band of generator i (Hz).
D_i^e / D_i	Equivalent droop/ governor droop of generator i (Hz/MW).
B_{sm}	Line admittance between s and m (S).
$W_{w,t,n}$	Wind farm w output power for scenario n in time interval t (MW).
π_n	Probability of scenario n .
$VOLL$	Value of loss load ($/MW-h).

LIST OF ABBREVIATIONS

The abbreviations used in the text have been defined at appropriate places, however, for easy reference, the list of abbreviations is given below.

Abbreviation	**Explanation**
ACF	Auto Correlation Function
ACE	Area Control Error
AGC	Automatic Generation Controller
ARIMA	Auto Regressive Integrated Moving Average
AR	Auto Regressive
ERCOT	Electric Reliability Council of Texas
FSM-O	Over Frequency Sensitive Mode
FSM-U	Under Frequency Sensitive Mode
KD	Kantorovich Distance
MA	Moving Average
MILP	Mixed Integer Linear Programming
MIUC	Modified Interval Unit Commitment
NERC	North American Electric Reliability Corporation
PACF	Partial Auto Correlation Function
PFR	Primary Frequency Response
PV	Photovoltaic
RES	Renewable Energy Sources
RTS	Reliability Test System
ROCOF	Rate of Change of Frequency
SUC	Stochastic Unit Commitment
SO	System Operator
UC	Unit Commitment
UFLS	Under Frequency Load Shedding

Chapter – 1

INTRODUCTION

1.1 Background

The dynamic behaviour of modern power systems poses a formidable challenge for SO to maintain generation-demand balance. Controlling the system frequency by maintaining the generation-demand balance is critical characteristics of power system security. Continuous variation in power consumption, because of switching on and off of loads cause generation-demand imbalance. This imbalance should be corrected within a short span of time otherwise, system frequency would vary from the nominal value. Large frequency variations due to contingency, like generation outage or loss of load, may cause serious threats to stability and security of the system. This may further lead to damage of important system equipment's or shut down of the system. Hence, constant frequency and generation-load balance are identified as the primary aspect for normal operation of power systems.

Conventional power systems have an inherent frequency response ability to stabilize initial frequency deviations, following generation-load imbalances [1], [2]. The term frequency response is traditionally used by the industry to describe how an interconnected system behaves on stabilizing the frequency, after a sudden loss of generation. According to North American Electric Reliability Corporation (NERC) standard, calculation of frequency response can be performed by calculating the size of the lost generation to the resulting net change in system frequency, once frequency has stabilized. Frequency response is measured as megawatts (MW) per 0.1Hz [1].

Modernization of electrical power generation technologies and global low carbon energy requirement provides opportunities for RES to meet the ever-increasing energy demand. Among the variety of RES, wind, and PV power are contributing the largest share with approximately 500 GW of wind and 300 GW of PV installed worldwide in 2017 [3],[4]. Larger integration of these RES into the grid will displace the conventional generation at a faster rate. Displacement of synchronous generation with non–synchronous generators have adverse effects on system frequency response [5]-[8]. The formidable challenge for the SO is to maintain the system frequency within the specified limits.

Frequency response adequacy assessment with large generation share from uncertain RES is a timely research challenge for the interconnections worldwide. The present work

considers several issues related to the development of frequency response mechanism, in low carbon power systems. Motivations for such issues are discussed in the next subsection.

1.2 Motivation for the Present Work

Uncertain RES generation characteristics would create several new challenges for SO in terms of frequency response adequacy. Recent studies on frequency response assessment in global interconnections like European interconnections, Western interconnection and Eastern interconnections, USA, indicate frequency response decline over the last decade [9]-[11]. One of the main reason for this declination is displacement of synchronous generators with non-synchronous RES generation. Hence, frequency response assessment with large RES is an issue of concern for the SO aiming to enhance the power system security. Frequency response capability of the system is highly dependent on system operation decisions. Thus, a detailed study of system operation under uncertain wind & PV generation is necessary for understanding SO's frequency response adequacy problem in the right perspective.

Due to wind/PV uncertainty, system operations like UC becomes a challenging decision-making problem [12]. Accurate modeling of involved uncertainties is necessary to solve these decision-making problem, which can be modeled in a stochastic optimization framework [13]. In such a framework, parameters affected by uncertainties are generally modeled as a stochastic process or scenarios. Scenarios are possible products of the arbitrary process with corresponding probabilities. A large number of scenarios are essential for precise modeling of any uncertainty. However, due to computational complexity and time limitations, generated scenarios are required to be reduced without changing their statistical properties significantly [14], [15]. For scenario reduction, two algorithms are generally used, namely backward reduction and forward selection [16], [17]. These algorithms have been used for modeling demand and financial market uncertainties, and the same can be extended to model wind/PV power uncertainty.

Scenario-based stochastic approach model RES uncertainty precisely, but requires computationally demanding simulations. This requires computationally fast algorithms to model the same. An interval forecast approach is discussed in the literature that requires less computational effort than the stochastic approach [18]. In Interval forecast, uncertainty is modeled with three non-probabilistic scenarios (*i.e.* central forecast, upper bound & lower bound). Hence, it requires less computational time but produces

conservative and thus expensive generation schedules [19]. Hence, the advantages of interval and scenario approaches could be incorporated to model the wind/PV power uncertainty.

Large wind/PV generation in existing power system would increase the requirement of frequency response, as these generators are weak in providing inertial response and PFR. This necessitates optimal PFR schedules from UC. As PFR was inherently available with conventional generation, it's scheduling within UC received relatively little attention [20]. Hence, a framework is required that contain initial transient frequency behavior within the prescribed limits and perform generator PFR scheduling to make frequency stable.

Another issue in addition to PFR scheduling under uncertainty is the prediction of system inertia condition and assessment of PFR requirement in the low carbon power system. Currently, SOs hardly assess system inertia impact to calculate future PFR requirement, which is planned/procured for an expected worst-case contingency [21]. System inertia is a key power system characteristic which provides instant support to the frequency, following contingencies like large infeed loss [2], [22]. There is a limited understanding of system behaviour to provide inertia & PFR with high RES generation. An understanding of these requirements during contingencies would provide knowledge about permissible renewable penetration that grids could withstand, following network regulations.

Frequency-related issues, such as the operation of frequency controlled reserves, ROCOF protection setting, UFLS, and PFR deployment need a proper assessment of system inertia condition for secure system operation. Future system operability requirements of interconnections strongly recommend development of methods for securing system inertia & PFR adequacy during normal and contingency conditions with evolving generation mix [23]. Increasing RES share in overall generation mix would pose additional formidable challenges from the technical and economical point of view. Reduced system frequency response would make system frequency more sensitive to changes in supply and demand. This would lead to quick frequency deviations, following the loss of generation and load.

Motivated from these aspects, the research work undertaken in this thesis aims to develop frequency response adequacy assessment under large integration of uncertain wind/PV generation. It characterizes uncertainty involved in the wind/PV power, further represent it to frequency response constrained generation and PFR scheduling framework. Uncertainties are represented through scenarios & modified interval forecast. In addition

to PFR scheduling, prediction of system inertia condition is performed to assess the PFR requirement under uncertain wind/PV generation. Further, optimal generation mix is assessed for securing inertia and PFR adequacy following frequency security criteria like ROCOF and frequency nadir.

1.3 Contributions of the Present Work

The objectives of this research work include the study of frequency response mechanism, particularly for system inertia and PFR adequacy under wind/PV power uncertainties. The main contributions of this thesis are follows:

i. On the basis of critical survey of literature pertaining to frequency response and large-scale wind/PV power penetration in the power systems, an overview of frequency response along with associated issues is presented. This detailed study helps to understand the considered problem in low carbon power systems.

ii. The initial part of this thesis work contributes by proposing wind/PV power uncertainty modelling techniques. To model these uncertainties through scenarios and computationally fast modified interval forecast, this thesis proposes efficacious algorithms for wind/PV power scenarios & modified interval forecast approach. Time series based ARIMA model is used for scenario generation and modified interval forecast, while probability distance based backward reduction is used for scenario reduction. In modified interval forecast five ramping scenarios are framed to accurately capture the expected wind/PV power output. Proposed modified interval algorithm is useful for the pragmatic characterization of wind/PV power uncertainties in frequency response constrained UC.

iii. Frequency response constraints modelling in SUC framework is computationally demanding. Hence, a novel computationally fast MIUC formulation framework to include the system's frequency response constraints is proposed. The framework directly aims to contain initial transient frequency behavior within the prescribed system security criteria. Further, it demonstrates the efficacy of proposed MIUC model through the systematic comparative assessment with SUC, for the impact of variation of frequency response parameters on operation cost and wind curtailment; and for computational and cost performance with varying wind penetration. MIUC formulation offers ultra-fast solutions, as it takes less than half the computational time as compared to SUC and has the potential to provide fast solutions to processes, like frequency response constrained dispatch and market clearing in low carbon systems.

iv. In addition to frequency response modelling in generation scheduling framework, PFR scheduling from committed generators is required to make frequency stable at quasi-steady-state, following generation outage. PFR was inherently available with conventional generation. Hence, its scheduling received little attention. In this work, novel exposition of PFR scheduling is proposed to find the PFR availability at frequency nadir and quasi-steady-state following the largest generation outage of the system. This assessment would help SO to estimate PFR requirement for worst-case contingencies.

v. As system inertia condition varies over a day's time, fixed PFR estimation based on the worst-case scenario is not efficient. Hence, it is imperative to forecast system inertia condition for upcoming hours, considering the current operation status of all generators. Hence, a novel exposition is proposed to predict system inertia condition with incremental RES generation, following the largest infeed loss. ROCOF and frequency nadir are considered as a security criterion to obtain maximum RES penetration limit considering network codes. Investigate the impact of variation in frequency security parameters on operation cost and wind & PV curtailment, to obtain suitable ROCOF setting for minimum RES curtailment.

vi. Large generation share from RES like wind and PV in overall generation mix would cater real-time operational issues for the utilities to deliver inertia and PFR. There is a need to find optimal generation mix for securing adequate inertia and PFR. Hence, a novel exposition of optimal generation mix is proposed with the objective of reduced operation cost while maintaining systems' frequency response. Assessment of PFR adequacy with diversified generation mix is carried out and overall cost performance is analysed for different generation mix cases. ROCOF setting and frequency nadir are considered as frequency security limit to obtain optimal generation mix. Results obtained through the proposed approach would be helpful for SO in order to obtain the optimal generation combination for maintaining system security and reliability.

1.4 Organization of the Thesis

Chapter organization is an important part of the thesis that provides a complete overview of the thesis. Current chapter introduces major issues involved in frequency response adequacy under uncertain wind/PV generation. It analyses the involved problems in this area that motivated the work, and further contributions to the present thesis. The pictorial representation of the thesis structure is shown in Fig. 1.1. Colored boxes are used to show

the flow of research objectives and theoretical background of the problem. White boxes indicate introductory literature related to the proposed approach, conclusion, summary of significant findings and future scope of the work. Blue boxes indicate the modelling of frequency response constraints implemented in proposed chapters. Yellow boxes demonstrate the use of uncertainty modelling in the proposed objectives. Violet boxes depict the UC modelling implemented in the proposed work. Green boxes show the system inertia and PFR estimation and red boxes represents the generation mix problem. Rest of the chapters of this thesis are organized as follows:

Chapter 2 provides a comprehensive literature review on issues pertaining to frequency response mechanism in low carbon power system, including those of uncertainty modeling, frequency response constrained generation and PFR scheduling, prediction of system inertia condition and optimal generation mix. It offers details on causes, models and solutions approaches of the associated issues. This study is helpful to understand the frequency response adequacy challenges with uncertain RES.

Chapter 3 discusses wind/ PV power uncertainty modelling though scenarios and modified interval forecast. In the proposed modified interval model, the advantages of interval and scenario approaches are incorporated. A time series based ARIMA model is used for interval forecast and scenario generation. Probability Distance Based Backward Reduction is used for scenario reduction. The wind/PV uncertainty modelling algorithms proposed in this work could be used for pragmatic characterization of uncertainty in decision making problems.

Chapter 4 proposes frequency response constrained computationally fast MIUC approach for generation and PFR scheduling under uncertainty. A comparative assessment is carried out between proposed MIUC and SUC approach in terms of operational cost, PFR cost, PFR schedule and computational time. MIUC formulation offers ultra –fast solution and could be used to obtain fast solutions to processes, like frequency response constrained dispatch and market clearing in low carbon systems.

Chapter 5 presents an exposition and methodology for prediction of system inertia condition and PFR requirement with incremental wind generation, following the largest infeed loss. ROCOF and frequency nadir are considered as a security criterion to obtain maximum wind penetration limit considering network codes. Further, impact assessment is carried out for variation in frequency security parameters on operation cost and wind curtailment. This assessment provides a system specific suitable ROCOF setting for minimum wind curtailment.

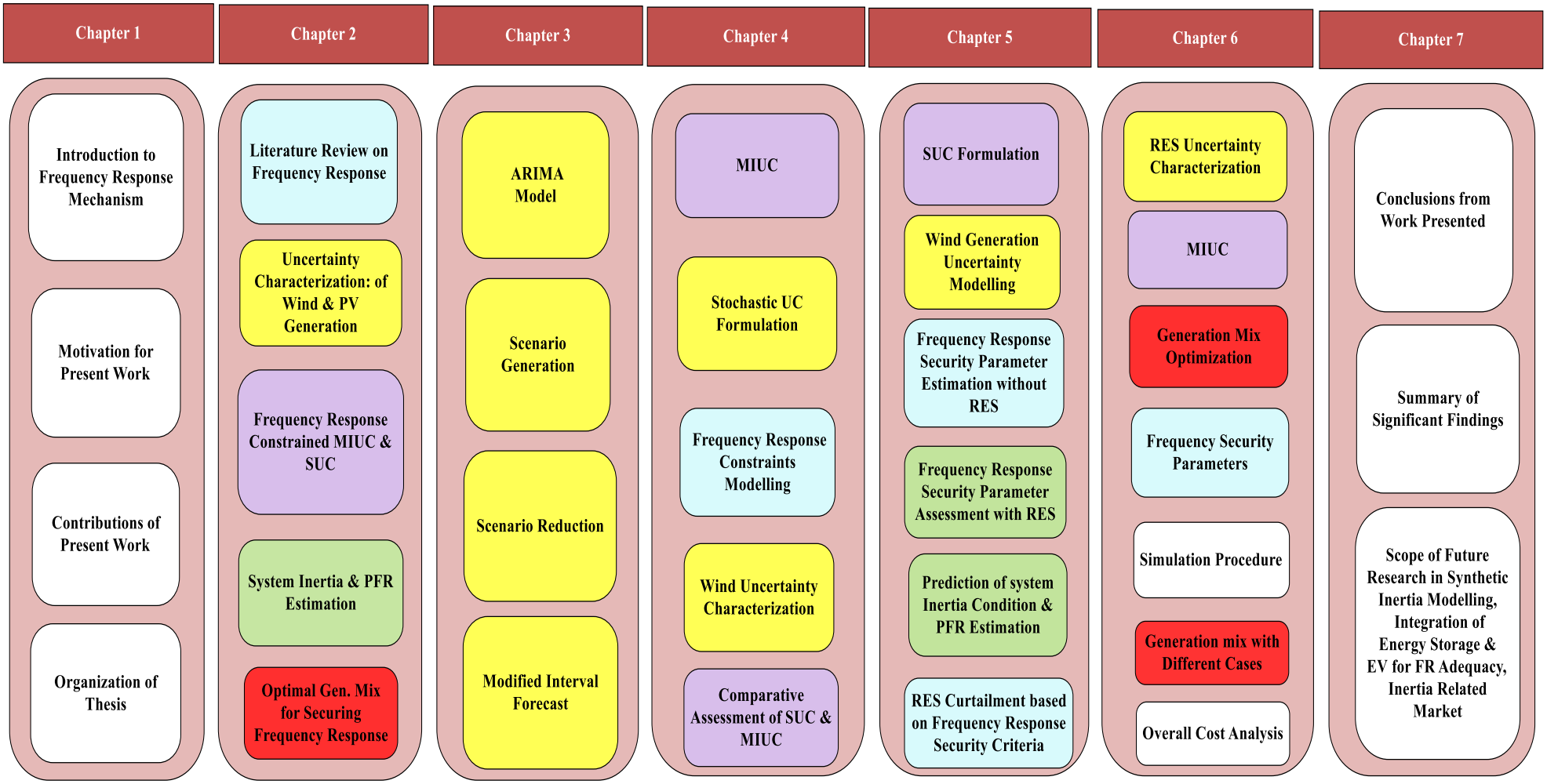

Fig. 1.1: Thesis Structure.

Chapter 6 investigates the optimal generation mix for system inertia and PFR adequacy in low carbon power system with the objective to reduce operation cost while maintaining systems' frequency response ability. Assessment of PFR adequacy with diversified generation mix is analysed with overall cost performance for different generation mix cases. Optimal generation mix is obtained through step by step evaluation of system frequency security criteria. Optimal combination of generators obtained through proposed approach would be helpful for SO to assess system inertia and PFR requirement for power system security and reliability.

Chapter 7 summarizes the main findings the work presented in this thesis and suggests directions for future research scope in this area.

Finally, Appendix A provides data of the one area IEEE Reliability Test System (RTS) used in the proposed case studies.

Chapter – 2

LITERATURE REVIEW

2.1 Introduction

Future low carbon power systems would see an enhancement in the frequency response requirement. This requirement is due to the rapid increase in the share of non-synchronous RES generation like wind and PV, in the interconnections over the world. A recent analysis at National Grid, United Kingdom reveals that PFR requirement would increase at a faster pace over the next two decades. Over the next few years, there would be an increase of about 30-40% [23]. An interconnected grid must have adequate frequency response to respond to a variety of inevitable contingency events and ensure quick restoration of the generation-demand balance. High RES penetration into the grid creates multiple system operational concerns for the SOs, such as declining quantum of system inertia & PFR, handling of uncertain & intermittent generation characteristics [5]-[8].

Frequency-related problems like frequency-controlled reserve requirement, ROCOF relay setting, UFLS, and PFR requirement, need wider investigation for secure power system operation. Future system operability framework of interconnections, strongly recommends the development of methods to accurately estimate frequency response requirement during normal and disturbance conditions [67], [68]. These challenges prompted industry-wide efforts by the national and regional operators to develop understanding and increase transparency by highlighting mitigation efforts to ensure frequency response adequacy.

Traditionally, India's electricity generation mix is dominated by thermal and hydro power. With the government's increased focus on greening the power sector, India targets to install 175 GW of grid-connected RES generation by 2022. This is expected to be around 37% of the installed capacity in 2022, which presently stands at 16% [115]. Most of the wind and PV generators are presently connected to an intra-State network and in future are likely to be connected to the inter-State transmission system as well. Wind and PV generation intermittency and uncertainty create challenges for balancing the grid and led the Central Electricity Regulatory Commission (CERC) to make provisions in the Indian Electricity Grid Code for sustainable system operation [116], [117]. CERC has proposed an ancillary services framework to manage power imbalances and congestion, aiming economy and efficiency in grid management, at the regional and national level.

In this regard, this chapter presents a theoretical background and review of literature pertaining to challenges for frequency response adequacy in uncertain low carbon power systems. Initially, a fundamental background on frequency response in terms of current scenario, conventional practice, reasons for frequency response declination and frequency response time frames have been provided. Next, issues pertaining to wind/PV power uncertainty modelling techniques required in decision-making problem are discussed. This uncertainty modelling is further represented in the novel framework of frequency response constrained MIUC approach of generation and PFR scheduling under wind penetration.

PFR schedule could vary with the system inertia condition over a day hence, approaches developed to estimate system inertia and requirement of prediction of system inertia condition have been discussed, which is not practiced in today's control rooms. Moreover, large integration of RES generation would affect the conventional generation mix and affect the system inertia and PFR capability. Thus, the last part of the chapter discusses optimal generation mix for securing system inertia and PFR adequacy.

2.2 Need to Maintain Frequency Balance

Larger frequency variations may cause serious threats to the stability and security of the system. This may lead to UFLS, damage of important system equipment's and sometimes shut down of the whole system. Hence, constant frequency and generation-load balance are imperative for a normally operating system.

There are a few reasons which give a basic idea about the need for maintaining frequency balance [27], [32]:

- Most of the ac motors are rotating with the speeds directly related to the frequency. The majority of ac motor driven loads may not be sensitive to larger frequency fluctuations.
- The turbine of generators especially thermal generators are designed to operate at a nearly constant speed. The velocity of expanding steam is uncontrollable and for higher turbine efficiency it is mandatory to have the synchronism of speed.
- The power system operations can be controlled in the more profound way if the frequency deviations are kept within the prescribed limits.
- Synchronous clocks are used and driven by synchronous motors, and the exactness of these clocks is a function of not only the frequency error but the integral of frequency error.

- UFLS, which is a drastic emergency frequency control that disconnects a large group of customers (loads) to protect the generator from damage at the time of extremely large frequency imbalance.

2.3 Frequency Response with Conventional Generation

According to NERC standard [1],[24] frequency response calculation can be performed by calculating the size of the lost generation to the resulting net change in system frequency, once frequency stabilizes (at Point B) as shown in Fig. 2.1.

During a contingent event, there is a generation–demand imbalance within the grid. This imbalance will cause system frequency deviation from the nominal value. Small power mismatches cause smaller deviation of frequency which can be handled easily. Large frequency deviations can be a problematic situation and may lead to damage of equipment and even blackouts [25]. For the reliable system operation, under frequency deviation due to loss of generation or over frequency deviation caused by loss of load are severe phenomena and have to be maintained within a tolerance level.

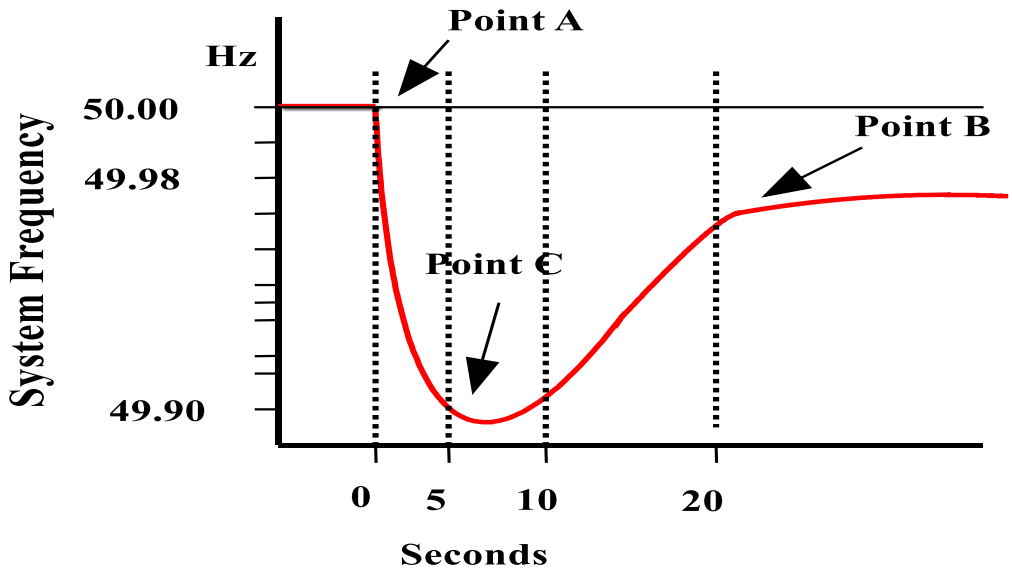

Fig. 2.1: Frequency response characteristics after generation outage event.

$$\text{Pre-disturbance Frequency; } \text{Frequency}_{\text{point A}}$$

$$\text{Settling Frequency; } \text{Frequency}_{\text{point B}}$$

$$\text{Frequency Nadir; } \text{Frequency}_{\text{point C}}$$

$$\text{Frequency Response} = \frac{\text{Generation Lost (MW)}}{\text{Frequency}_{\text{point A}} - \text{Frequency}_{\text{point C}}}$$

Frequency is closely related to the active power balance [26], [27]. The balance between generation and load demand has to be maintained by suitable control actions. When there is a sudden increase in active and reactive power demand and no control actions are taken. Neglecting losses (transmission losses, core losses in transformers and generators), the active power balance equation can be written as:

$$P_m = P_e + P_a \tag{1.1}$$

Where,

P_m : The mechanical power supplied to the generator by the prime mover [W].

P_e : The electrical power output of the generator [W].

P_a : The power accelerating (or slowing down) the generator [W].

Now, considering a situation when there is a balance between the electrical energy production and the consumption rate (*i.e.*, $P_m = P_e$ & $P_a = 0$), and there is a sudden increase of active power demand occurs ($P_e \uparrow$). In order to maintain the active power balance (Eq. 1.1), the generator speed slows down ($P_a \downarrow$) and the frequency of the system drops. In order to maintain the active power balance and thus the frequency without the control actions, the mechanical power input has to be increased but the deceleration continues [26], [27]. The active power and frequency balance can be achieved by control actions within the suitable frequency response delivery time frames. These control time frames are broadly classified as: Primary Frequency Control and Secondary Frequency Control. The primary frequency control is achieved by speed governor control system and secondary frequency control can be achieved by load frequency control. These controls are described in the subsequent sections in detail.

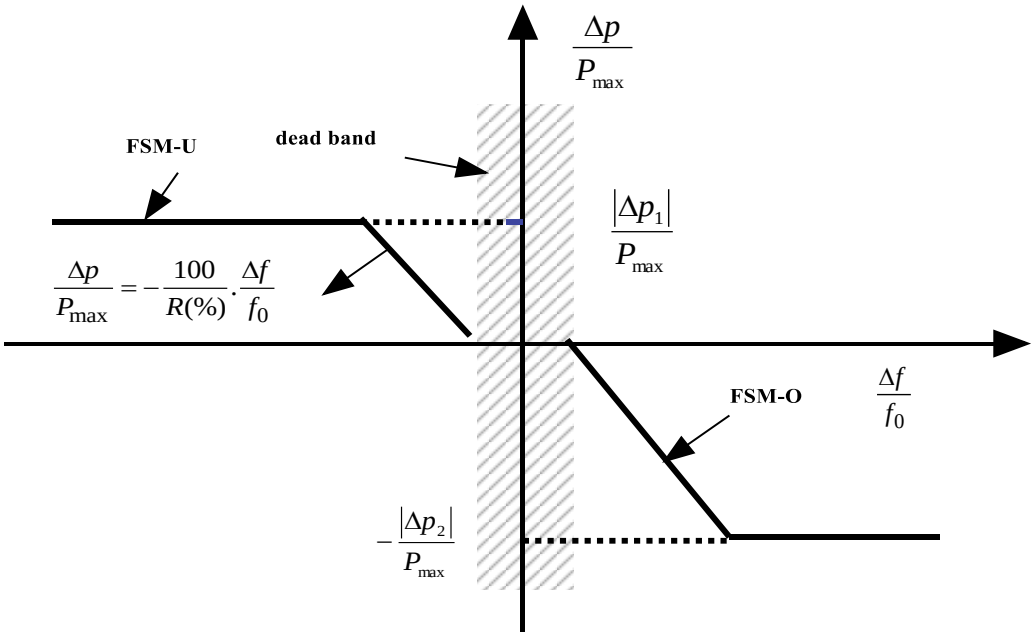

Fig. 2.2: Generator frequency sensitive modes.

The generator can vary its active power in the range of 1.5 to 10%. Response dead band range and the dead band is in the range 0-500 mHz & 2-12%, respectively [28]. Fig. 2.2, depicts the frequency sensitive modes of generators *i.e.* over frequency sensitive mode (FSM-O) & under frequency sensitive mode (FSM-U) of generator governor based on droop and dead band setting.

In FSM-O, generators reduce its active power output in proportion to the frequency rise $\frac{\Delta f}{f_0}$, where, f_0 is the nominal frequency of the system. The minimum regulating level is $\frac{-\Delta p_2}{P_{max}}$, where, P_{max} is the maximum capacity. In FSM-U, generators release additional active power up to its maximum capacity, P_{max} [29].

2.2.1 Reasons for Frequency Response Declination

In the USA, North American Electric Reliability Corporation (NERC) has done a lot of research work on the frequency response. Recent studies have shown that there is a declination in the frequency response in the last several years. Many physical reasons are responsible for this declination, these are listed below [1], [24], [30]:

- Steam power plant working on sliding pressure operating mode (In this mode plant cannot meet the quick demand variations, because quick-responding valves are

engaged for protection of unexpected steam pressure increase that is why in this mode it can't contribute to frequency response).

- Nuclear units working in blocked governor modes.
- Combined cycle gas-based generation gives positive frequency response this means that when there is a drop in frequency, the power output will also drop. This frequency response mode may cause serious issues like blackouts at the time of emergency.
- Due to the deregulation and present structure of market, there is a lack of individual reserves available with utilities.
- Less inertia in the new generator designs *i.e.*, less mass/ MW of output.
- Lack of incentives available for providing frequency response in the market design.

2.2.2 Frequency Response Time Frames

Frequency response can be classified into four different types based on the response delivery time, as shown in Table 2.1 [1], [2], [5]. It is the inertia of the system that provides the ability to arrest the initial frequency deviation. The ROCOF depends upon the system inertia. Higher system inertia is desirable as it provides more time to generator governors to respond to a frequency deviation [2], [26].

Table 2.1: Frequency Response Time Frame

Response	**Time frame**
Inertial Frequency Response	0-5 Seconds
Primary Frequency Response	1-20 Seconds
Secondary Frequency Response	4 Secs-3 Minutes
Tertiary Frequency Response	Minutes- Hours

PFR is the control action provided by the generator governor against the frequency deviation. It is generally delivered completely within 20 seconds [5]. PFR role is to stabilize the frequency at some intermediate state (as shown in Fig. 2.1). It is delivered by governor controller assisted by the system inertia and frequency sensitive load response. A governor controller adjusts the rotation speed of the shaft by changing the supply to the turbine and thus controls frequency. Governor controller also maintains system stability at the time of contingencies and line outages. Generator governor responds to frequency variations according to its droop characteristics. Generator governor droop provides the generator's PFR response capability. Primary frequency controller contains a feedback

loop and the gain of this loop is known as speed droop and denoted by D_i. It is given by Eq. (1.2) as:

$$D_i = \frac{df \,/\, f_0}{\Delta P / G_i} \tag{1.2}$$

Where, f_0 is nominal frequency, ΔP is change in power output and G_i is the output of the generator i.

In North America, industry practice for generator governor droop is 5 % [25]. Droop percentage signifies that generator output should vary from minimum to its maximum capacity if the system frequency varies by 5 %.

Inertial response and PFR only limit the frequency deviation but couldn't bring back the system frequency to its nominal value. Secondary frequency control is an autonomous action to restore the frequency to its predefined value. It is implemented by Automatic Generation Controller (AGC) also termed as Load Frequency Controller. The AGC is installed in the system which controls multiple generators inside a control area and bring back the frequency to its nominal value [25], [27]. It deploys reserves to restore the frequency closer to nominal value. AGC delivers response in seconds to minutes for the frequency restoration. The Governor and AGC work together, after the initial response from the governors (PFR). If the frequency deviation is not controlled by the primary response, AGC deploys regulating reserves so that frequency could be recovered back. The balancing authority monitors the supply-demand balance and area frequency for computation of the Area Control Error (ACE). ACE is the difference between net scheduled power and actual interchange of power at real time. If ACE is not zero, the balancing authority sends a signal to regulating units to drive ACE to zero. There are three common AGC implementation techniques [25]:

- **Constant Frequency Control**: In generator power output is based only on the frequency deviations. This type of control is common for interconnection with a single balancing authority like ERCOT. If it is used in interconnections with more than one balancing authority, it would result in power swings.
- **Constant Net Interchange Control**: AGC controls the interchange of power flows and avoid response to frequency deviations.
- **Tie-line Bias Control**: It is the commonly used control in grids with number of balancing authorities. In this strategy, balancing authority is responsible for returning frequency to its nominal value, once the frequency get stabilize at an intermediate state.

Tertiary frequency control is the manual actions taken by the SO or the automatic change in the system to avoid the current and future contingencies. It operates on even longer time duration (minutes to hours). This control is used to restore the primary and secondary frequency control reserves, when the secondary control fails to restore the system frequency at the desired level [32]. Tertiary frequency control actions necessitate synchronised changes in generator scheduling and dispatch. It means that implementation of this control requires dispatch of one generator down to restore its reserve capability, while simultaneously dispatch another generator up to replace the power provided by the first generator.

Reliability of power supply is one of the important aspects of the system operation. To ensure reliable operation of the system, sufficient primary and secondary frequency control reserves are required to accomplish demand variations during normal operations as well as to respond to sudden, large imbalances these are collectively known as Operating Reserves [10], [33]. Operating reserves can be distinguished on the basis of online, offline and response time.

- **On-line reserves:** These resources are connected and synchronized at the real time with the interconnection. It includes spinning, regulating, and other on-line reserves.
- **Off-line reserves:** These resources are not synchronized with the interconnection at the real time but could be made available at the time of emergency. It includes non-spinning and other off-line reserves.
- **Contingency reserves:** These component of operating reserves are specifically designed to operate at generation outage events. Therefore, they response time is very fast. Both spinning and non-spinning type of reserves could be used as contingency reserves.
- **Regulating reserves**: These are another component of operating reserves that provide regulation. The output from generation resources is controlled centrally via dispatch signals from AGC systems. Therefore, these reserves must be online.
- **The remaining reserves**: These type of reserves are synchronised with the system but running at less than full capability. These reserves are sluggish and may not respond quickly to the contingency events. These are also termed as other online or offline reserves.

PFR and in emergency conditions, UFLS are capable of frequency stabilization after the sudden loss of generation. The spinning reserve component of contingency reserves is intentionally designed to respond to these events. Actually, when generation outage event

takes place, primary frequency control actions would be taken up by synchronised generation sources. Regulating reserves and other on-line reserves would also participate automatically in response to the sudden loss of generation.

After the contingency events, frequency variations would be controlled by the mutual effect of all sources that are capable of providing primary frequency control. This is regardless of whether they are formally designated as on-line contingency (*i.e.*, spinning) reserves.

2.4 Frequency Response with Penetration of Renewable Energy Sources

RES generation is weak in providing an inertial response (as mentioned in Table 2.2). As RES would displace synchronous generator, the system's inherent ability to arrest and stabilize initial frequency deviation also gets reduced. Reduced system inertia would make system frequency more prone to supply and demand imbalance. This would lead to quick frequency deviations, following the loss of generation and/or load.

Table 2.2: Inertial Capability of Generators

Generator Type		**Inertia Constant**	**Inherent Inertial response**
Conventional Generators	Hydro Turbine	2-9 s [26]	Yes
	Steam Turbine	2-9 s [26]	Yes
Renewable Generators	FSIG		Yes (lower than steam turbine)
	PMSG		Negligible [34]
	DFIG	2-6 s [35],[36]	Limited
	PV	Not Applicable	No

*FSIG: Fix Speed Induction Generator, PMSG: Permanent Magnet Synchronous Generator, DFIG: Doubly Fed Induction Generator, PV: Photo Voltaic.

Generation characteristics of RES, like wind and PV, are different from those of conventional generation. Uncertainties, such as wind speed, cloud transients, solar insolation, increase the operational risk and affect generator output continuously [37], [38], [39]. Normally, RES is equipped with frequency relay that disconnects after a frequency disturbance. When the RES penetration of a grid is large, a massive RES disconnection can lead to power system oscillations [40], [41]. As RES penetration

increases, the fluctuations of generated power increases whilst overall system inertia is reduced [9], [42]-[44]. There is a reduction in the frequency nadir and settling frequency because of the lack of inertial response and PFR from RES and the displacement of responsive conventional generation.

There is limited understanding of required frequency response that could stabilize system frequency with large renewable penetration and inertia variation conditions. An understanding of frequency response requirement during such conditions would enhance flexible frequency operation strategy. This necessitates a wider understanding of the research challenges arising out of large penetration of uncertain RES generation in the grid and how uncertainty modelling techniques could be used to characterize wind/PV power uncertainty for reliable and secure system operation.

2.5 Wind & PV Generation Uncertainty Characterization

Due to wind/PV power uncertainty, system operations like scheduling and dispatch becomes challenging decision-making problem [12]. Accurate modeling of involved uncertainties is necessary to solve these decision-making problems. Uncertainties are generally modeled using deterministic forecasting models, which focus on the use of point forecast. Point forecast provides a single value of expected wind/PV power for a given lead-time, without any information about the possible deviation from forecasted value. Use of deterministic forecast for modeling decision-making problems may not provide the desired accuracy in solutions [12], [13], [38].

Decision-making problems are generally formulated using stochastic optimization [13], [45]. In this formulation, the randomness of input parameters can be described by a stochastic process. Stochastic process can be characterized by scenarios. These scenarios are possible results of arbitrary input with corresponding probabilities. Large quantum of scenarios are necessary for precise characterization of any stochastic process. The computational time required to solve scenario-based approaches, depends on the scenario number [14]-[17], [46]. Therefore, it is required to reduce the number of scenarios, in a manner that the reduced scenario set has a smaller number of scenarios, with minimally changed statistical properties [15], [16].

Generated scenarios need to be reduced via scenario reduction techniques [16], [17], [47]-[50]. Scenarios can be reduced by using fast forward selection and simultaneous backward reduction methods [16], [17]. These methods are iterative and their mathematical formulation is complicated. The complexity of scenario reduction

algorithms can be simplified by using a probability distance based backward reduction algorithm, however, scenario elimination is still an iterative process. Iterative elimination of scenario requires large computational time when the preserved scenarios are mini scale as compared to generated scenarios. This reduction process needs to be accelerated for reducing the computational time [48]-[51].

Scenario-based stochastic approach model RES uncertainty precisely, but requires computationally demanding simulations. This problem is handled using interval forecast in the literature. It is a robust technique, which requires less computational effort than the stochastic approach [18], [52]. In Interval forecast, uncertainty is modeled with three non-probabilistic scenarios (*i.e.* central forecast, upper bound & lower bound). Hence, it requires less computational time but produces conservative and thus expensive generation schedules [19]. This is because of the constraints imposed on the feasibility of transitions, from lower to upper bound of wind/PV power interval, and vice versa, between any two consecutive time periods. Such extreme transitions have a low probability and could be replaced by less severe ramp constraints. Hence, this requires a modified interval approach that could consider inter hour ramp requirements and accurately capture the expected wind/PV output.

On the basis of a critical review of literature pertaining to approaches or algorithms that have been used for modeling uncertainties through scenarios and interval forecast, following challenges are identified. Existing algorithms for scenario generation as well reduction has been used for modeling electric load and financial market uncertainties and their application needs to extend for modeling wind/PV power uncertainty. Uncertainty modelling through scenarios provides precise solutions but requires computationally demanding simulations. Interval approach requires less computational time but gives conservative solutions. Additionally, existing algorithms are complex and need to be simplified for modeling wind/ PV power uncertainties. Quality and stability of scenarios need to be considered for improving uncertainty modeling.

2.6 Frequency Response Constrained Generation & PFR Scheduling Under Uncertainty

Large wind/PV generation in existing power system increase the requirement of FR services, as the existing wind/PV generators are weak in providing inertia and PFR. This necessitates optimal PFR schedules from UC. Various computational techniques have been proposed to obtain the cost-efficient combination of controllable generation units,

which may effectively respond to penetration from intermittent wind/PV generation while maintaining minimal generation cost.

Deterministic UC is widely used to schedule the reserves, while demand is modelled by a point forecast, and the associated uncertainty is characterised using ad-hoc reserve rules [53]. However, these formulations do not consider probabilistic modeling and cost benefits of maintaining reserves. SUC with Mixed Integer Linear Programming (MILP) formulation can schedule operating reserves, while wind scenario generation techniques can be used to address the associated uncertainty [54], [55]. These techniques consider probabilistic modeling and reduce the expected operating cost, however obtaining SUC solution is computationally challenging, as it considers a large number of scenarios [56]. Scenario reduction techniques are widely used to mitigate the computational burden [45]-[50]. However, an insufficient number of scenarios usually led to a less accurate solution and in turn increases the operating cost [57].

As PFR was inherently available with conventional generation, it's scheduling within UC received relatively little attention [20]. PFR requirement with large renewable penetration has increased, as non- synchronous generation sources are weak in providing PFR. PFR scheduling is particularly challenging as the deployment timeframe does not possess the broad freedom, as available in tertiary regulation. This is a rapid response following a contingency and has to be deployed in first 5-10 seconds [58]. Most of the electricity markets do not have explicit provisions for incentivizing or mandating PFR. Markets over the world are realizing this necessity, and are adopting it progressively. Presently, PFR scheduling practice in real time is available in Australian and New Zealand electricity market [58], [59]. PFR in day-ahead scheduling is considered in ERCOT and Nordic electricity markets [11], [21]. In the day-ahead market, PFR ancillary service is usually a multi-period security-constrained UC (SCUC) and in the real-time market, it is a single or multi-period security-constrained economic dispatch (SCED) [60]-[62]. PFR control in real-time operations makes sense from the market perspective. However, from a system security perspective, it makes more sense to procure PFR in day-ahead for the worst case contingency.

PFR ancillary service market design incorporates reliability requirements of PFR and ensures incentives for synchronous inertia, PFR capacity, and responsive droop curves. This provides a stable and sustainable response by reduced insensitivity to frequency, triggering speed and full deployment of PFR [63]. Generators' frequency response is modeled as a constraint of MILP based UC model [20], [53], [60]-[65]. Primary regulation

constraints in the UC model has been modeled, explicitly covering only steady-state system frequency deviation and governor droop to determine if sufficient primary reserves are committed [20]. However, the assessment of transient frequency behavior and consideration of frequency droop parameter for unit regulation has not been investigated. PFR and steady-state frequency response with uncertainties like thermal generation outage, wind generation, and demand are included along with SUC model [63]. However, the impact of system inertia level on PFR and frequency nadir has not been thoroughly investigated. Security-constrained UC with linearised system frequency constraints has been proposed considering inertial and PFR response [64]. The response time of all generators has been considered identical. However, these assumptions may not provide the exact deployment time of the reserves. Stochastic generation scheduling has been enhanced to include frequency response constraints while considering wind uncertainty [65]. Despite that SUC formulation is cost-effective, the need to reduce computational burden can't be overlooked, considering operational time constraints.

From the literature reviewed in this section, it can be understood that a computationally fast system operation framework is required to include frequency response constraints under uncertain wind/PV generation.

2.7 Prediction of System Inertia Condition for PFR Adequacy

System inertia is a key power system characteristic which provides instant support to the frequency, following contingencies like large infeed loss [66]. There is a limited understanding of system behaviour to provide inertia & PFR with high renewable penetration. An understanding of these requirements during such contingencies would provide knowledge about permissible renewable penetration that grids could withstand, following network regulations. Frequency-related issues, such as the operation of frequency controlled reserves, ROCOF protection setting, UFLS, and PFR deployment speed requirement need a proper assessment of available system inertia for secure system operation. Future system operability requirements of interconnections strongly recommend the development of methods to accurately estimate system inertia during normal and disturbance conditions [67], [68].

Inertia estimation methods may require knowledge of the frequency and electrical power of every system generator, which is scantly available [69]. Inertia estimation using

simultaneous assessment of disturbance time and inertia uses frequency and active power measurement from a single location and is applicable for small systems only [70]. Theoretically, least square approximation based frequency disturbances estimation could be used to calculate system inertia [71]. System inertia calculation for Western Interconnection in North America is presented based on the measured frequency during disturbances [72]. However, its performance assessment is difficult, as it is not tested in a simulation environment. Great Britain system's inertia is estimated based on aggregated estimates at the regional level using phasor measurement unit data [73]. An online inertia estimation tool prototype for ERCOT analyses the performance between generation outage events and maximum instant frequency deviation [5], [21].

System inertia estimation is essential considering grid's frequency security, but the prediction of system inertia condition for coming hours is always a concern for the SO [21], [68], [74], [75]. It is required to handle unwanted contingencies, like large infeed loss or loss of load, estimation of PFR requirement, UC decision making, and system frequency stability. As system inertia condition varies over a day's time, fixed PFR estimation based on worst-case scenario is not efficient. Hence, it is imperative to forecast system inertia for upcoming hours, considering the current operation status of all generators. Using this information, expected system inertia could be calculated for each hour. Prior information of system inertia condition would be useful for the estimation of PFR requirement.

2.8 Optimal Generation Mix for System Inertia and PFR Adequacy

RES generation mix is integrated into the interconnections, in order to limit the fossil fuels and meet the government policy targets [76], [77]. As the generation mix on a power system evolves, moving away from traditional generation units, behavior of the power system in response to a power imbalance also changes [76], [80]. Increasing RES share in overall generation mix would pose additional formidable challenges from the technical and economical point of view. RES integration could lead to both diversifications of generation sources and an increase in overall cost due to the additional resource requirement for flexibility and hence secure system operation [85].

Recent analysis in the interconnection globally reveals that, PFR requirements are expected to increase significantly over the next 15 years. Over the next 5 years, this amounts to an increase of 30-40% [23], [75]. This requires efficient generation mix by balancing the profits of generation source variation and cost of security with the PFR provision. PFR requirement analysis is done for the quantification of variability and uncertainty of the RES [77], [86], [87]. It is observed that the PFR requirements could be partly compensated by the interaction of different type of loads and wind power [77]. Another scenario-based study is performed for different combinations of wind & solar power generation for the computation of PFR requirements caused due to uncertainty [86]. It is concluded that PFR requirements and uncertainty is reduced with RES mix [87]. Diversified RES mix provides smooth generation portfolio. Hence, generation predictability would increase and the probability of extremes values would decrease. This would result in a reduction in overall system frequency response requirements.

Conventional and RES generation technology have distinctive effect on system frequency and there is limited understanding of frequency response adequacy with various generation mix characteristics. There is a need to obtain optimal generation mix for securing adequate inertia and PFR. This would support SO to maintain reliable and stable power system.

2.9 Research Challenges

Large-scale RES generation penetration in power systems poses formidable challenges for SO to meet the frequency response requirements. Development of modelling techniques for frequency response adequacy under wind/PV power uncertainties is a challenge considered for investigation in this thesis. Excellent bibliographical surveys and research reviews on such challenges have been published in recent years. These indicate that frequency response service is a potentially interesting and timely research problem for interconnections and power management research community over the globe. On the basis of critical review of literature pertaining to the considered problem, following research challenges have been identified.

- Development of efficacious algorithms for wind/PV power uncertainty modelling through scenarios and modified interval forecast.
- Development of novel, computationally fast MIUC formulation framework to include system's fast frequency response constraints. The framework directly aims to contain

initial transient frequency behavior within the prescribed system security criteria, following the largest infeed loss.

- PFR scheduling of committed generators, required to make frequency stable at intermediate state, following the largest infeed loss.
- Prediction of system inertia condition for PFR adequacy under uncertain wind generation.
- Development of novel exposition for optimal generation mix with the objective of reduced operating cost while maintaining systems' frequency response.

Chapter – 3

WIND & PV GENERATION UNCERTAINTY MODELLING THROUGH SCENARIOS AND MODIFIED INTERVAL FORECAST

3.1 Introduction

Power system operations like generation scheduling and dispatch are decision-making problem. Decisions obtained through these operations impact the system security and reliability. Wind and PV power uncertainty makes this problem more critical [12]. Accurate modeling of involved uncertainties is necessary to solve these decision-making problems. The uncertainty of input parameters could be described by a stochastic process. The stochastic process could be characterized by scenarios. Scenarios are probable outcomes of arbitrary input with corresponding occurrence probability. Large quantum of scenarios are required for precise modeling of any stochastic process. Computational time required to solve scenario-based approach depends on the quantum of scenarios. Therefore, it is required to reduce original scenarios set, in a manner that reduced set has a lesser number of scenarios, with minimally changed statistical properties. However, an insufficient number of scenarios usually lead to a less accurate solution and in turn, increase the operating cost of the problem [14]-[17], [46].

In this work modified interval forecast approach is proposed along with the scenario approach. Interval forecast already exists in literature and it is a robust technique, which requires less computational effort than the stochastic process. In interval forecast, uncertainty is modeled with three non-probabilistic scenarios (*i.e.* central forecast, upper bound & lower bound). Hence, it requires less computational time but produces conservative and thus expensive generation schedules [18], [52]. This is because of the constraints imposed on the feasibility of changeovers, from lower to upper bound of wind power interval, and vice versa, between any two consecutive time periods. Such extreme changeovers have a low probability and could be replaced by less severe ramp constraints.

In the proposed modified interval model, the advantages of interval and scenario approaches are incorporated. Uncertainty is modeled using upper and lower bounds, as in the interval formulation, but inter-hour ramp requirements are based on net load scenarios

and hence accurately capture the expected wind and PV output. A time series based ARIMA model is used for interval forecast and scenario generation [51]. Probability Distance Based Backward Reduction is used for scenario reduction. The algorithms have been implemented for wind power scenario generation of wind speed historical time series data for the duration 01.01.2010 to 31.12.2010, online available from Illinois Institute of Rural Affair, USA [88] and PV irradiation time series data from Chicago, USA for the duration 01.01.2010 to 31.12.2010 [89]. Proposed modified interval and scenario-based uncertainty characterization models are useful for system operators to optimize system operations pragmatically under uncertainty.

3.2 ARIMA Model

Statistical ARIMA model is used to model random time series based on a number of historical data, pattern identification, and parameter estimation [51], [90]. This is a hybrid of autoregressive and moving average model. The typical ARIMA (p,d,q) model is expressed as

$$\alpha_p(\beta)(1-\beta)^d \lambda_t = \psi_0 + \psi_q(\beta)\zeta_t \tag{3.1}$$

where λ_t is the prediction limit of wind & PV power at time interval t, d is the degree of differentiation, β is the backshift operator, $\alpha_p(\beta)$ is the AR operator of order p, and $\psi_q(\beta)$ is the MA operator of order q. ζ_t is a random number distributed normally with zero mean and constant variance. This is also known as white noise or error signal. If q is assumed to be zero in ARIMA model, it behaves like an autoregressive (AR) model.

3.2.1 Distribution Transformation

The random time series of wind speed scenario generated by the ARIMA model are not actual wind speed scenarios. This is because generated series is in terms of white noise and follows a normal distribution, while actual wind speed is always greater than or equal to zero and follows Weibull distribution [12], [91]. For wind speed analysis, Weibull distribution is a widely accepted function as compared to other functions, and has advantages of flexibility, simplified parameter estimation, *etc.* [47], [92], [93]. Therefore, the generated wind speed scenarios are transformed into actual wind speed scenarios by distribution transformation process. In this process, cumulative distribution function (CDF)

of generated random wind speed scenarios series is considered by the ARIMA model. This provides a probability of occurrence of each scenario. For these probabilities, inverse Weibull CDF is considered to generate actual wind speed scenarios. The scale and shape parameters used in inverse Weibull distribution are estimated from actual historical wind speed data of any specified site. The shape of the probability distribution plot is decided by shape parameter while the distribution range is decided by scale parameter. Mathematically, the distribution transformation process is expressed as

$$V = \phi^{-1}\left[F_Z\left(Z\right)\right] \tag{3.2}$$

where, $F_Z\left(Z\right)$ is cumulative distribution function of randomly generated wind speed scenario series, and $\phi(V)$ is cumulative distribution function of actual historical wind speed data. PV radiation data follows a normal distribution; hence distribution transformation is not required.

3.2.2 Wind Speed to Power Conversion

In scenario generation, wind speed time series data, as measured by anemometers installed at different heights is used [94]. These scenarios are transformed into power scenarios, considering the preferred hub-height. This is an important process because of the hub height of installed turbines and anemometer's height differs in some cases. This process could be expressed as:

$$V\left(h\right) = V\left(h_r\right)\left(\frac{h}{h_r}\right)^{\alpha} \tag{3.3}$$

where,

$V\left(h\right)$: Estimated average wind speed (m/sec)

$V\left(h_r\right)$: Recorded wind speed at known hub height (m/sec)

h : Generator hub height (m)

h_r : Known Anemometer height (m)

α : Shear coefficient depending on atmosphere stability and surface roughness

The generated desired hub height scenarios are converted into power scenarios, by utilizing power curve of considered wind turbine model. The power curve shows the

relationship between power and wind speed. This relationship is mathematically expressed as Eq. (3.4) and depends on swept area, air density, efficiency, cut-in, and cut-out speed:

$$P(V)=\begin{cases}0 & V \le V_{cut-in} \\ \frac{1}{2}C_p(V)\rho AV^3 & V_{cut-in} \le V \le V_{Rated} \\ P_{max} & V_{Rated} \le V \le V_{cut-out} \\ 0 & V \ge V_{cut-out}\end{cases} \quad (3.4)$$

where,

A : Swept area of wind turbine rotor (m^2)

ρ : Air density at wind site (kg/m^3)

$C_p(V)$: Overall efficiency of wind turbine expressed as a function of wind speed

V : Wind speed (m/sec)

V_{cut-in} : Cut-in speed of wind turbine (m/sec)

$V_{cut-out}$: Cut-out speed of wind turbine (m/sec)

V_{Rated} : Rated speed of wind turbine (m/sec)

P_{max} : Maximum power output of wind generator (MW)

3.2.3 PV Radiation to Power Conversion

The power output of PV plant is modelled using global horizontal irradiation series, panel efficiency, performance factor of plant and total solar panel area. Power output is given by

$$PV_{power} = Ar * \eta * GHI * PF \quad (3.5)$$

Here, PV_{power} is generated PV power in Watt, Ar is PV panel area in m^2, η is the efficiency of PV panel, GHI is Global Horizontal Irradiance in W/m^2 and PF is the performance factor.

3.3 Scenario Generation

In stochastic optimization models, parameters affected by uncertainties are generally modeled as stochastic processes [12], [45]. A stochastic process can be represented either by continuous or discrete random variables or scenarios. Availability of generating units is

a discrete random process while wind speed/PV radiation is represented by continuous random variables [90].

In this section, models and process used in wind/ PV power scenario generation are discussed, followed by the proposed algorithms.

3.3.1 Proposed Wind/PV Power Scenario Generation Algorithm

In this section, the stepwise procedure for wind/PV power scenario generation is described. The algorithm is also illustrated in the flowchart of Fig. 3.1.

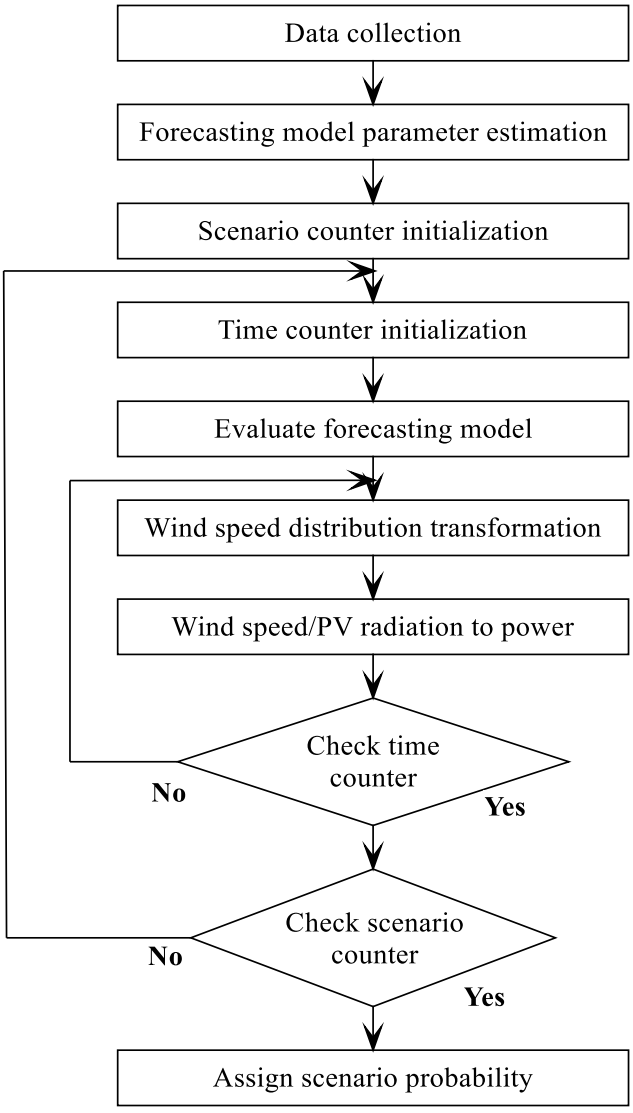

Fig. 3.1: Wind/PV power scenario generation algorithm.

Step 1: Distribution Fitting: Take historical wind speed/PV radiation data of any specified site. Fit these data into known probability distribution and estimate the parameters of this distribution.

Step 2: Time Series Analysis: Order and parameter of time series ARIMA model, for collected historical wind speed/ PV radiation data is estimated. The order of AR terms is decided by sample Partial Auto-correlation Function (PACF) plot at different lag (time step), while the order of MA terms is decided by observing ACF plot. Thereafter, parameters of the ARIMA model, *i.e.* AR coefficients, MA coefficients, and variance of white noise are estimated.

Step 3: Scenario Counter Initialization: Assume the required number of scenarios be N_ω. Start with the scenario $\omega = 1$.

Step 4: Time Counter Initialization: For day-ahead scenarios generation, 24-time periods are considered. Start with time $t = 1$.

Step 5: White Noise Generation: Generate normal distribution random number with zero mean and standard deviation σ, as estimated in Step 2. White noise is mathematically expressed as $\varepsilon_t = N(0, \sigma)$.

Step 6: Evaluate ARIMA Model: Evaluate the ARIMA expression in Eq. (3.1) for random generation of wind speed scenarios.

Step 7: Distribution Transformation: The generated random wind speed scenarios are not actual wind speed scenarios. Therefore, actual wind speed scenarios are generated by using distribution transformation described above and mathematically shown in Eq. (3.2).

Step 8: In case of Wind Speed Conversion at Desired Hub Height: The generated wind speed scenario for anemometer height is converted for desired hub height scenario by using Eq. (3.3).

Step 9: Wind Speed/PV Radiation to Power Conversion: When wind speed scenario for desired hub height is generated, it is transformed into power scenario through the power curve associated with turbine model, installed in wind farm. The typical power curve expressed in (3.4) is used to determine power at any wind speed. Solar radiation is converted to power using the panel area, performance factor, panel efficiency & GHI as shown in (3.5)

Step 10: Check Time Counter: If time period counter, *i.e.* 24 is achieved, go to next step, otherwise update $t = t + 1$ and go to step 5.

Step 11: Check Scenario Counter: If the desired number of scenario N_ω is achieved, go to next step, otherwise update scenario $\omega = \omega + 1$ and go to Step 5.

Step 12: End

3.4 Scenario Reduction

Large scenario quantum is necessary to precisely model any stochastic process. However, computational burden for solving scenario-based optimization models would increase due to the huge number of scenarios. This necessitates reduction of original scenario set in a manner to obtain reduced number of scenario without changing the statistical properties [12], [45]-[50], [95]. The reduced scenario number is based on the problem type, which is to be optimized, and it must be less than one-fourth of generated scenarios [96].

The basic idea of scenario reduction is to remove scenarios with very low occurrence probability and bundle scenarios that are very close. Accordingly, scenario-reduction algorithms determine a subset of scenarios and calculate probabilities for new scenarios, such that the reduced probability measure is closest to the original probability measure, in terms of a certain probability distance between the two measures [46], [48].

The scenario-reduction algorithm reduces and bundles the scenarios using the Kantorovich Distance (KD) matrix. KD is the probability distance between two different scenario sets that represent the same stochastic process. It is generally used to quantify the closeness of different scenario sets. KD assures that maximum possible scenario are reduced, without violating given tolerance criteria. Probability of all deleted scenarios is assumed to be zero. The new probability of preserved scenarios is equal to sum of its former probability and the probability of deleted scenarios that are closest to it [48], [97].

3.4.1. Probability Distance Based Scenario Reduction

Let the initial probability distribution Q is considered over the scenario set Ω. The problem of optimal reduction of set Ω could be described as follows: obtain a scenario subset $\Omega_S \subset \Omega$ of prescribed cardinality or accuracy $N_{\Omega S}$, and assign new probabilities to the preserved scenarios such that the corresponding reduced probability distribution Q', defined over the subset Ω_S, is closest to the original distribution Q in terms of probability distance. The KD can be equivalently determined as

$$KD\left(\omega,\omega^{'}\right)=\sum_{\omega\in\Omega/\Omega_S}\pi_{\omega}v\left(\omega,\omega^{'}\right) \tag{3.6}$$

where, π_{ω} is an occurrence probability of scenario ω and $v\left(\omega,\omega^{'}\right)$ is a cost function. It is vector distance between scenario subsets estimated by following expression:

$$v\left(\omega,\omega^{'}\right)=\left\|P_{\omega}-P_{\omega}^{'}\right\|,\forall\omega,\omega^{'}\in\Omega\quad\Omega=1,2.....N_{\omega} \tag{3.7}$$

where, P_{ω} and P_{ω}' are values of wind & PV power generation for scenario ω and ω' respectively. The cost matrix consists of cost function for all generated scenario sets. KD matrix consists of the product of cost function and corresponding occurrence probability of all generated scenarios. The expression in Eq. (3.7) can be used to derive several heuristics for generating reduced scenario sets, which are close enough to the original set. Two heuristic algorithms are proposed in the literature, namely backward reduction and forward selection. In backward reduction, optimal deletion of single scenario is an iterative process until a prescribed number of scenarios are eliminated. Forward selection is used when the preserved number of scenarios are small. In this approach, selection of single scenario is repeated, until a desired number of scenarios are selected. In this work, backward reduction approach is employed for wind & PV power scenario reduction.

3.4.2. Proposed Algorithm

In this section, step-wise procedure for wind & PV power reduction is described. The algorithm is also illustrated through the flowchart depicted in Fig. 3.2.

Step 1: Collect Generated Scenarios: All scenarios generated by using algorithm described in previous section are collected. Assign probabilities of collected scenarios in such a way that sum of probability of all scenarios at any time step must be unity. Probability of each scenario ω is $1/N_{\omega}$, where N_{ω} is total number of generated scenarios.

Step 2: Compute KD Matrix: Compute the cost matrix for each pair of scenarios and determine the KD matrix by multiplication of scenario probabilities, using Eqs. (3.6) and (3.7).

Step 3: Scenario Selection: Determine the scenario with lowest KD. The lowest KD is obtained for scenarios with equal magnitude and probability.

Step 4: Scenario Elimination: Select the scenario with lowest KD, and the scenario having KD closest to it. The lowest KD scenario is removed on the basis of its relative closeness to the other scenarios and low occurrence probability. Its probability is added to the probability of nearest identified scenario. This ensures that sum of the occurrence probability of all the remaining scenarios is

always unity. This process of scenario reduction gives rise to a new probability matrix with the reduced order.

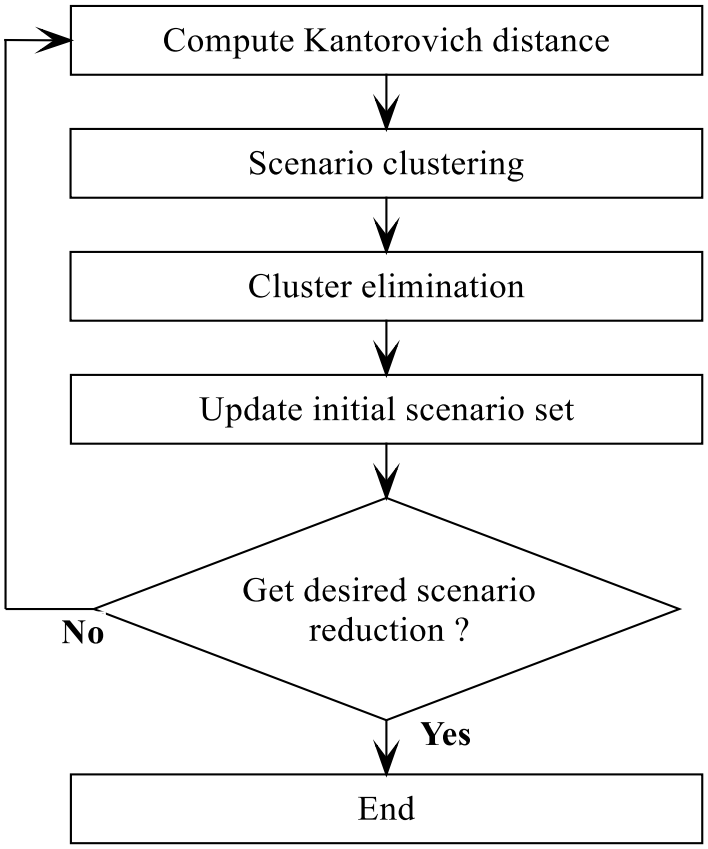

Fig. 3.2: Flow diagram of scenario reduction algorithm.

Step 5: Update Probability Matrix: Update the initial probability matrix by new matrix.

Step 6: Update Initial Scenario Set Matrix: After deletion of the selected scenario, the initial scenario matrix is updated. This matrix now has $N_{\omega}-1$ scenarios. One scenario is eliminated during each iteration.

Step 7: Repeat Step 2 to Step 6 until desired numbers of reduced scenarios are obtained.

Step 8: End

3.5 Modified Interval Forecast

Scenario approach is one of the benchmark methods for uncertainty characterization. However, this approach is computationally demanding because of large number of probabilistic scenarios. In view of this, in this work Modified Interval approach of uncertainty characterization is proposed that incorporates advantageous features of interval

and scenario-based approach. Uncertainty is modeled using upper and lower bounds, as in the interval formulation, but inter-hour ramp requirements are formulated based on net load scenarios and hence accurately captures the expected wind and PV output.

Prediction interval is an interval within which power generation may lie, with a certain probability. Forecast intervals considered are normally distributed. For 95% prediction interval, the h step forecast is

$$y_{T+h|T} \pm c\sigma_h \tag{3.8}$$

σ_h is an estimate of standard deviation of h step forecast distribution. Multiplier c depends on coverage probability.

As compared to stochastic scenario-based approach, interval approach is computationally fast because the generation uncertainty is represented by three non-probabilistic scenarios (black lines in Fig. 3.3): the central forecast (black circles), lower limit and upper limit (red circles).

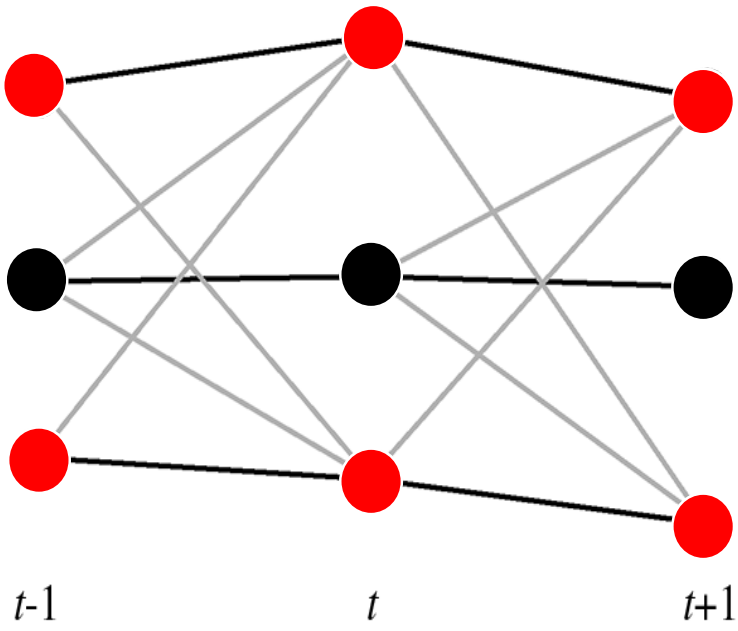

Fig. 3.3: Interval scenarios (red) with changeover constraints (grey).

Interval approach gives conservative results because of constraints forced on the changeovers from lower to upper limit, and vice versa, between any two successive time periods, as depicted by the grey lines in Fig. 3.3. These changeovers have low probability and could be substituted by less severe ramp constraints. Comparative assessment of

uncertainty modelling through stochastic scenarios, interval and modified interval approach is illustrated in Fig. 3.4

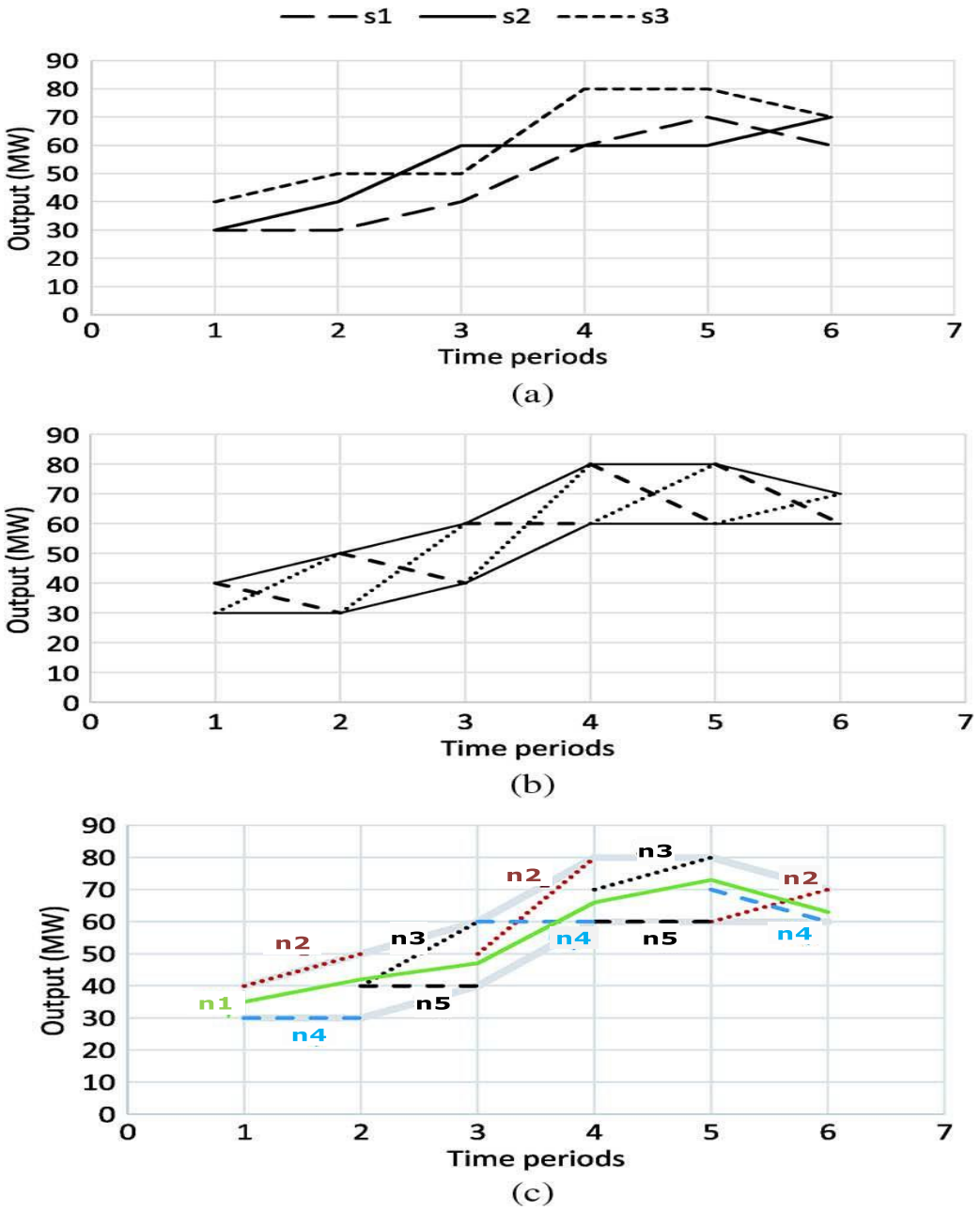

Fig. 3.4: Uncertainty modeling illustration: (a) Stochastic Scenarios; (b) Limits (lines), up ramps (dotted lines) & down ramps (dashed lines) considered in Interval; (c) central forecast (green line), limits (thick grey lines), up ramps (dotted lines) and down ramps (dashed lines) considered in Modified Interval with five ramping scenarios.

Fig. 3.4 (a) depicts the scenarios used by the stochastic approach. Limits for both interval and modified interval are formed based on the minimum and maximum values of scenarios at each hour. For instance, lower limit in hours 1–4 and 6 is set by scenario s1.

However, in hour 5 it is set by scenario s2. Fig. 3.4 (b) shows the interval limits with up and down ramps. Fig. 3.4 (c) shows artificial modified interval ramping scenarios with ramp requirements between successive hours. Five ramping scenarios are considered as $n1, n2, n3, n4 \& n5$. Here, $n1$ is central forecast scenario. Scenario $n2$ is up ramp requirement for odd and even hours. Up ramp requirements for even and odd hours are shown by $n3$. Down ramp requirements for odd and even hours is considered as $n4$, while down ramp requirements for even and odd hours is $n5$. It could be observed, each ramp ends at one of the limits, while its tail at the hour before is obtained by the highest slope over all stochastic scenarios. In same manner each dotted fragment in Fig. 3.4 (c) shows up ramp and upper limit, while each dashed fragment defines down ramp & lower limit. To obtain ramp needs and limits for each wind farm & PV plant in a given power system, the procedure explained in Fig. 3.4 is applied to each wind farm and PV plant individually.

3.5.1 Proposed Algorithm

In this section, the step-wise procedure for wind/ PV power interval forecast is described. The algorithm is also illustrated through the flowchart depicted in Fig 3.5.

Step 1: Distribution Fitting: Take historical wind speed/PV power data of any specified site. Fit these data into known probability distribution and estimate the parameters of this distribution.

Step 2: Time Series Analysis: Estimate the order and parameter of time series ARIMA model.

Step 3: Time Counter Initialization: Here 24-time periods are considered for day-ahead scenarios generation. Start with time $t = 1$.

Step 4: Evaluate forecasting model.

Step 5: Prediction of intervals with 95% confidence intervals at step of 10% for capturing the accurate inter hour ramp requirement for wind/ PV output.

Step 6: Wind Speed/Solar Radiation to Power Conversion:

Step 7: Check Time Counter: If desired time period counter, *i.e.* 24 is achieved, go to next step, otherwise update $t = t + 1$ and go to step 3.

Step 8: Obtain modified interval scenarios with upper and lower bound and central forecast with inter hour ramping scenarios.

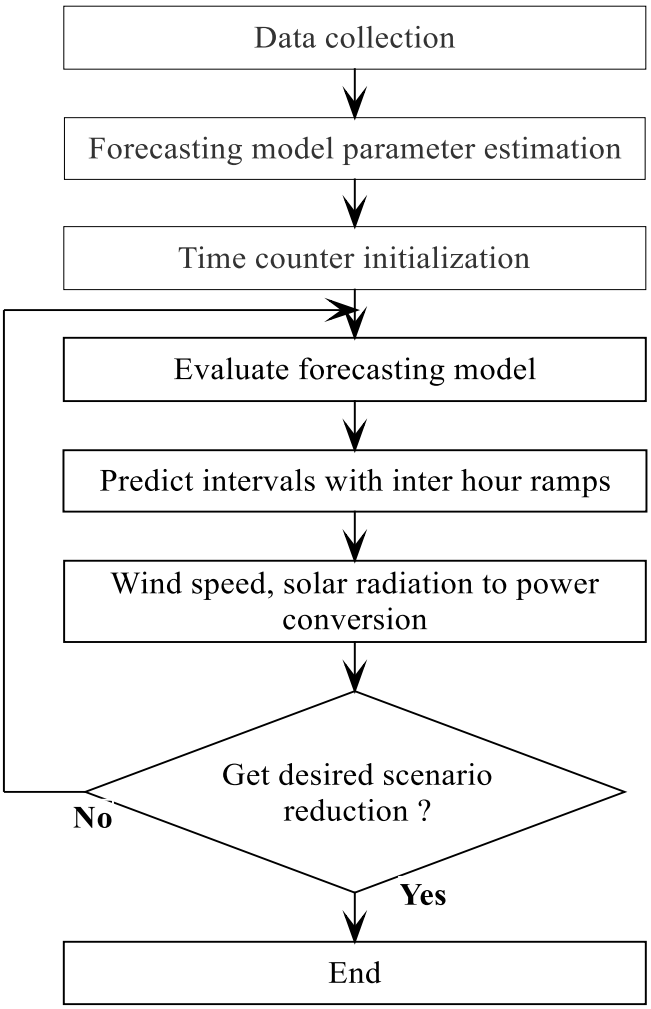

Fig. 3.5: Flow diagram of modified interval algorithm.

3.6 Case Studies

To illustrate the proposed uncertainty characterization with scenarios and modified interval forecast algorithms two practical case studies are presented in this section. First case study is based on wind/PV power uncertainty modeling through stochastic scenarios while second is based on uncertainty modeling through modified interval forecast.

3.6.1 Data

The historical wind speed used for wind power scenario-generation and reduction algorithms is obtained from publicly available data Illinois Institute of Rural Affairs, USA [88]. The hourly mean wind speed of August 2016, recorded at 39 m of anemometer height, is used in this study. The shear coefficient of selected site at the time of data

collection is 0.35. The air density is 1.242 kg/m^3 . To convert wind speed into wind power, power curve of the standard simulated turbine model VESTAS, with 3 MW of capacity and 100 m of hub height, is used [98]. Historical PV radiation data is taken from Chicago, USA [89]. PV panel area, efficiency & performance factor considered for this study are 3.5 Km Sq., 15% and 75% respectively.

3.6.2 Case Study I: Wind & PV Scenario Generation and Reduction

To generate next-day wind & PV power scenarios, the algorithm described in Section 3.3 is simulated. In case of wind power scenario generation, the historical data is fitted into Weibull distribution with an estimated scale parameter and shape parameter as 4.4338 and 3.0486, respectively. Order of the ARIMA model is determined by observing the sample ACF and PACF plots shown in Figs. 3.6 and 3.7, respectively. The PACF of sample data determines the order of AR terms, and the ACF determines the order of MA terms in the ARIMA model. In the ACF plot, exponential or sinusoidal delay is one, and in the PACF plot, spikes cut off to zero after lag 1. Therefore, the ARIMA (1, 1, 1) model is suitable for analysis of historical data. The estimated values of the AR, MA coefficient and the variance of white noise are 0.619 and 0.614, 0.983 respectively.

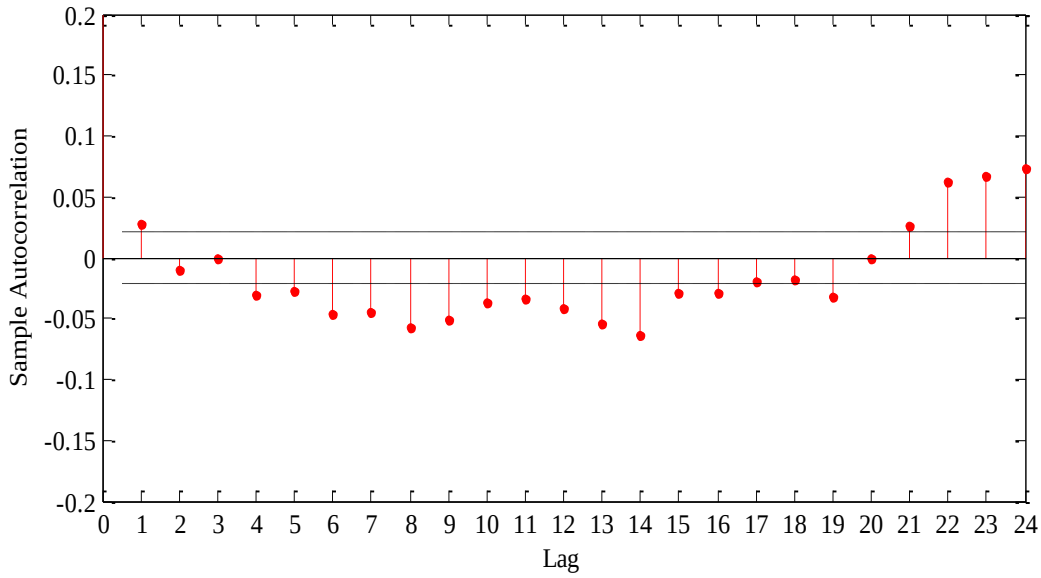

Fig. 3.6: ACF plot of sample wind speed data.

Generated wind power scenarios are shown in Fig. 3.8. In this study, 1000 scenarios are generated for each hour of the next 24 hours. After scenario generation, the reduction algorithm is utilized to obtain ten representative scenarios, as shown in Fig. 3.9. The

probability-distance-based backward algorithm is used for scenario reduction. The minimum KD is set as zero, and the maximum KD is set as 3000 kW. A single scenario is deleted in each iteration; it is proposed to reduce 1000 generated scenarios to 10. Thus, to obtain 10 scenarios, 990 iterations are performed. The sum of probabilities of all generated and reduced scenarios is always one at any particular time instant.

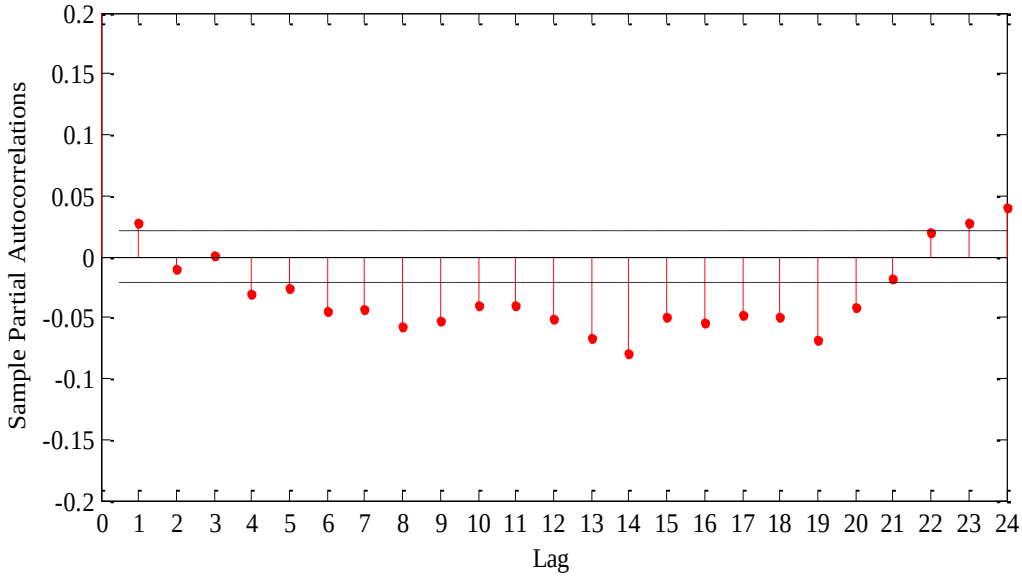

Fig. 3.7: PACF plot of sample wind speed data.

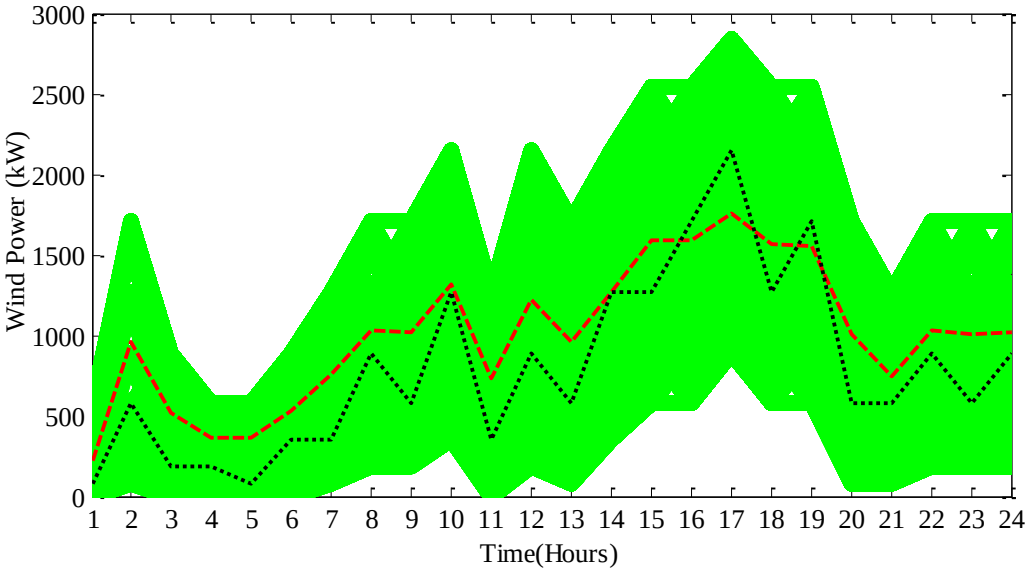

Fig. 3.8: Generated wind power scenarios.

Table 3.1 gives the reduced wind power scenario with corresponding probabilities and KDs for eleventh hour. This table shows that Scenario 3 has the lowest KD and would be

selected for elimination in the next iteration. Scenario 9 is closest to the selected scenario. The new probability of Scenario 8 would be the sum of its previous probability and probability of Scenario 3.

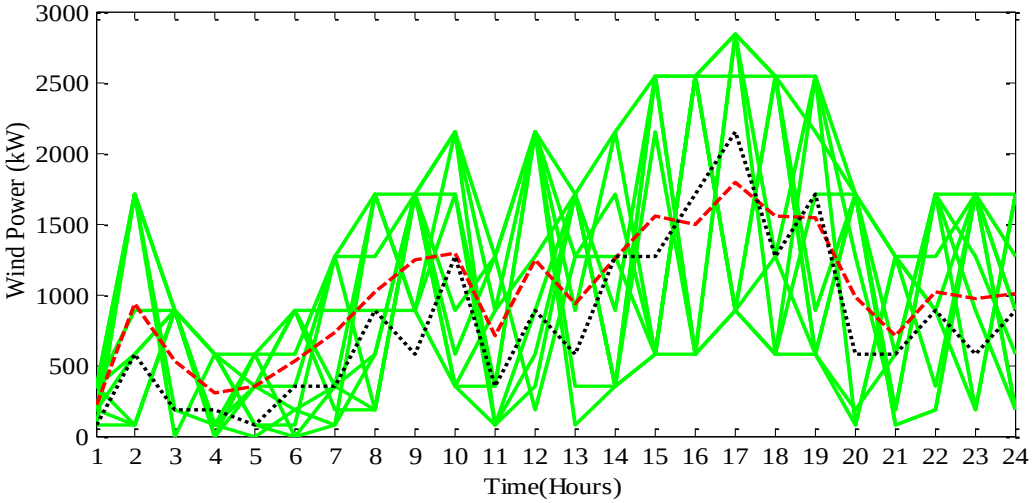

Fig. 3.9: Reduced wind power scenarios.

Table 3.1: Reduced Wind Power Scenarios, Probabilities and KD of Eleventh Hour

Scenario Index	Wind Power (kW)	Probability	KD
1	1273	0.001	133.665
2	1273	0.001	133.665
3	**77**	**0.001**	**8.085**
4	353	0.001	37.065
5	77	0.001	8.085
6	1273	0.415	133.665
7	353	0.213	37.065
8	886	0.001	93.03
9	**77**	**0.281**	**8.085**
10	886	0.085	93.03

In case of PV, PACF of sample data determines the order of AR terms, and the ACF determines the order of MA terms in the ARIMA model. In the ACF plot, shown in Fig. 3.10, exponential or sinusoidal delay is zero, and in the PACF plot, shown in Fig. 3.11, spikes cut off to zero after lag 3. Therefore, the ARIMA (3, 0, 0) model is suitable for analysis of historical data. The estimated values of the AR1, AR2, AR3 and the variance are 1.820 and -1.031, 0.383, 0.236 respectively. Here, negative sign of AR2 reflects negative value of PACF for second lag.

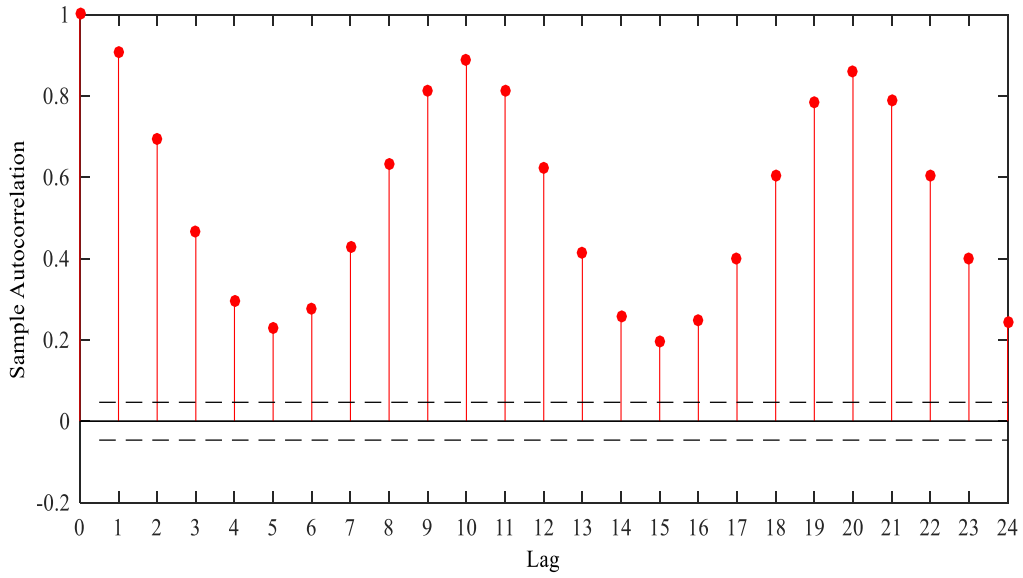

Fig. 3.10: ACF plot of sample PV radiation data.

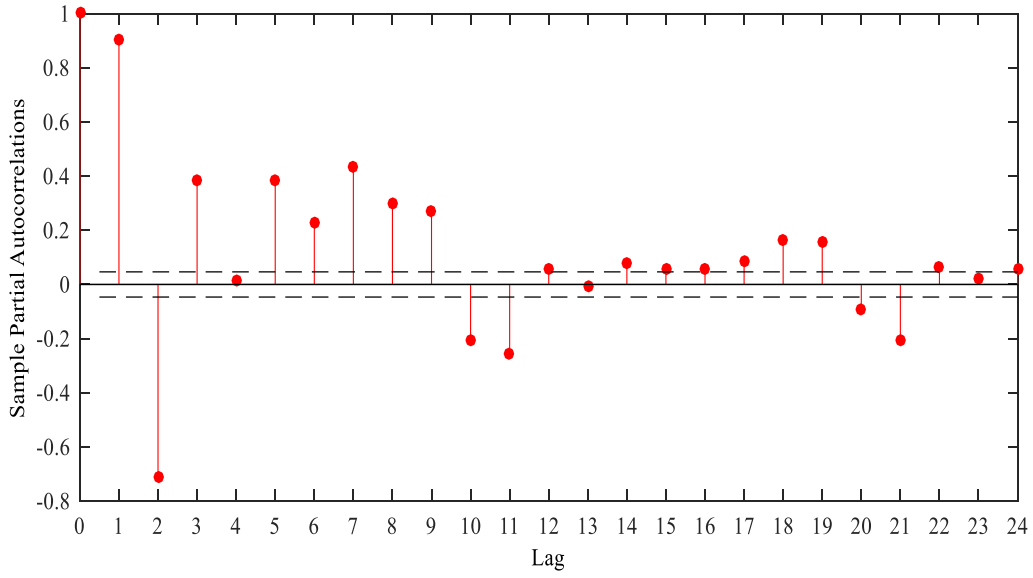

Figure 3.11: PACF plot of sample PV radiation data.

Fan plot for probabilistic normalized PV power with prediction intervals from 10% to 90%, in a step of 10% confidence interval is demonstrated in Fig. 3.12. This consideration reduces prediction error and hence accurately captures expected PV output.

The generated PV power scenarios are shown in Fig 3.13. In a similar manner of previous case study, 1000 PV power scenarios are generated in this study, for each hour of the forthcoming 24 hours. Thereafter, generated scenarios are reduced to ten representative scenarios, as shown in Fig. 3.14.

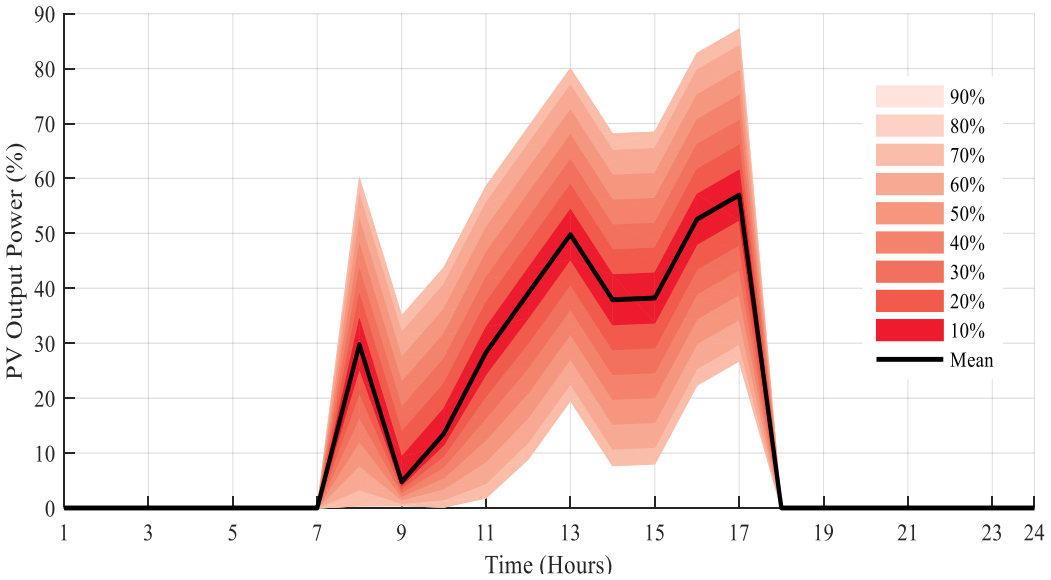

Fig. 3.12: Fan plot of probabilistic normalized PV power with different prediction interval with mean scenario (black solid line).

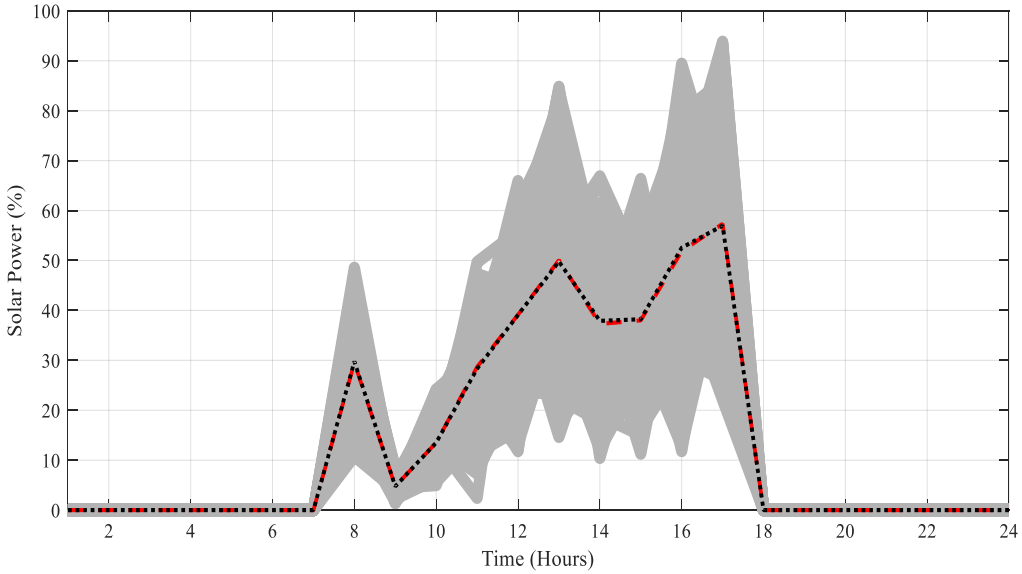

Fig. 3.13: PV power scenario generation (grey-solid), mean scenario (red-dash) and forecasted PV power (black-dotted).

It is found that both generated and reduced scenarios vary around their mean value within 95 % confidence interval. For scenario reduction, lowest and largest values of KD are set as zero and 200 MW, respectively. Table 3.2 shows the reduced PV power scenarios with corresponding probabilities and KDs for representative first hour. This reflects that Scenario 2 has the lowest KD and would be selected for elimination in next

iteration. Scenario 9 is closest to the selected scenario. The new probability of Scenario 8 would be the sum of its former probability and probability of Scenario 2.

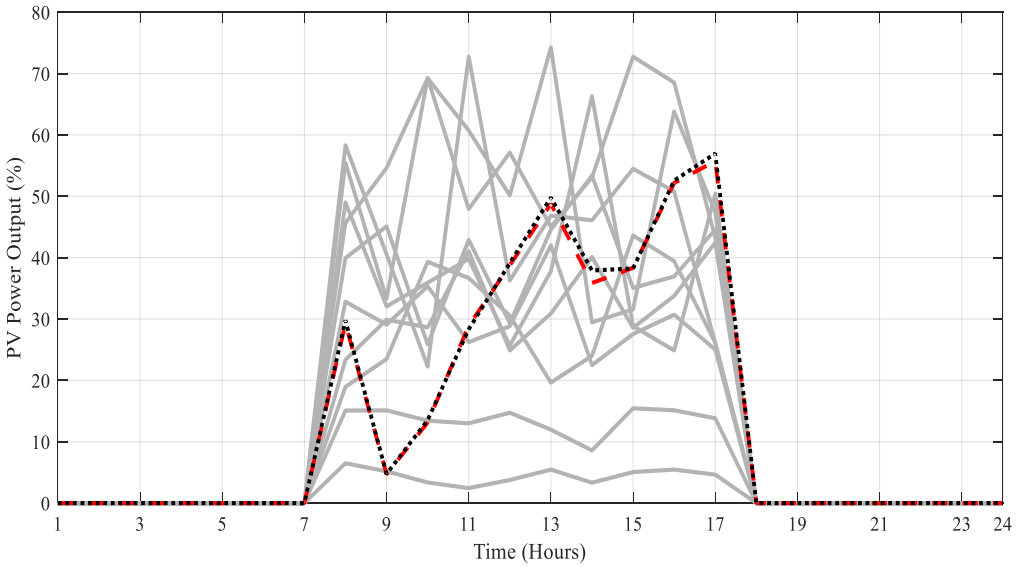

Fig. 3.14: Reduced 10 PV power scenarios (green-solid) along with mean scenario (red-dashed) and forecasted wind power (black-dot).

Table 3.2: Reduced PV Power Scenarios, Probabilities and KD of First Hour

Scenario Index	PV Power (kW)	Probability	KD
1	37.900	0.071	0.392301
2	**46.931**	**0.104**	**0.378336**
3	78.635	0.013	1.153745
4	73.352	0.087	1.35347
5	61.099	0.392	0.557562
6	39.280	0.024	1.831448
7	47.989	0.031	3.395021
8	87.220	0.053	0.221976
9	**78.851**	**0.028**	**0.374087**
10	52.276	0.197	0.973555

3.6.3 Case Study II: Wind & PV Power Interval Forecast

Figs. 3.15 & 3.16 shows the obtained upper and lower limits of wind & PV power prediction intervals with central forecast. Inter hour ramp variation of odd and even hours are shown by dotted lines in Fig. 3.15 and followed for PV ramping scenarios in similar manner.

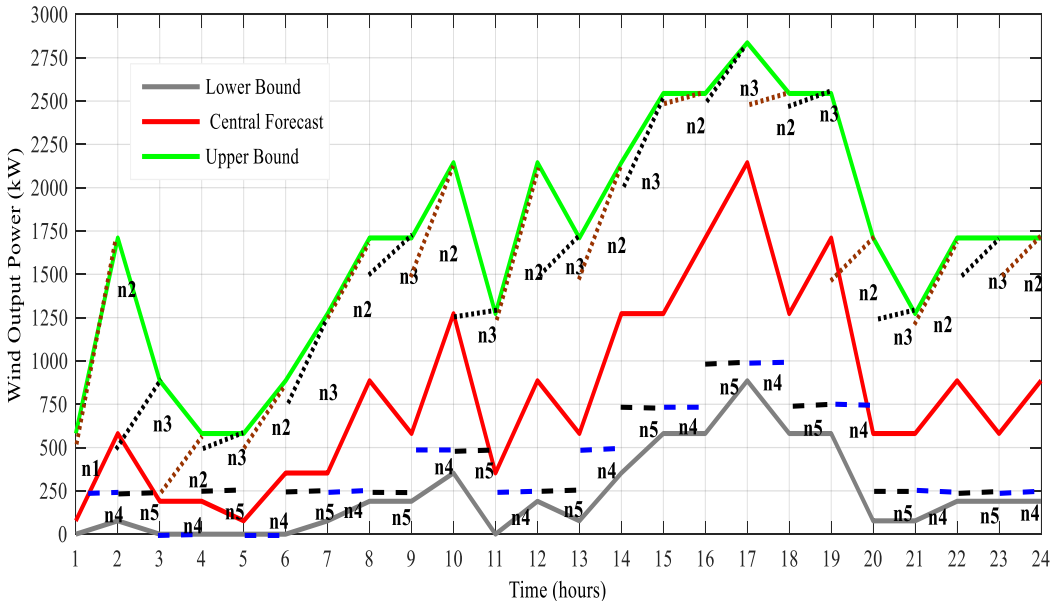

Fig. 3.15: Hourly wind power intervals: up ramp requirements (dotted line) and down ramp requirement (dashed lines).

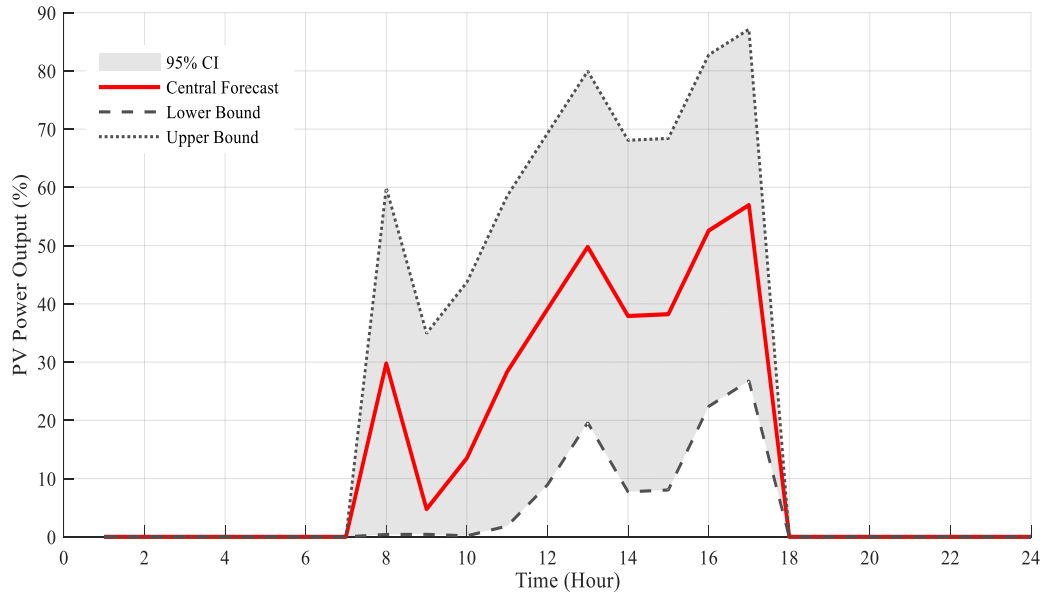

Fig. 3.16: PV power interval forecast with upper and lower bound and central forecast at 95% confidence interval.

Variation of power output is captured for each hour and used in calculation of net load calculation in generation scheduling problem in following chapters. This consideration characterizes the uncertain wind & PV power output pragmatically. Uncertainty characterization through this approach is represented in frequency response constrained

Modified Interval unit commitment (MIUC) approach for generation & PFR scheduling and optimal generation mix formulation in the following chapters.

Simulations are performed using the MATLAB platform [99], on a Windows® based DELL personal computer, with a 2.2-GHz processor and 8 GB RAM.

3.7 Conclusions

This chapter presents efficacious algorithms for uncertainty characterization through scenarios and modified interval forecast. The stochastic scenario generation algorithm is based on time series, while the reduction algorithm utilizes the concept of probability distance. Modified interval forecast algorithm is utilized to generate five artificial ramping scenarios for representation of wind & PV power uncertainty. Upper & lower bounds with central forecast scenario is predicted with 95% confidence interval. Both the algorithms are implemented for next-day wind & PV generation of wind farm & PV plant. The results clearly showcase the strength of proposed algorithms for wind & PV power uncertainty characterization with both the approaches. Owing to quantum scenario reduction, stochastic properties of generated scenarios are maintained, with a minimum variation in mean and standard deviation. In case of Modified Interval inter hour ramping scenarios are considered to accurately capture the wind/PV output.

Proposed algorithms are utilized for wind & PV power uncertainties characterization in the formulation of frequency response constrained Stochastic and Modified Interval unit commitment along with optimal generation mix formulation in following chapters.

Chapter – 4

FREQUENCY RESPONSE CONSTRAINED MODIFIED INTERVAL SCHEDULING UNDER WIND UNCERTAINTY

4.1 Introduction

Large penetration of asynchronous generation in evolving green power systems, particularly in the form of wind generation, would reduce power system's inertial and PFR capability [5],[7]. Reduced overall system inertia, along with network security constraints, could curtail and restrict the maximum instantaneous penetration of wind generation [100]. Maintaining system frequency within the prescribed limits and handling uncertainty associated with wind generation forecast requires large reserve capacity, which could increase operating costs [101]-[103]. Various computational techniques like deterministic, stochastic, interval optimization *etc.* have been proposed to obtain the cost-efficient combination of controllable generation units, which may effectively respond to penetration from intermittent wind generation, while maintaining minimal generation cost.

Deterministic UC is widely used to schedule the reserves, while demand is modelled by a single forecast, and the associated uncertainty is handled using ad-hoc reserve rules [53]. However, these formulations do not consider probabilistic modeling and cost benefits of maintaining reserves. SUC with MILP formulation can schedule operating reserves, while wind scenario generation techniques can be used to address the associated uncertainty [54], [55]. These techniques consider probabilistic modeling and reduce the expected operating cost, however obtaining SUC solution is computationally challenging as it considers a large number of scenarios [56]. Scenario reduction techniques are widely used to mitigate the computational burden [45]-[50]. However, an insufficient number of scenarios usually lead to a less accurate solution and increase the operating cost [57].

As PFR was inherently available with conventional generation. It's scheduling within UC received relatively little attention [20]. PFR requirement with large renewable penetration has increased, as non- synchronous generation sources are weak in providing PFR. PFR scheduling is particularly challenging as the deployment time frame does not possess the broad freedom of minutes to hours, as available in tertiary regulation. This is a rapid response following a contingency and has to be deployed in first 5-10 seconds [58].

Most markets do not have explicit provisions for incentivizing or mandating PFR. Markets world over are realizing this necessity, and are adopting it progressively. Presently, PFR scheduling practice in real time is available in Australian and New Zealand electricity market [58], [59]. PFR in day-ahead scheduling is considered in ERCOT and Nordic electricity markets [11], [21]. In the day-ahead market, PFR ancillary service schedules are usually a SCUC and in the real-time market, it is a single or multi-period SCED [60]-[62]. PFR control in real-time operations makes sense from the market perspective. However, from a system security perspective, it makes more sense to procure PFR in day-ahead for the worst case contingency.

PFR ancillary service market design incorporates reliability requirements of PFR and ensures incentives for synchronous inertia, PFR capacity, and responsive droop curves. This provides a stable and sustainable response by reduced insensitivity to frequency, triggering speed and full deployment of PFR [63].

Generators' frequency response is modeled as a constraint of MILP based UC model [20], [53], [60]-[65]. Stochastic generation scheduling has been enhanced to include frequency response constraints while considering wind uncertainty [65]. Despite that SUC formulation is cost-effective, the need to reduce computational burden can't be overlooked, considering operational time constraints.

In this context, this chapter contributes by:

(i) Proposes a novel, computationally fast MIUC formulation framework to include the system's fast frequency response constraints. The framework directly aims to contain initial transient frequency behavior within the prescribed system security criteria, following the largest infeed loss.

(ii) Performs PFR scheduling, required to make frequency stable at intermediate state, following the largest infeed loss.

(iii) Characterizes wind generation uncertainty pragmatically in the proposed MIUC and SUC problem using ARIMA model, through rigorous scenario analysis.

(iv) Demonstrates the efficacy of proposed MIUC model through the systematic comparative assessment with SUC, for their PFR scheduling performance; the impact of variation of frequency response parameters on operation cost and wind curtailment; and for computational and cost performance with varying wind penetration.

Computationally fast solutions obtained through the proposed MIUC model, within acceptable time intervals, can strongly benefit system operations with the fast frequency response in future low carbon power system.

4.2 Problem Formulation

This section characterizes MIUC and SUC formulation with frequency response constraints and wind uncertainty. The IUC formulation has been modified to include inertial and PFR constraints requirements.

4.2.1 MIUC Formulation

IUC is a robust technique, which requires less computational effort than SUC. In IUC, uncertainty is modeled with three non-probabilistic scenarios (*i.e.* central forecast, upper bound & lower bound). Hence, it requires less computational time but produces conservative and thus expensive generation schedules [18], [19], [52]. This is because of the constraints imposed on the feasibility of transitions, from lower to upper bound of wind power interval, and vice versa, between any two consecutive time periods. Such extreme transitions have a low probability and could be replaced by less severe ramp constraints [19].

IUC model is modified to incorporate fast frequency response constraints that directly aim to contain the initial transient frequency behavior, within the prescribed system security criteria. Advantages of IUC and SUC models are incorporated in MIUC to improve day-ahead UC and PFR schedules. In MIUC, wind uncertainty is characterized by ramping scenarios, constructed within forecasted upper and lower bound. Inter-hour ramp requirements of constructed scenarios are based on net load. Hence, it accurately captures the expected wind output.

MIUC is mathematically modelled as MILP constraints. The objective function is formulated to minimize the expected operating cost of the forecasted wind generation, *i.e.* the central forecast scenario $n1$. The objective function includes the cost of start-up, running and no-load of each generating unit, along with the lost load cost.

$$\min \sum_{t\in T}\sum_{i\in I}(S_{i,t} + Nl_i.\chi_{i,t} + LS_t.VOLL + \sum_{b\in B} Cs_{i,b}.G_{i,b,t,n1}) \tag{4.1}$$

Operational constraints of the objective function are:

1) Generator Start Up/Shut Down Status:

Constraint (4.2) sets the generating unit startup or shutdown status $t-1$ and t. Constraint (4.3) restricts the generating unit to start up and shut down within the same time interval.

$$\chi_{i,t}^{up} - \chi_{i,t}^{dn} = \chi_{i,t} - \chi_{i,t-1}, \quad \forall t \in T, i \in I \tag{4.2}$$

$$\chi_{i,t}^{up} + \chi_{i,t}^{dn} \leq 1, \quad \forall t \in T, i \in I \tag{4.3}$$

2) Minimum Up/Down Times:

Constraint (4.4) sets the on/off status based on the initial generator status. t_0 equals 0 if the first $TI_i^{mu} + TI_i^{md}$ hours is 0. Constraints (4.5) and (4.6) provide minimum up and down time for the remaining time intervals.

$$\chi_{i,t} = \chi_{i,t_0}, \quad \forall t \in [0, TI_i^{mu} + TI_i^{md}], i \in I \tag{4.4}$$

$$\sum_{t-TR_i^{mu}+1} \chi_i^{up} \leq \chi_{i,t}, \quad \forall t \in [TI_i^{mu}, T], i \in I \tag{4.5}$$

$$\sum_{t-TR_i^{md}+1} \chi_i^{dn} \leq 1 - \chi_{i,t}, \quad \forall t \in [TI_i^{md}, T], i \in I \tag{4.6}$$

3) Generator Start-Up Cost:

The start-up cost of each generating unit depends on the service time interval. Constraint (4.7) determines the exact points of the start-up curve at which the generator has not been in service. One element j of $Su_{i,t,j}$ is given value 1 if $\chi_{i,t}^{up} = 1$, ensured by constraint (4.8). An accurate value of start-up cost is assigned by constraint (4.9).

$$Su_{i,t,j} \leq \sum_{TO_{i,j}^{lo}}^{TO_{i,j}^{up}} \chi_{i,t}^{dn}, \quad \forall t \in T, i \in I, j \in J \tag{4.7}$$

$$\sum_{j \in J} Su_{i,t,j} = \chi_i^{up}, \quad \forall t \in T, i \in I \tag{4.8}$$

$$S_{i,t} = \sum_{j \in J} Suc_{i,j} . Su_{i,t,j}, \quad \forall t \in T, i \in I \tag{4.9}$$

4) Generator Constraints:

The power output of individual generators is taken as the addition of the output from each segment of its cost curve, as defined by Eqn. (4.10). Generating unit output limits are mentioned in (4.11). Constraints (4.12)-(4.16) set the generator ramping constraints for MIUC. Wind uncertainty is characterized by ramping scenarios, termed as

$n1, n2, n3, n4 \& n5$. Here, $n1$ denotes central forecast scenario. Up ramp limits between odd and even hours is considered as Scenario $n2$. Scenario $n3$ is up ramp limits between even and odd hours. Scenario $n4$ shows down ramp limits between odd and even hours, and Scenario $n5$ is down ramp limits between even and odd hours. Constraint (4.12) sets the upper and lower ramp bounds for the central forecast scenario $n1$.

$$G_{i,t,n} = \sum_{b \in B} G_{i,b,t,n}, \quad \forall t \in T, i \in I, n \in N \tag{4.10}$$

$$G_i^{\min} . \chi_{i,t} \le G_{i,t,n} \le G_i^{\max} . \chi_{i,t}, \quad \forall t \in T, i \in I, n \in N \tag{4.11}$$

$$-R_i^{dn} \le G_{i,t,n1} - G_{i,t-1,n1} \le R_i^{up}, \quad \forall t \in T, i \in I \tag{4.12}$$

Constraint (4.13) sets the ramp up limit for scenario $n2$, which is only between alternate hours. Constraint (4.14) sets up ramp bounds for $n3$. Modulo function is used to implement these conditions, which assign 0 for even time periods and 1 for odd time periods. In the same manner, constraints (4.15) and (4.16) set the lower ramp bounds for scenario $n4$ and $n5$, between alternate hours.

$$G_{i,t,n2} - G_{i,t-1,n2} \le R_i^{up}, \forall t \in T \,|\, t \equiv 0, i \in I \tag{4.13}$$

$$G_{i,t,n3} - G_{i,t-1,n3} \le R_i^{up}, \forall t \in T \,|\, t \equiv 1, i \in I \tag{4.14}$$

$$-R_i^{dn} \le G_{i,t,n4} - G_{i,t-1,n4}, \forall t \in T \,|\, t \equiv 0, i \in I \tag{4.15}$$

$$-R_i^{up} \le G_{i,t,n5} - G_{i,t-1,n5}, \forall t \in T \,|\, t \equiv 1, i \in I \tag{4.16}$$

5) Transmission Constraints:

Power balance equation at each node is given by Eqn. (4.17). Eqn. (4.18) defines limits of wind power loss at each wind generator.

$$\sum_{i \in s} G_{i,t,n} + \sum_{w \in s} (W_{w,t,n} - W_{w,t,n}^{curt}) - \sum_{\{s,m\} \in L} B_{sm}(\theta_{s,t,n}) = LN_{t,s}, \forall t \in T, s \in S, n \in N \tag{4.17}$$

$$0 \le W_{w,t,n}^{curt} \le W_{w,t,n}, \forall t \in T, w \in W, n \in N \tag{4.18}$$

If the line flow limits mentioned in Eqn. (4.19) could not be a specific value of wind power available at the wind farm w, the wind power is curtailed by $Cu_{t,w,n}$. Voltage angle limits are set by Eqn. (4.20), which is set to 0 for reference bus in (4.21).

$$-L_{sm} \le B_{sm}(\theta_{m,t,\mathrm{n}} - \theta_{s,t,n}) \le L_{sm}, \forall t \in T, \{s,m\} \in L, n \in N \quad (4.19)$$

$$-\pi \le \theta_{s,t,n} \le \pi, \forall t \in T, s \in S \setminus s_{ref}, n \in N \quad (4.20)$$

$$\theta_{s_{ref},t} = 0, \forall t \in T \quad (4.21)$$

4.2.2 SUC Formulation

SUC objective aims to minimize the operating cost. It considers the cost of each scenario, with its existence probability:

$$\min \sum_{t\in T}\sum_{i\in I}(Nl_i.\chi_{i,t} + S_{i,t} + LS_t.VOLL + \sum_{n\in N}\pi_n \sum_{b\in B} Cs_{i,b}.G_{i,b,t,n}) \quad (4.22)$$

Here, SUC is a two-stage optimization problem. First, here-and-now decisions are made on the on/off status of generators. Wait-and-see decisions are made after the dispatch of each generator committed at the first stage, for all scenarios. n scenarios are considered for SUC ramp constraint (4.23). Scenario generation and reduction technique (discussed in Chapter 3) is used to obtain these scenarios. Hence, SUC ramping scenarios represent actual scenarios and are different from the ramping scenarios used in MIUC formulation. Other constraints are similar to MIUC constraints.

$$-R_i^{dn} \le G_{i,t,n} - G_{i,t-1,n} \le R_i^{up}, \quad \forall t \in T, i \in I \quad (4.23)$$

4.2.3 Modeling of Frequency Response Constraints

Frequency response constraints model the control of initial frequency deviation within the prescribed limit, following maximum infeed loss. Constraint (4.24) ensures that enough inertial response should be available so that the maximum ROCOF does not trigger protective relays like UFLS relay or cause instability. Constraint (4.25) ensures PFR adequacy.

$$\sum_{i\in I}\left\{x_{i,t} * H_i * G_i^{\max}\right\} + H^{eqload} * LN_{t,s} \ge H^{req} - R_t^{ins} \quad \forall t \in T \quad (4.24)$$

$$\sum_{i\in I} P_{i,t} \ge P^C - LD * T^{de} * \frac{\Delta f^{\max}}{f_0} - R_t^{ins}, \quad \forall t \in T \quad (4.25)$$

Constraints (4.26)-(4.32) deal with the droop setting and governor enabling for PFR. Constraint (4.26) generates the equivalent droop curve, represented as Hz/MW. Eqn.

(4.27) ensures that adequate PFR is available during large frequency variations. Eqns. (4.28) and (4.29) ensure that adequate headroom is available with enabling of the governor, for providing PFR and maintaining droop curve relationship. Constraint (4.30) requires the generator to be online when its governor is enabled.

$$D_i^e = \frac{D_i * f_0}{G_i^{\max}}, \qquad \forall i \in I \tag{4.26}$$

$$P_{i,t} \le \frac{\delta_{i,t}}{D_i^e}(\Delta f^{\max} - G_i^{db}), \quad \forall i \in I, \forall t \in T \tag{4.27}$$

$$\frac{1}{D_i^e}(\Delta f^{\max} - G_i^{db}) \ge G_i^{\max} * \delta_{i,t} - G_i^{\max} * \Upsilon_{i,t}, \forall t \in T \tag{4.28}$$

$$P_{i,t} \ge \frac{\Upsilon_{i,t}}{D_i^e}(\Delta f^{\max} - G_i^{db}) - G_i^{\max}(1-\delta_{i,t}), \forall i \in I, \forall t \in T \tag{4.29}$$

$$\delta_{i,t} \le \chi_{i,t} \; \forall i \in I, \forall t \in T \tag{4.30}$$

Constraint (4.31) sets δ equal to 0, for generators, which are working in a mode that cannot provide PFR (*e.g.* generators with blocked or no governor mode, sliding pressure mode), while constraint (4.32) also sets δ equal to 0 for the generators having large governor deadband.

$$\delta_{i,t} = 0 \quad \forall i \in G_{ng}, \quad \forall t \in T \tag{4.31}$$

$$G_i^{db} \le G_i^{db\max} + f_0(1-\delta_{i,t}), \forall i \in I, \forall t \in T \tag{4.32}$$

Eqns. (4.33) - (4.36) ensure frequency behavior during large unit outages follow the security criteria of frequency nadir and steady-state frequency, as mentioned in Section II.

$$\begin{aligned} \left|\Delta f^{nadir}\right| &= \Delta f^{db} + \frac{\Delta P - (LD * LN_{t,s}) * \Delta f^{db}}{LD * LN_{t,s}} \\ &+ \frac{2P_{i,t} * H_i}{T^{de} * (LD * LN_{t,s})^2} \log\left(\frac{2P_{i,t} * H_i}{LN_t * (LD * LN_{t,s}) + 2P_{i,t} * H_i}\right) \le \Delta f^{\max} \end{aligned} \tag{4.33}$$

In Eqn. (4.33), frequency nadir depends on the inertial and PFR response. The value of frequency nadir Δf^{nadir} should not exceed $\Delta f^{\max}$ and should satisfy sufficient conditions [65]. Eqn. (4.34) determines the frequency value at point B (Fig.1) which depends on the PFR delivered at Δt_2 and should be less than Δf^{nadir}. At this level, it is assumed that ROCOF is zero, which means that frequency has attained some steady-state value.

$$\Delta f^{ss} = \frac{\Delta P - P_{i,t}}{LD * LN_{t,s}} \leq \Delta f^{nadir} \tag{4.34}$$

Eqns. (4.35) and (4.36) assess the PFR requirements and ensure that adequate PFR is available at t^{nadir} and t^{ss}.

$$\sum_{i \in I} P_{i,t}^{ss} \geq P_{i,t} - P^{Css} \quad \forall \ i \in I, t \in T \tag{4.35}$$

$$\sum_{i \in I} P_{i,t}^{nadir} \geq P_{i,t} - P^{Cnad} \quad \forall t \in T \tag{4.36}$$

The Flow chart of the proposed formulation is shown in Fig. 4.1. It demonstrates the relation between both the proposed model.

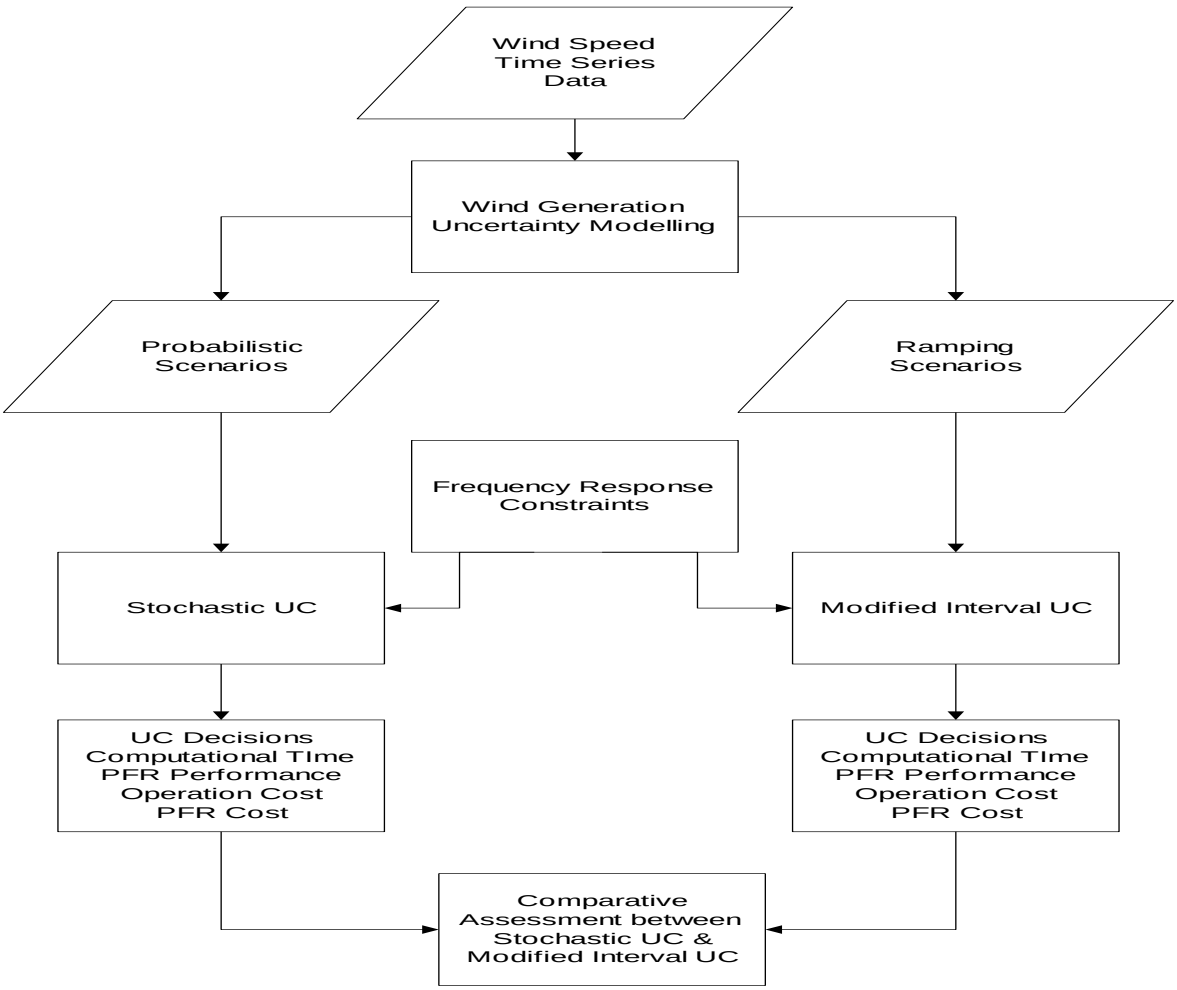

Fig. 4.1: Flow chart of simulation procedure

4.2.4 Wind Generation Uncertainty Characterization

Variable nature of wind power can be modeled using the ARIMA model. Wind power variation with weather conditions leads to non-stationary time series data. ARIMA model

works on stationary time series data. Hence, wind power is initially transformed into a stationary time series by data differentiation. Here, ARIMA model forecasts the upper and lower limit of wind power to construct ramping scenarios for MIUC model and to generate wind power scenarios for SUC model. Detailed formulation of uncertainty modelling is discussed in Chapter 3.

4.3 Case Study

One area IEEE reliability test system, a sub-system of large synchronous interconnection is used to implement the frequency response constrained improved interval and stochastic scheduling problem [104]. There are 24 buses, 17 load buses, 38 transmission lines and 32 generators in the system. The generation mix includes eleven oil/steam turbine units, nine coal/steam turbine units, six hydro turbine units, four oil/combustion units, and two nuclear units. The total installed capacity of generators in one area is 3405 MW and peak load is 2850 MW. The data is modified to accommodate nine wind farms with a generation capacity of 1020 MW (30% penetration). Wind farm locations are mapped respecting the transmission lines lengths. Wind units consist of VESTAS V90 turbines, the details of which are available at the manufacturer database [98]. Wind speed historical time series data for the duration 01.01.2010 to 31.12.2010 is used, online available from Illinois Institute of Rural Affair, USA [88].

Table 4.1: Generator Frequency Response Parameters

Unit	$G_i^{\max}$ **(MW)**	H_i **(s)**	D_i **(p.u.)**	G_i^{db} **(mHz)**
U12	12	2.6	0.05	15
U20	20	2.8	0.05	15
U50	50	3.5	0.05	15
U76	76	3.0	0.05	15
U100	100	2.8	0.05	15
U155	155	3.0	0.05	15
U197	197	2.8	0.05	15
U350	350	3.0	0.05	15
U400	400	5.0	0.05	15

Generator characteristics like unit startup costs, heat rates, ramping rates, maximum and minimum capacities, minimum up and minimum down times, transmission data and

dynamic system parameters are provided in [104]. Fuel cost is obtained from [105]. Frequency response characteristics of each generation unit are mentioned in Table 4.1.

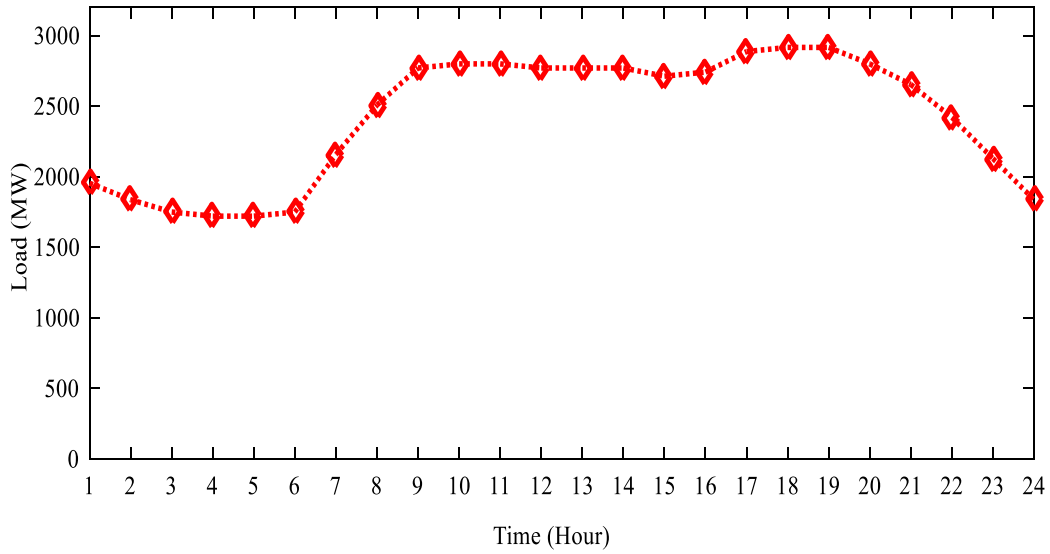

Fig. 4.2: Load profile of peak load day [104].

This characterization represents different generation types, thus avoiding the need to adopt a separate model for different generation types. The load profile for peak load day from Week 51 is shown in Fig. 4.2. Value of inertia constant is attained from [104], nominal frequency (f_0 =50 Hz), governor droop (D_i = 5%), frequency dead band (G^{db} =15 mHz), load damping rate (LD =1%/Hz) and delivery time (T^{de} =10 s) are chosen according to National Grid standards [106]. ROCOF of 0.5Hz/s is considered [31]. The largest generators in the system are two nuclear units of 400 MW, and a loss of supply of one of this unit is considered. Δf^{ss} and t^{ss} should not be more than 49.5 Hz and 60 s respectively. System PFR capacity should limit $\Delta f^{\max}$ above the minimum value of 49.2 Hz [106]. The maximum P^C requirement is assumed to be 30% of the total responsive capacity and $G^{db\max}$ for all governors should at least be greater than 100 mHz. *VOLL* is assumed to be 10000 $/MW-h.

4.3.1 Wind Generation Uncertainty Modeling

Wind power uncertainty would impact the generation scheduling decisions. Hence, it is important to characterize and represent wind power uncertainty for accurate generation scheduling decisions. In this work, wind uncertainty is modeled through scenarios and

modified interval forecast. Algorithms for both the approaches used in wind power uncertainty modeling is provided in Chapter 3.

Table 4.2: Generator PFR Scheduling Performance

Unit	$P_{i,t}$ **(MW)**			
	$P_{i,t}^{nad}$ (MW) at (Δf^{nadir} = 0.6 Hz)		$P_{i,t}^{ss}$ (MW) at (Δf^{ss} = 0.4Hz)	
	SUC	MIUC	SUC	MIUC
U12	3.2	3.0	2.3	2.1
U20	5.4	5.2	2.8	2.3
U50	0	0	6.58	5.48
U76	20.3	19.8	10.6	9.8
U100	27.72	26.18	14.78	14.21
U155	0	0	21.88	20.68
U197	55.28	54.67	27.14	26.54
U350	19.45	18.34	50.08	49.21

4.3.2 Frequency Response Performance

This section details the performance of frequency response parameter, considering large generation outage. The response provided by each unit when frequency reaches nadir and intermediate steady state point is shown in Table 4.2. It may be observed that both the formulations provide a similar level of PFR. However, flexible generators like U197 provides a better response at Δf^{nadir}, and U350 provides a better response at Δf^{ss}.

Table 4.3: Impact of Frequency Response Parameter Variation

Frequency response parameter	**Variation range**	**Impact on operation cost**		**Impact on wind curtailment**	
		SUC	**MIUC**	**SUC**	**MIUC**
ROCOF Setting (Hz/s)	0.5 - 0.2	20% (↑)	22% (↑)	25% (↑)	26% (↑)
PFR Delivery Time (s)	10 - 03	05% (↓)	04% (↓)	49% (↓)	48% (↓)
Load Damping Rate (1%/Hz)	1-0	06% (↑)	07% (↑)	08% (↑)	09% (↑)

Better PFR from these units leads to a reduction in spinning reserves requirement and possible integration of more wind generation, which in turn reduces the total operation

cost, as shown in Table 4.3. PFR schedules expected in day-ahead may differ with real-time inertia conditions and would require real-time dispatch.

4.4 Impact of frequency response parameter variation

This section explores the impact evaluation of variation in frequency response related parameters, like ROCOF protection setting, PFR delivery time, and load damping rate, on the operation cost and wind curtailment in both the formulations. Hence, the impact of variations is highlighted as the maximum possible increase or decrease in operation cost and wind curtailment. Table 4.3 summarizes the results of parameter variation.

4.4.1 ROCOF Setting Variation:

Impact analysis of ROCOF setting helps to understand the required setting for including non- synchronous generation. The ROCOF setting depends on the available system inertia and increasing this setting would lead to RES disconnection. The ROCOF setting at 0.2 Hz/s would result in high operation cost (about 20% with SUC and 22% with MIUC) and increased wind curtailment (about 25% with SUC and 26% with MIUC). There is no significant increase in the operation cost with the setting variation from 0.4 Hz/s to 0.5 Hz/s, and wind curtailment is also less than 10% with both the formulations.

4.4.2 PFR Delivery Time Variation:

PFR is delivered by the governor at the time of contingent condition within few seconds. T^{de} =10s is considered here. It is assumed that the governor is enabled for all the generators and all the generators have similar response capability. PFR delivery time is varied from 10s to 3s. The results show that as the delivery time is reduced, operation cost reduces (by up to 5% with SUC and 4% with MIUC) and there is a significant reduction in wind curtailment (up to 49% with SUC and 48% with MIUC). When the delivery time is between 5s-3s, there is no significant reduction in operational cost and wind curtailment. This happens because additional power required to arrest the frequency deviation would be limited by the intermediate steady-state frequency requirement.

4.4.3 Load Damping Rate Variation:

Reduction in load damping rate from 1%/Hz to 0%/Hz would increase the operation cost (by up to 6% with SUC and 7% with MIUC) and wind curtailment (by up to 8% with SUC

and 9% with MIUC). Enhanced use of power converter interfaced generation would decline the damping effect but may increase the operation cost and reduce the ability to integrate more wind generation, if not considered in the UC.

4.4.4 Cost Performance with Varying Wind Penetration:

This section presents comparative cost analysis with increasing wind penetration level and consideration of PFR constraints, in both SUC and MIUC formulation. PFR constraints consideration reduces the average number of units committed online per hour. PFR constraints add only about 0.22% in total operation cost, which is not substantially higher than the considered duality gap of MILP solver (0.1%). This is because of the committed inertial and PFR response of the system. Here, the synchronous inertial cost is assumed zero for all hours, as the system has sufficient committed inertial and PFR response.

In both the formulations, wind uncertainty impact on system inertia is directly considered. Such consideration allows the peak load plants to provide required frequency response for the low probability scenarios but very high response requirements. This, in turn, reduces the total spinning headroom, and therefore permits higher penetration of wind generation and reduces the overall operation cost.

Table 4.4: Cost Comparison with Varying Wind Penetration

Wind Penetration (%) →	**10%**		**20%**		**30%**	
Modeling Techniques →	SUC	MIUC	SUC	MIUC	SUC	MIUC
Operation Cost $*10^6$($)	0.988	0.998	0.966	0.978	0.916	0.927
Total PFR Payments ($)	1696	1709	2350	2362	2502	2518
Standard Deviation $*10^3$ ($)	0.398	0.288	2.556	2.438	4.308	3.961

Table 4.4 compares the cost performance of both the scenarios with varying wind penetration. For 10% penetration, the cost difference is less, SUC operating cost and PFR payment is about 0.5 % less than the MIUC formulation (Figs. 4.3 & 4.4). However, standard deviation (SD) is the same in both the cases as 0.078%. For 20% and 30% penetration, cost difference increases by less than 2% and may increase with increased penetration, as shown in Fig. 4.2. However, the overall cost reduces with increasing wind penetration. SD is 0.17% for the two cases at 20% and 30% penetration, it is 0.29% for

SUC and 0.27% for MIUC. SD calculations are useful to validate uncertainty characterization of day-ahead scheduling.

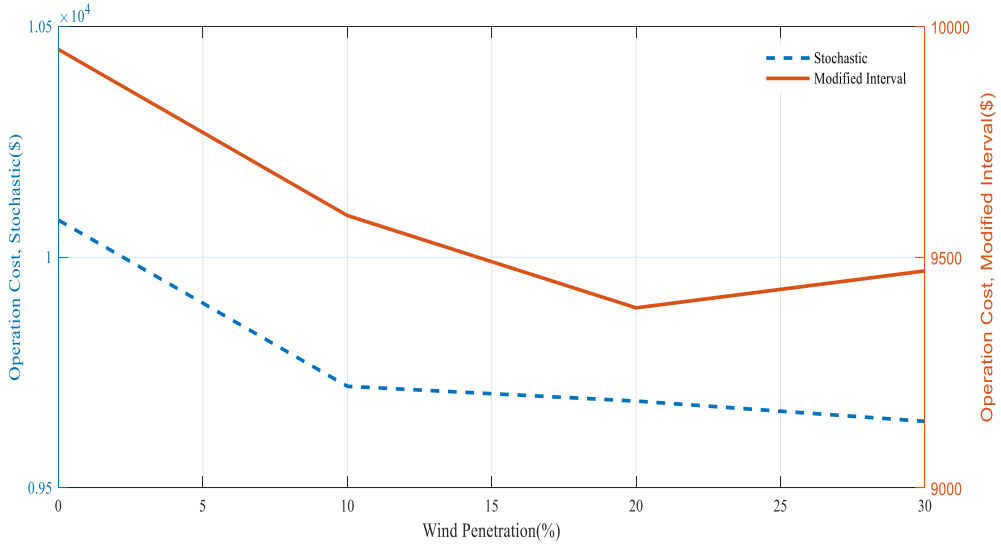

Fig. 4.3: Operation cost with increasing wind penetration level.

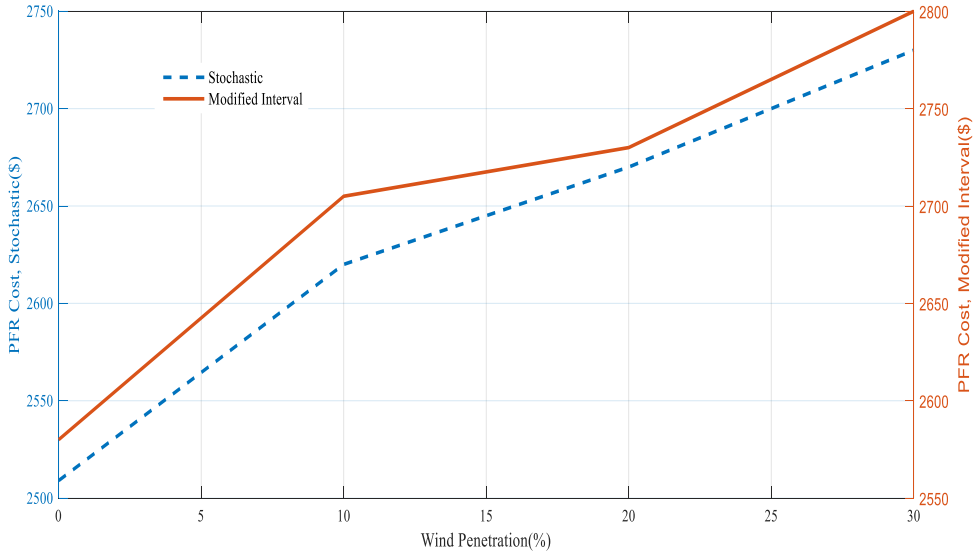

Fig. 4.4: PFR payments with increasing wind penetration level.

4.4.5 Computational Performance

Simulation work is carried out on GAMS 24.2.3 using CPLEX solver with 0.1% duality gap on Intel Core i5 2.20 GHz processor. MIUC and SUC with PFR constraints, on an average, took 1.5 times simulation time than the basic scheduling formulation. However,

for MIUC, computation time is reduced by around 50% in both cases, *i.e.* SUC with and without PFR constraints, as shown in Table 4.5.

Table 4.5 Comparison of MIUC and SUC on the Basis of Time Elapsed

Scheduling Model	**Time Elapsed (Seconds)**
SUC without PFR	680
SUC with PFR	819
MIUC without PFR	324
MIUC with PFR	403

4.5 Conclusions

This chapter presents computationally efficient MIUC model incorporating frequency response and transmission network constraints, while considering wind uncertainty at different penetration levels. Case studies are performed to compare the proposed method with efficient SUC model. Numerical results show that the SUC model with frequency response constraints is an economical and effective way to handle wind uncertainty, as compared to MIUC. However, there is marginal cost difference with similar PFR performance. Moreover, comparison of computational time for the two models reveal that MIUC formulation offers ultra –fast solutions, as it takes less than half the computational time as compared to SUC and has the potential to provide fast solutions to processes, like frequency response constrained dispatch and market clearing in low carbon systems. MIUC based market clearing and dispatch formulation could be used to co-optimize energy, PFR, and inertia. Minimum frequency value and ROCOF could be the control variables for dispatch. Low-carbon systems could be optimally dispatched, by appropriate uncertainty and variability modelling in accordance with frequency control criteria.

Chapter – 5

PREDICTION OF SYSTEM INERTIA CONDITION FOR PRIMARY FREQUENCY RESPONSE ADEQUACY

5.1 Introduction

System inertia is a key power system characteristic which provide instant support to the frequency, following generation-load imbalance or contingencies like large infeed loss [66]. With strong policy targets to achieve high renewable penetration, wind generation is likely to be major contributors to total grid generation capacity. There is a limited understanding of system behaviour to provide inertia & PFR with high wind penetration. An understanding of these requirements during such contingencies would provide knowledge about permissible wind penetration that grids could withstand, following network regulations.

As a non-synchronous generation, like wind and PV, starts to displace conventional generation, the system's inherent ability to resist transient changes in frequency decreases [1], [5]-[7]. Reduced system inertia would make system frequency prone to changes in supply and demand. This would lead to quick frequency deviations, following the loss of generation and/or load. Large PFR capacity is required to stabilize the system and prevent large frequency variations [2], [65].

PFR service this rapid has been defined in few restructured power markets, like Australian National Electricity Market and New Zealand [58]. In view of future low inertia conditions arising due to high renewable penetration, some markets are considering even faster PFR market products. ERCOT has proposed a fast frequency response service expected to provide a rapid response within 0.5 seconds, to be sustained for at least 10 minutes [58], [62]. However, scheduling a unit to provide such a quick response, would gratuitously increase the overall cost of maintaining frequency stable.

Inertia estimation methods may require knowledge of the frequency and electrical power of every system generator, which is scantly available [69]. Inertia estimation using simultaneous assessment of disturbance time and inertia uses frequency and active power measurement from a single location and is applicable for small systems only [70]. Theoretically, least square approximation-based frequency disturbances estimation could be used to calculate system inertia [71].

System inertia calculation for Western Interconnection in North America is presented based on the measured frequency during disturbances [72]. However, its performance assessment is difficult, as it is not tested in a simulation environment. Great Britain system's inertia is evaluated based on aggregated estimates at the regional level using phasor measurement unit data [73]. An online inertia estimation tool prototype for ERCOT analyses the performance between generation outage events and maximum instant frequency deviation [5], [21], [67].

Currently, SOs hardly assess system inertia impact to calculate future PFR requirement, which is planned/procured for an expected worst-case contingency [21]. Accurate system inertia estimation is essential considering grid's frequency security, but the prediction of system inertia is always a concern for the SO. It is required to handle unforeseen contingencies, *viz.* large infeed loss or loss of load, estimation of PFR requirement, UC decision making, and system frequency stability. As system inertia condition varies over a day's time, fixed PFR estimation based on worst-case scenario is not efficient [21], [68]. Hence, it is imperative to predict system inertia for upcoming hours, considering the current operation status of all generators. Using this information, expected system inertia could be calculated for each hour. This could provide the prediction of future system inertia condition and thus, required PFR can be estimated.

In the above context, the key contribution of this chapter is to:

(i) Propose a novel framework for day-ahead prediction of system inertia condition and PFR in stochastic generation scheduling framework mapped with frequency security criteria like ROCOF, Frequency nadir, and quasi-steady-state frequency.

(ii) Provide information of maximum wind penetration that a system could withstand, without violating network regulation of ROCOF and frequency nadir.

(iii) Investigate the impact of variation in frequency security parameters on operation cost and wind curtailment, to obtain suitable ROCOF setting for minimum wind curtailment.

5.2 Problem Formulation

This section provides detailed formulation of the stochastic scheduling model enhanced to incorporate frequency response constraints [109]. In the proposed formulation, demand & uncertain wind generation is forecasted and based on that net load is estimated. In this work, wind generation uncertainty is modelled using scenario generation & reduction approach.

5.2.1 Stochastic Scheduling Model

The aim of objective function is to minimize operation cost of all generating units, over the optimization time horizon, while serving forecasted demand. To forecast 24-hour demand, Grey system theory based model is used, as this model provides sufficient accuracy and requires minimal training data, due to its momentum transfer behavior [110]. This model considers cost of each reduced scenario in proportion to its probability π_n. The objective function includes start-up cost, no-load cost and operating cost of all the generators, as shown by Eqn.

$$\sum_{n\in N} \pi_n \left(\sum_{t\in T}\sum_{i\in I} (Nl_i * \chi_{i,t} + S_{i,t} + \sum_{b\in B} Cs_{i,b}.G_{b,i,t})\right) \tag{5.1}$$

The optimization problem is subject to following operational constraints:

1) Power Balance Constraints

In (5.2), the power balance equation is given as total generation output equal to LN_t. Eqn. (5.3) calculates net load, which is a difference of forecasted load and available wind capacity. W^{curt} denotes the curtailment in wind capacity. Eqn. (5.4) provides wind curtailment limits.

$$\sum_{i\in I} G_{i,t} = LN_t \quad \forall t \in T \tag{5.2}$$

$$LN_t = LF_t - \sum_{t,w} (W_{t,w}^{av} - W_{t,w}^{curt}) \tag{5.3}$$

$$0 \le W_{t,w}^{curt} \le W_{t,w}^{av} \quad \forall t \in T, w \in W \tag{5.4}$$

2) Generator Start Up/Shut Down Status

Constraint (5.5) determines the generator startup or shutdown status at the time t, based on its 0/1 status between hours t–1 and t. Constraint (5.6) restricts the generator to start up and shut down within the same time interval.

$$\chi_{i,t}^{up} - \chi_{i,t}^{dn} = \chi_{i,t} - \chi_{i,t-1}, \quad \forall t \in T, i \in I \tag{5.5}$$

$$\chi_{i,t}^{up} + \chi_{i,t}^{dn} \le 1, \quad \forall t \in T, i \in I \tag{5.6}$$

3) Minimum Up/Down Times

Constraint (5.7) sets the on/off status based on initial generator status. t_0 equals 0 if the first $TI_i^{mu} + TI_i^{md}$ hours is 0. Constraints (5.8) and (5.9) give minimum up and down time for the remaining time intervals respectively.

$$\chi_{i,t} = \chi_{i,t_0}, \quad \forall t \in [0, TI_i^{mu} + TI_i^{md}], i \in I \tag{5.7}$$

$$\sum_{t-TR_i^{mu}+1} \chi_i^{up} \le \chi_{i,t}, \quad \forall t \in [TI_i^{mu}, T], i \in I \tag{5.8}$$

$$\sum_{t-TR_i^{md}+1} \chi_i^{dn} \le 1 - \chi_{i,t}, \quad \forall t \in [TI_i^{md}, T], i \in I \tag{5.9}$$

4) Generator Start-Up Cost

The start-up cost of each generator depends on the service hours. Constraint (5.10) finds the start-up curve points at which the generator is off. An element j of $Su_{i,t,j}$ has value 1 if $\chi_{i,t}^{up} = 1$, ensured by Constraint (5.11). The exact value of start-up cost is assigned by Constraint (5.12).

$$Su_{i,t,j} \le \sum_{TO_{i,j}^{lo}}^{TO_{i,j}^{up}} \chi_{i,t}^{dn}, \quad \forall t \in T, i \in I, j \in J \tag{5.10}$$

$$\sum_{j \in J} Su_{i,t,j} = \chi_i^{up}, \quad \forall t \in T, i \in I \tag{5.11}$$

$$S_{i,t} = \sum_{j \in J} Suc_{i,j} . Su_{i,t,j}, \quad \forall t \in T, i \in I \tag{5.12}$$

5) Generator Constraints

The power output of individual generators is the sum of output on each part of its cost curve indexed by b, as defined by Eqn. (5.13). Minimum and maximum generator output limits are mentioned in Eqn. (5.14). Eqn. (5.15) sets the hourly upper and lower ramp bounds for each unit.

$$G_{i,t} = \sum_{b \in B} G_{b,i,t}, \quad \forall t \in T, i \in I \tag{5.13}$$

$$G_i^{\min} . \chi_{i,t} \le G_{i,t} \le G_i^{\max} . \chi_{i,t}, \quad \forall t \in T, i \in I \tag{5.14}$$

$$-R_i^{dn} \le G_{i,t,n} - G_{i,t-1,n}, \le R_i^{up} \; \forall t \in T, \forall i \in I, \forall n \in N \tag{5.15}$$

5.2.2 Modelling of Frequency Response Security Standards

The objective of frequency response is to contain the dynamic frequency evolution after an infeed loss within prescribed limits. Frequency security criteria used to characterize the initial transient behaviour of the frequency in this study are:

(1) ROCOF;

(2) Frequency nadir;

(3) Steady-state frequency;

(4) Frequency Response Index (β)

ROCOF attains its highest magnitude just after any severe contingency; initially, the frequency deviation is contained by the inertial response of the synchronous generators. After deployment of inertial response, PFR has to limit the frequency above a minimum prescribed limit, in the case of the largest infeed loss. Further, PFR enables meeting the quasi-steady-state condition at which frequency should stabilize above UFLS limit within few seconds to a minute.

This section discusses the mathematical formulation to explicitly incorporate the transient frequency behaviour within the stochastic scheduling framework. The differential equation (5.16) is mapped into the stochastic scheduling model by considering three characteristic periods in the form of constraints associated with the frequency security criteria discussed above.

Frequency behaviour after large imbalances, like large infeed loss, could be described using the motion equation of synchronously connected rotating mass, known as swing equation, as shown in Eqn. (5.16) [26].

$$2H_i \frac{df_i}{dt} = \frac{{f_0}^2}{Ap_i f_i} \Delta P \tag{5.16}$$

Here, $Ap^{sys} = \sum_{i \in I} Ap_i$, Ap_i is the rated apparent power of generator i (VA).

1) The rate of Change of Frequency (ROCOF)

ROCOF depends on inertial response capability of the system. Autonomous spontaneous actions taken by the system or elements of the system to arrest initial frequency deviation

is known as the inertial response of the power system. Total system inertial response is estimated using Eqn. (5.17).

$$H^{sys} = \frac{\sum_{i \in I} Ap_i H_i}{Ap^{sys}} \tag{5.17}$$

Synchronously connected motors also contribute to system inertia. This could be considered in a similar manner as generators. In this work, system frequency is calculated by aggregating all generators as one fictitious generator [68], [111]. This is expressed by Eqn. (5.18).

$$f^{eq} = \frac{\sum_{i \in I} H_i f_i}{\sum_{i \in I} H_i} \tag{5.18}$$

where, f_i denotes the frequency of individual generator i (Hz), $\frac{df_i}{dt}$ is the ROCOF (Hz/s).

Eqn. (5.16) could be expressed in terms of total system inertia and equivalent system frequency as:

$$ROCOF = \frac{df^{eq}}{dt} = f_0 \frac{\Delta P}{2H^{sys} Ap_i} \tag{5.19}$$

From Eqn. (5.19), it could be observed that as H^{sys} decreases, ROCOF would increase. That would lead to a higher frequency excursion and deeper frequency nadir, f^{nadir} at nadir time, t^{nadir}. Governor response during the inertial response time frame is negligible, as Δf is approximately zero. Hence, the maximum value of ROCOF should satisfy the minimum H^{sys} in case of maximum infeed loss, as mentioned in Eqn. (5.20).

$$H^{sys} = \frac{\sum_{i \in I} H_i * Ap_i * \chi_{i,t} - \Delta P * H_i^L}{f_0} \geq \left| \frac{\Delta P}{2 * ROCOF^{\max}} \right| \tag{5.20}$$

Constraint (5.21) ensures that enough inertial response is available, so that $ROCOF^{\max}$ does not trigger protective relays like UFLS relay or cause instability.

$$\sum_{i \in I} \left\{ \chi_{i,t} * H_i * G_i^{\max} \right\} + H^{eqload} * FL_{t,} \geq H^{req} \quad \forall t \in T, \forall i \in I \tag{5.21}$$

2) Frequency nadir

Frequency nadir is the minimum value of system frequency during the transient period. Frequency value at nadir depends on system inertia & PFR capability. After deployment of inertial response available with the system, governor PFR is deployed with maximum ramp rate. Constraint (5.22) ensures that adequate PFR is available.

$$\sum_{i\in I} P_{i,t} \geq P^{C} - LD * T^{de} * \frac{\Delta f^{\max}}{f_0}, \quad \forall t \in T \tag{5.22}$$

Constraints (5.23)-(5.29) describe the droop setting requirement and governor response. Constraint (5.23) represents the equivalent droop curve, in terms of Hz/MW. Eqn. (5.24) ensures PFR adequacy during large frequency deviation.

$$De_i = \frac{D_i * f_0}{G_i^{\max}}, \qquad \forall i \in I \tag{5.23}$$

$$P_{i,t} \leq \frac{\delta_{i,t}}{De_i}(\Delta f^{\max} - G_i^{db}), \quad \forall i \in I, \forall t \in T \tag{5.24}$$

Eqns. (5.25) and (5.26) ensure headroom availability with the enabling of governor. This would provide PFR and maintain droop curve relationship.

$$G_{i,t} + \frac{1}{De_i}(\Delta f^{\max} - G_i^{db}) \geq G_i^{\max} * \delta_{i,t} - G_i^{\max} * \Upsilon_{i,t}, \forall t \in T \tag{5.25}$$

$$P_{i,t} \geq \frac{\Upsilon_{i,t}}{De_i}(\Delta f^{\max} - G_i^{db}) - G_i^{\max}(1-\delta_{i,t}), \forall i \in I, \forall t \in T \tag{5.26}$$

Constraint (5.27) restricts the generator to be online when its governor is enabled. Constraint (5.28) sets $\delta_{i,t}$ equal to 0 for generators working in blocked or no governor mode. In this mode, these generators cannot provide PFR. Constraint (5.29) sets $\delta_{i,t}$ equal to 0, for generators with large governor deadband.

$$\delta_{i,t} \leq \chi_{i,t}, \forall i \in I, \quad \forall t \in T \tag{5.27}$$

$$\delta_{i,t} = 0, \quad \forall i \in G_{ng}, \quad \forall t \in T \tag{5.28}$$

$$G_i^{db} \leq G_i^{db\max} + f_0(1-\delta_{i,t}), \forall i \in I, \forall t \in T \tag{5.29}$$

$$\Delta f^{nad}(t) = -1/H^{sys}(t) * ((\Delta P^2 / 2P_{i,t}) + \Delta P * t^{de}) \tag{5.30}$$

Frequency deviation at nadir could be expressed by Eq. (5.30). The value of frequency nadir Δf^{nadir} should not exceed $\Delta f^{\max}$ [65]. In terms of system inertia and PFR delivered after largest infeed loss, frequency nadir at the time t could be expressed in simplified form as Eq. (5.30)

3) Frequency at Quasi-Steady -State

The frequency at intermediate quasi-steady-state condition depends on the PFR capacity delivered by generators at T^{de} and could be determined by Eq. (5.31). At this state, ROCOF is zero, which means that frequency has attained some quasi-steady-state value.

$$\Delta f^{ss} = \frac{\Delta P^{\max} - P_{i,t}}{LD * LF_t} \leq \Delta f^{ss\max} \tag{5.31}$$

Here, $\Delta f^{ss\max}$ is considered as maximum permissible frequency deviation at quasi-steady-state and its value should be less than the frequency deviation at nadir.

In addition to these constraints; Eqns. (5.32) and (5.33) determines the required PFR and ensure PFR adequacy at t^{nadir} and t^{ss}.

$$\sum_{i \in I} P_{i,t}^{ss} \geq P^{css} \quad \forall t \in T \tag{5.32}$$

$$\sum_{i \in I} P_{i,t}^{nadir} \geq P^{cnadir} \quad \forall t \in T \tag{5.33}$$

4) Frequency Response Index (β)

Frequency response index (β, MW/0.1 Hz) is a parameter to indicate the quantum of MW imbalance between load and generation that corresponds to 0.1 Hz frequency deviation from its nominal value [111], [112]. This information helps to assess the inertia and PFR adequacy of the studied system. β value could be estimated by Eqns. (5.34) and (5.35). Regression between f^{nadir} and corresponding power outages (ΔP) could be used to obtain λ and β progressively.

$$f^{nadir} = (\lambda * \Delta P) + f^{c} \tag{5.34}$$

$$\beta = (1/|\lambda|) * 0.1 \tag{5.35}$$

Where, λ & f^{c} denote the slope (Hz/MW) and constant part of the regression model in terms of frequency, respectively.

5.3 Methodology

In this work, two stages are proposed for the prediction of system inertia condition. Day-ahead stochastic scheduling is performed for forecasted wind generation and demand. Hence, solution obtained in forecasted framework would provide prior information of system parameters. Flow diagram of the proposed method is shown in Fig. 5.1.

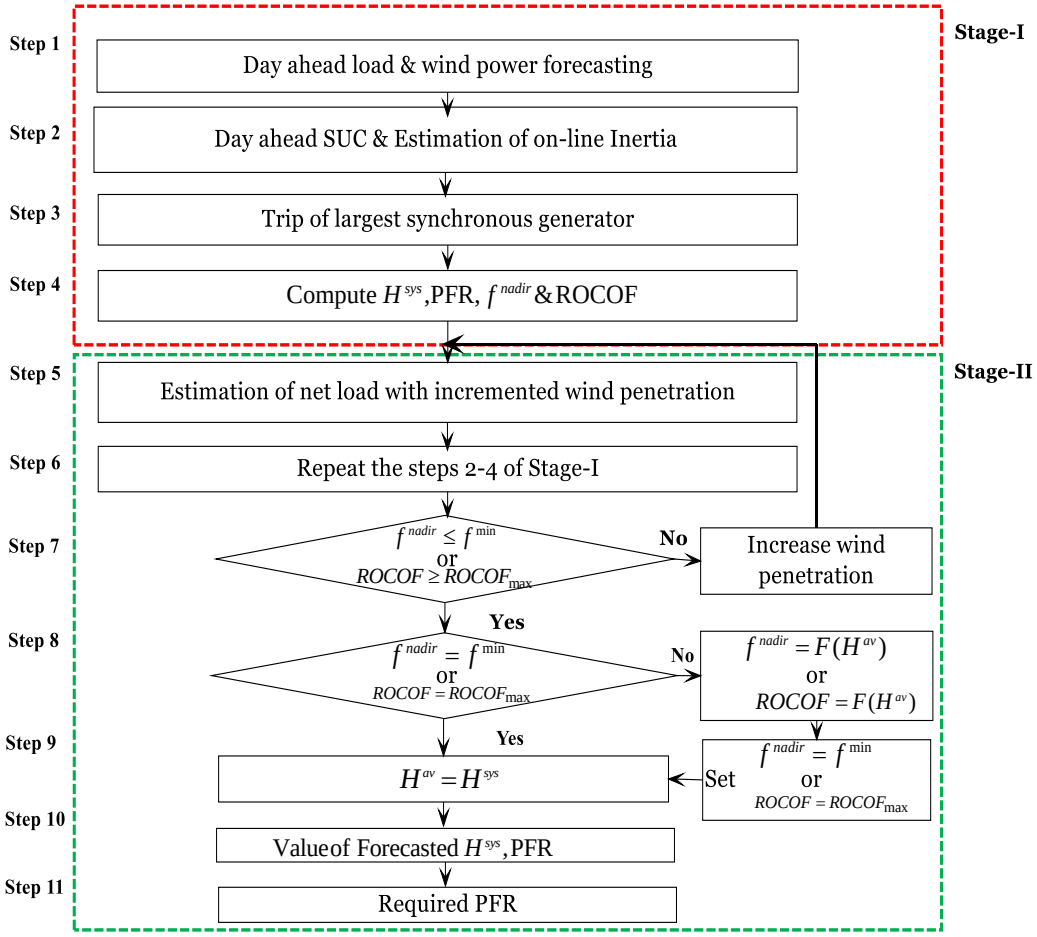

Fig. 5.1: Flow diagram of the proposed two-stage model.

In the first stage, system inertia and PFR is estimated without wind penetration, considering the largest infeed loss from the committed generators. For this, load is forecasted from historical load data and day-ahead stochastic scheduling is performed from the forecasted value. This would provide information about number of committed generators and hence system inertia condition over a day. From the committed generators, one of the largest infeed loss is considered. After this event, system inertia (H^{av}), ROCOF and frequency deviation are estimated and compared with the prescribed security criteria. If security criteria are not violated, calculations are performed for second stage.

In the second stage, net load is initially estimated with 5% wind penetration and system inertia is evaluated from committed generators. If sufficient system inertia is available penetration level is incremented. After each addition, minimum frequency and ROCOF are updated. This carries on until either ROCOF or minimum frequency value attains the UFLS margin. A mathematical functional relationship between f^{nadir} and H^{av} or ROCOF and H^{av} is formed as mentioned in Step 8 of Fig. 5.1. This functional relationship would consider security criteria, like ROCOF and f^{nadir}, whichever approaches prescribed security limit first. At this stage, information of wind penetration and frequency security parameters are collected. This is the maximum wind penetration that system could withstand in a secure fashion, considering network frequency security regulation. The results obtained is system specific and would vary according to the system parameters and dynamic conditions.

5.4 Wind Generation Uncertainty Characterization

Prediction of system inertia condition would be affected by the availability of wind power. Uncertain generation characteristics of wind power would affect UC decisions and would make it difficult to meet the system demand. Inaccurate scheduling decisions may result in over and under estimation of overall system inertia and PFR requirement. This would create challenges for SO to meet the inevitable contingencies like largest generation outage or loss of large chunk of load. Hence, modeling of wind uncertainty plays an important role in prediction of system inertia condition and estimation of PFR requirement. In this work, wind uncertainty is modeled through scenario generation and reduction. Reduced wind power scenarios reflect expected power generated by the wind power plants. The algorithms used for wind power scenario generation and reduction is provided in Chapter 3.

5.5 Case Study

The present section considers two stages for prediction of system inertia condition over a day mapped with frequency security parameters like ROCOF, maximum frequency deviation. The results illustrate effectiveness of the proposed model for estimation of system inertia, PFR requirement and investigate the impact of frequency security criteria on wind curtailment.

5.5.1 Data

Proposed work is carried out on one area IEEE 24 –Bus RTS with installed capacity of 3405 MW [104]. The study considers 11 oil/steam turbine units, 9 coal/steam turbine units, 6 hydro turbine units, 4 oil/combustion units and 2 nuclear units. System peak load is 2850 MW. The data is modified to accommodate wind farms with installed capacity varied from 5% to maximum penetration limit. Wind units consist of VESTAS V90 turbines, the details of which are available at manufacturer database [98]. Wind speed historical time series data for the duration 01.01.2010 to 31.12.2010 is used, online available from Illinois Institute of Rural Affair, USA [88].

Table 5.1: Generator Frequency Response Parameters

Unit	G_i^{up} **(MW)**	H_i **(s)**	De_i **(p.u.)**	G_i^{db} **(mHz)**
U12	12	2.6	0.05	15
U20	20	2.8	0.05	15
U50	50	3.5	0.05	15
U76	76	3.0	0.05	15
U100	100	2.8	0.05	15
U155	155	3.0	0.05	15
U197	197	2.8	0.05	15
U350	350	3.0	0.05	15
U400	400	5.0	0.05	15

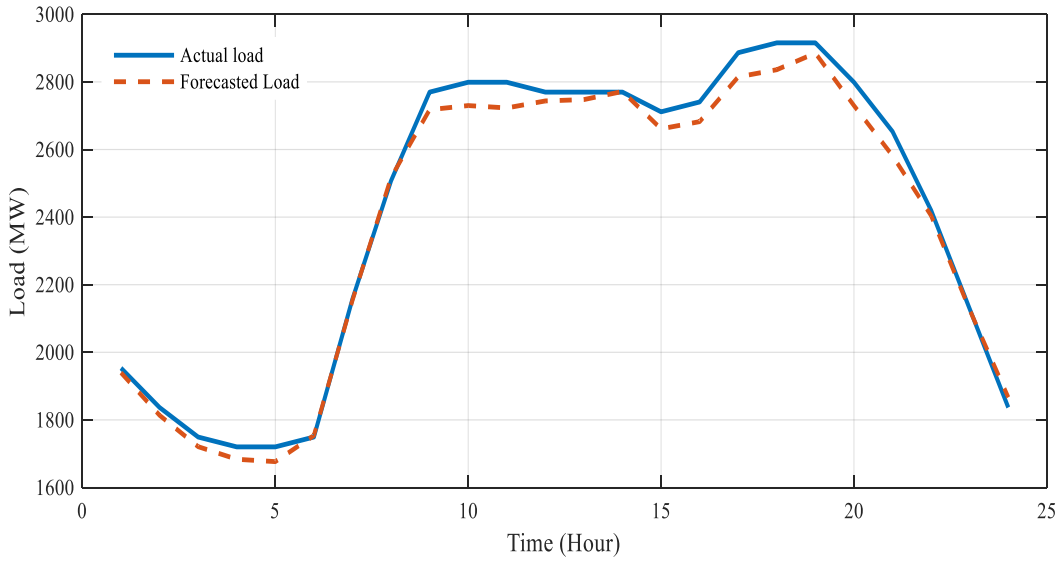

Fig. 5.2: Actual and forecasted load curve for peak load day [104].

Generator frequency response parameters are shown in Table 5.1. Nominal frequency (=50 Hz), governor droop (= 5%), dead band (=15 mHz), load damping rate (=1%/Hz), and PFR delivery time (=10 s) are as per National grid standards [106]. There are two nuclear generators of 400 MW each, which represent system's largest capacity units. Out of these 2 units, outage of one is considered. PFR capacity should limit frequency above 49.5 Hz. Maximum PFR requirement is taken as 30% of system's total responsive capacity and it should be greater than 100 mHz for all generator units. Generator fuel cost is obtained from [105]. Maximum ROCOF of 1.176 Hz/s is considered for the studied test system, to avoid UFLS after largest infeed loss [111], [113]. Fig. 5.2 shows actual and forecasted demand for peak load day.

5.5.2 Stage I: System Inertia Condition without Wind Penetration

This section examines the system's frequency response ability to arrest frequency deviations after largest infeed loss. At this stage, generation share from wind is not considered. Conventional generators are scheduled for the estimation of ROCOF and frequency deviation limits over a day.

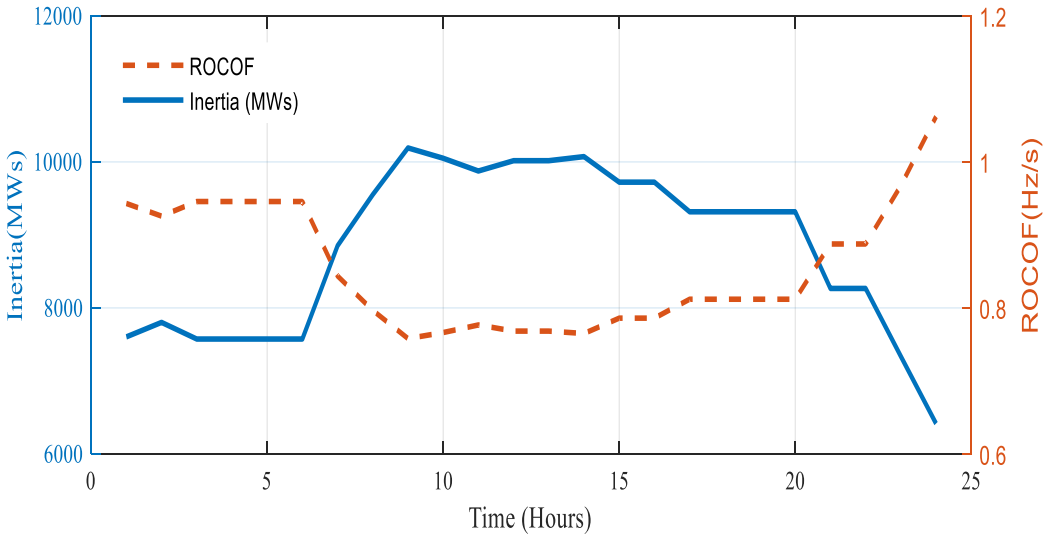

Fig. 5.3: ROCOF variation in response to inertia variation for 24 hrs.

Figs. 5.3 and 5.4 highlights that decreasing inertia quantum for different loading condition over a day results in high ROCOF and frequency deviation. In case of low load conditions, like in Hour 24, few generators get committed, resulting in lower inertia and in turn higher ROCOF. Fig. 5.5 shows PFR variation over 24-hours.

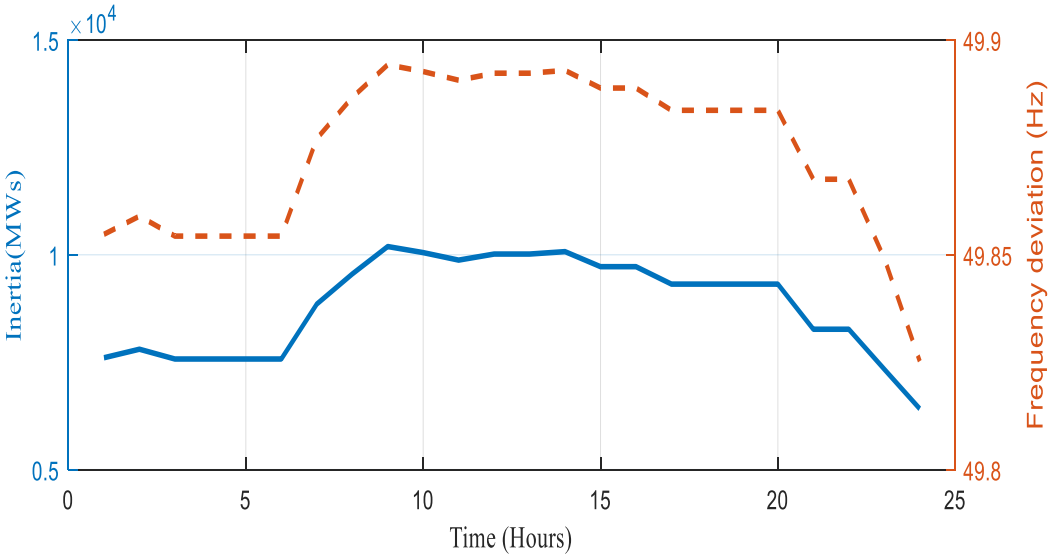

Fig. 5.4: Frequency deviation in response to inertia variation.

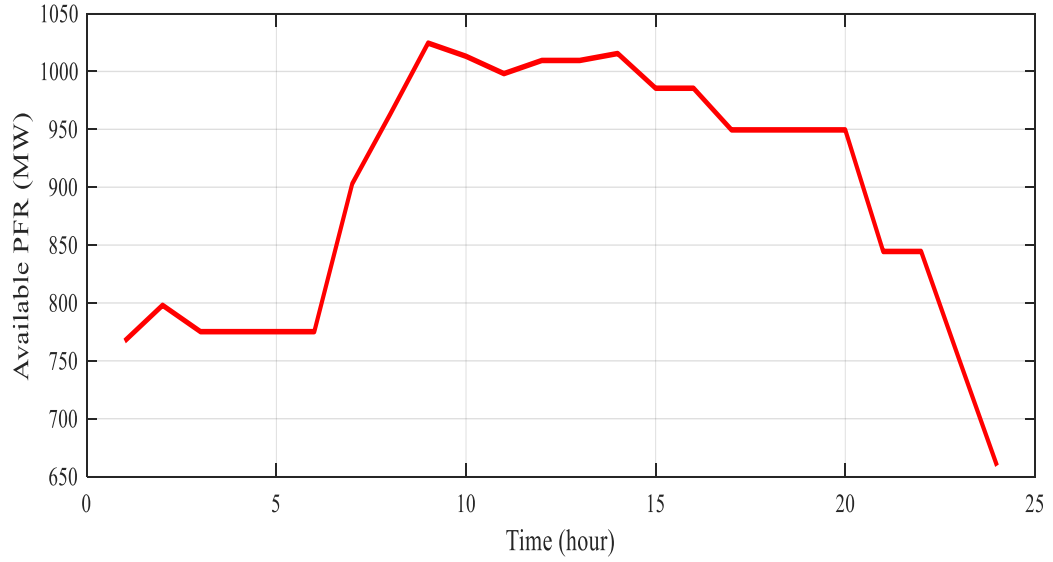

Fig. 5.5: PFR variation based on forecasted load.

Table 5.2 summarizes different observations from Stage-I, *i.e.*, minimum and maximum quantum of inertial response, PFR, ROCOF and frequency deviation.

Table 5.2: Frequency Response Parameters after Stage-I

Parameters	**Minimum Value**	**Maximum Value**
Inertial (MWs)	6415.8	10191.8
PFR (MW)	659.4	1024.5
ROCOF(Hz/s)	0.7682	1.0620
Frequency deviation (Hz)	49.82	49.89

5.5.3 Stage II: System Inertia Condition with Incremental Wind Penetration

This section investigates the impact of increasing wind penetration on frequency response parameters. At this stage, wind is incrementally added, and net load is calculated for each penetration level, as shown in Fig. 5.6.

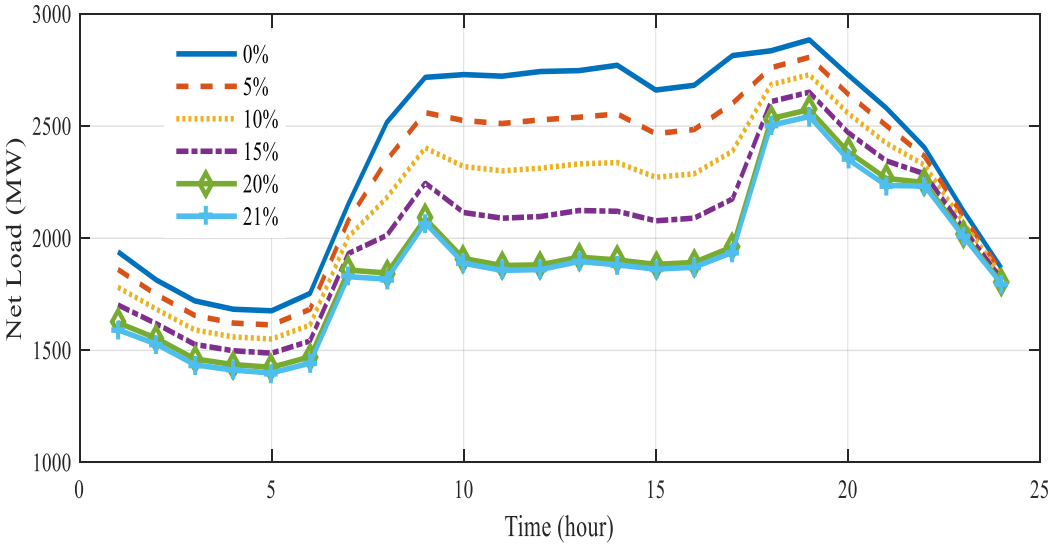

Fig. 5.6: Net load variation with varying wind penetration.

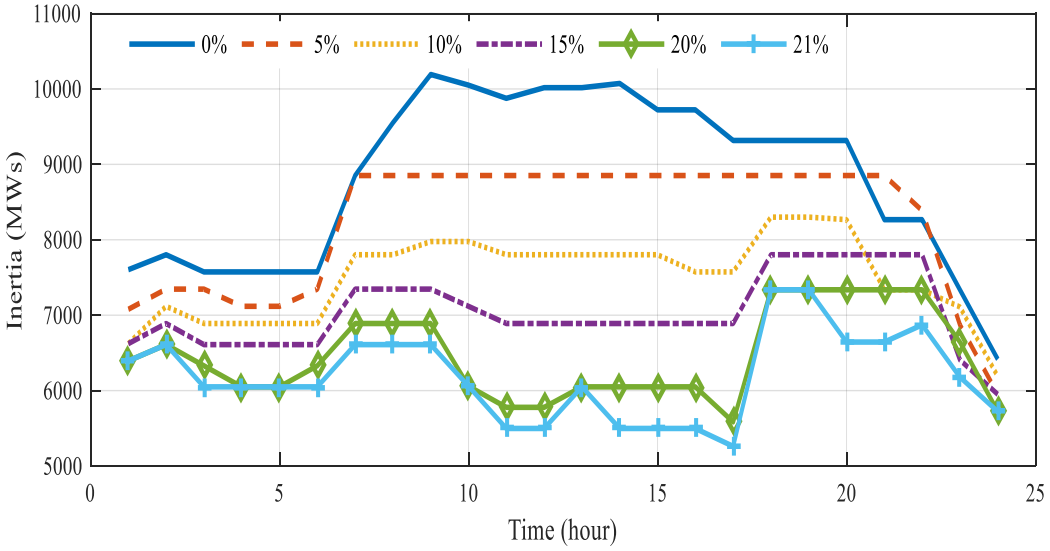

Fig. 5.7: Inertia variation with varying wind penetration.

It is observed that increasing wind penetration level from 0% to 21% reduces the overall net load. Hence, commitment decisions are changed with decreasing net load. This results in reduced

overall inertia as shown in Fig.5.7. Thus, increases ROCOF and frequency deviation for varying net load, as shown in Figs. 5.8 and 5.9. It is further observed, that for 20% penetration, ROCOF variation is higher and almost reaching the prescribed security limit of 1.176 Hz/s in Hour 24, prior to approaching the frequency deviation limit.

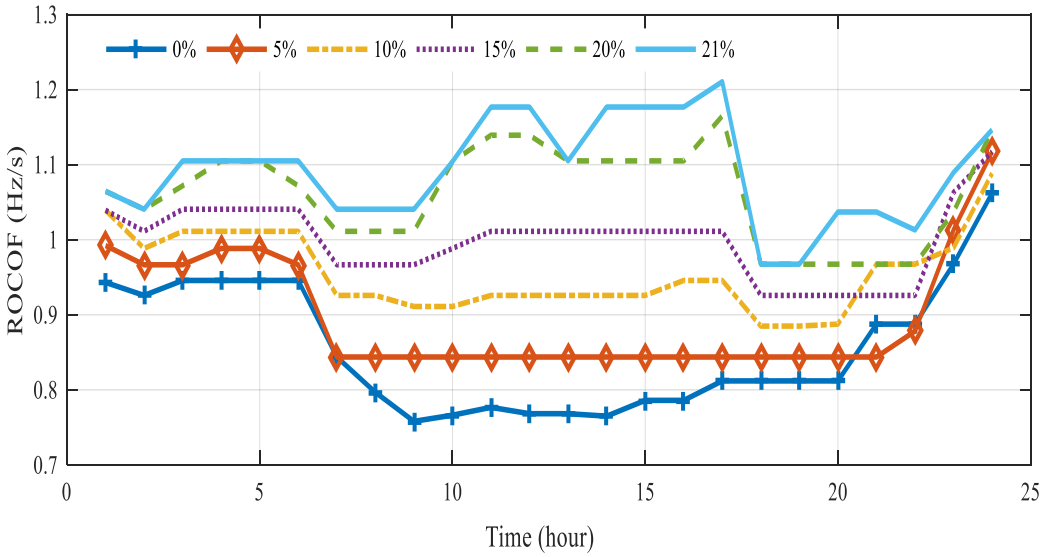

Fig. 5.8: ROCOF variation with variation in wind penetration.

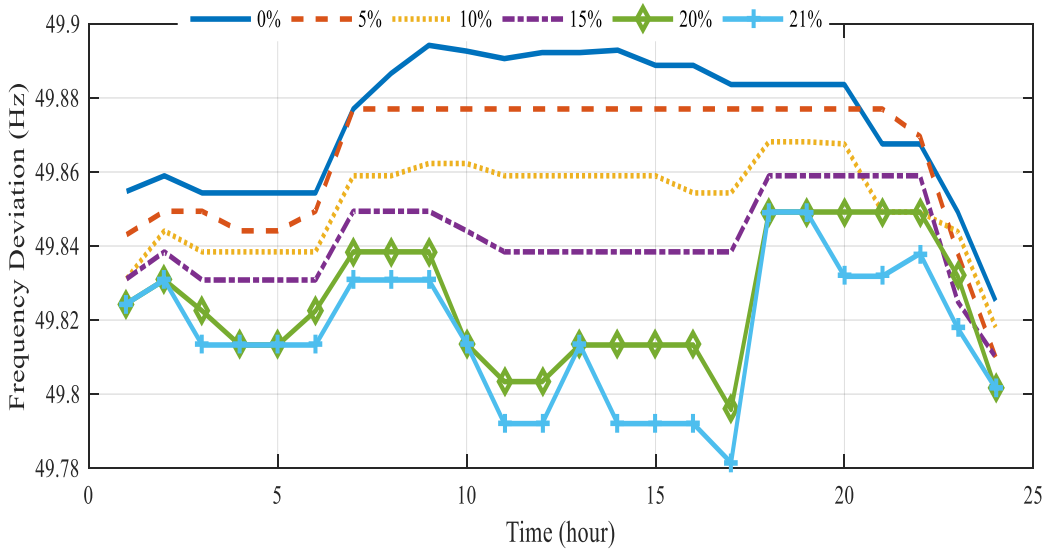

Fig. 5.9: Frequency deviation with varying wind penetration level.

Table 5.3 summarizes the variation in quantum of inertial response, PFR, ROCOF and frequency deviation, with varying wind penetration after Stage-II. Although, these results are system specific, it is observed that further increment in wind power penetration would

violate the frequency stability. This would require large PFR capacity to maintain the system frequency within the prescribed security limits.

Table 5.3: Frequency Response Parameters after Stage-II

Wind (%)	Inertia (MWs)	PFR (MW)	ROCOF (Hz/s)	Frequency deviation (Hz)
5%	5950.8 – 8851.8	612.9 – 903	0.8437– 1.1172	49.81 – 49.877
10%	6187.8– 8300.4	636.6 –848.1	0.8849– 1.0883	49.818 – 49.868
15%	5950.8 – 7801.8	612.9 – 798	0.9275– 1.1172	49.81 – 49.85
20%	5722.8 – 7336.8	570.3 –751.5	0.9674– 1.1464	49.795 – 49.849
21%	5722.8 – 7336.8	557.7 –751.5	0.9674 - 1.1767	49.781 - 49.849

5.5.4 PFR Requirement at Frequency nadir

In this section β, f^{nadir} and PFR requirement are estimated for the largest infeed loss of 400 MW, as discussed in Section III C. Regression between f^{nadir} and infeed loss of 400 MW is shown in Fig. 5.10.

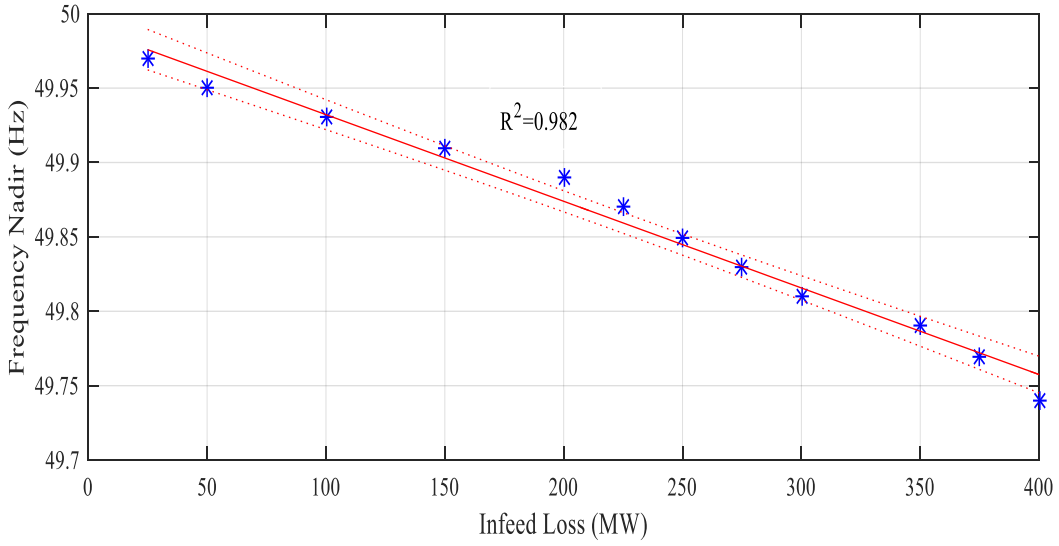

Fig. 5.10: Regression between frequency nadir and infeed loss.

$$f^{nadir} = (-0.000582 * 400) + 49.98 \tag{5.36}$$

$$\beta = \left(\frac{1}{|-0.000582|} \right) * 0.1 \tag{5.37}$$

From Eqns. (5.36) and (5.37), it could be analysed that for specific load condition, β value for studied system is 171.82 MW/0.1 Hz and f^{nadir} is 49.747. Hence, approximately 412.36 MW of response is required, to maintain generation demand imbalance. It could be observed from Table 5.3, that sufficient PFR is available with the system for all conditions, to maintain frequency above the minimum value. Hence, there is no requirement of additional PFR for the stated conditions. However, this requirement would be higher with lower frequency nadir as shown in Fig. 5.11. Further, PFR procured in day ahead may differ in real-time with variation in system inertia conditions, and requires real-time dispatch.

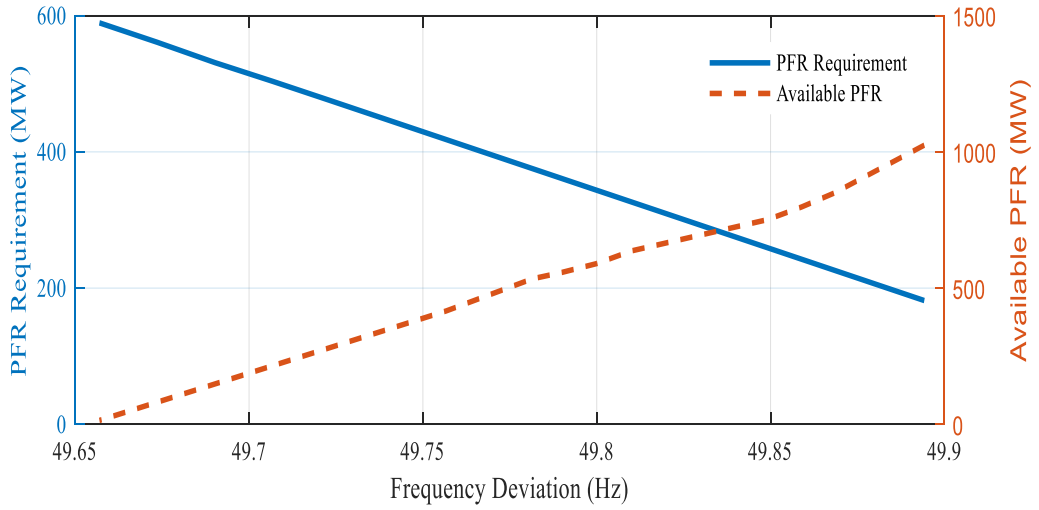

Fig. 5.11: PFR availability and PFR requirement at frequency nadir.

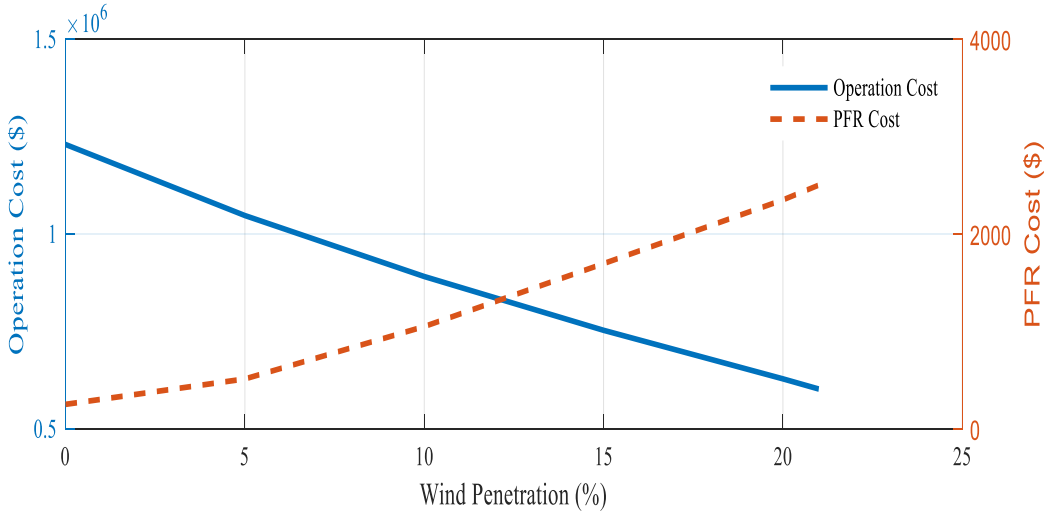

Fig. 5.12: Operation cost & PFR cost with varying wind penetration.

5.5.5 Overall Cost Analysis

With increasing wind penetration, operation cost reduces. Increasing wind penetration reduces the average number of conventional units committed online per hour.

It could be observed from Fig. 5.12, there is marginal increment in PFR cost. PFR constraints add only about 0.3% to total operation cost. This marginal increment in PFR cost is because of system's inertia and PFR adequacy. Synchronous inertial cost is considered zero for scheduling horizon, as system has sufficient inertial response and PFR.

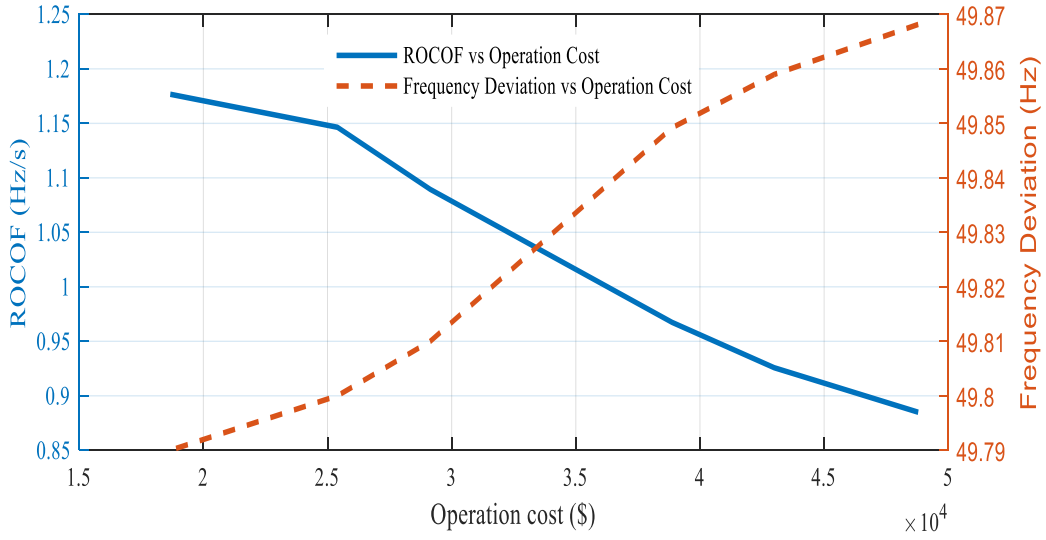

Fig. 5.13: Operation cost with variation in ROCOF & frequency deviation.

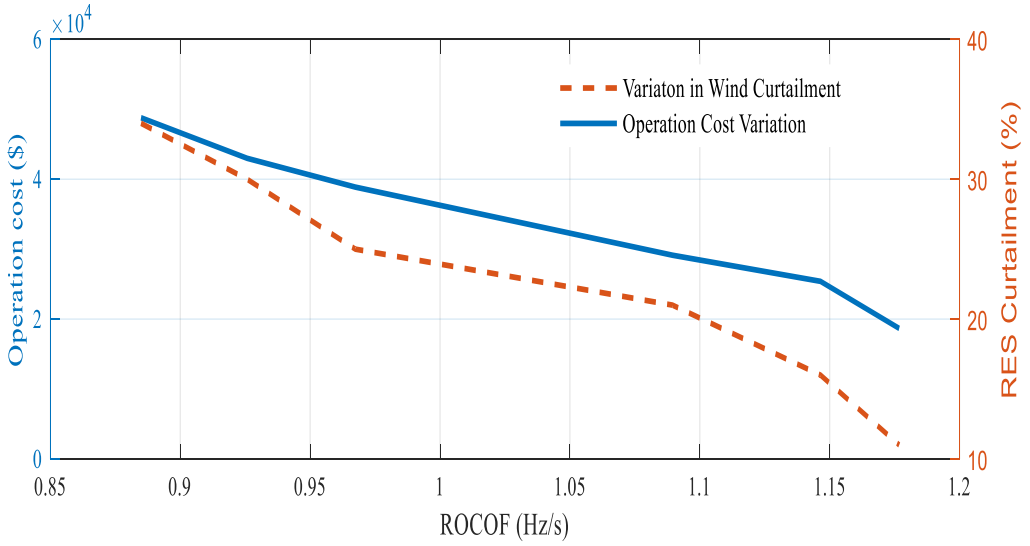

Fig. 5.14: Operation cost & wind curtailment with variation in ROCOF setting.

5.5.6 Wind Curtailment Based on Frequency Security Criteria

This section explores the impact of system frequency security parameters, like ROCOF, and frequency deviation on operation cost and wind power curtailment. ROCOF depends on the system inertia condition and increasing this setting leads to significant wind power disconnection.

It could be observed from Figs. 5.13 & 5.14, ROCOF setting variation from 1.176 to 0.869 Hz/s would result in increased operation cost of about 20% and wind curtailment of about 22%.

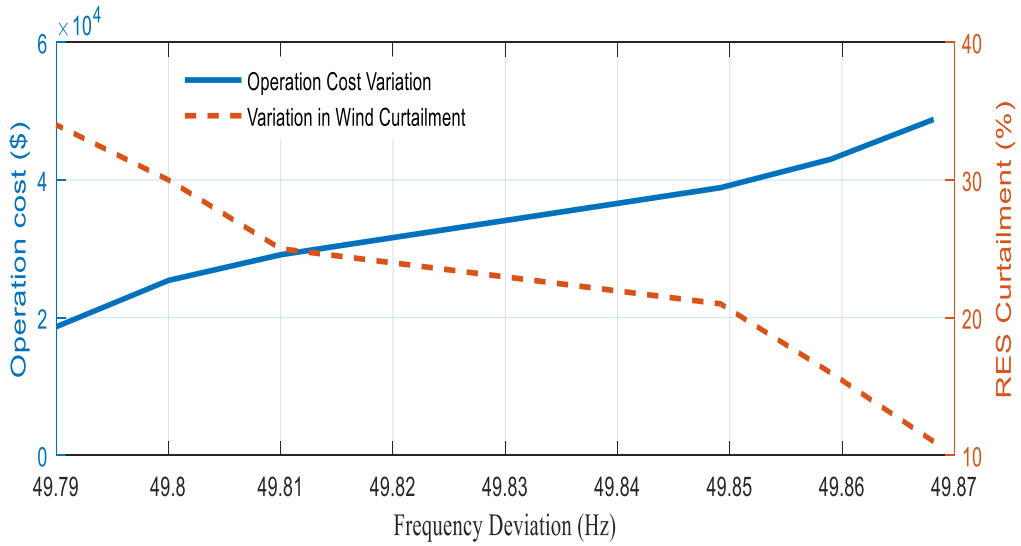

Fig. 5.15: Operation cost & wind curtailment with variation in frequency deviation.

Similarly in Fig.5.15, frequency deviation from 49.87 Hz to 49.79 Hz results in increased wind curtailment and decrease in operation cost of about 18%. This is because of reduction in number of committed conventional generators and hence reduced operation cost. Observation obtained from this study would be helpful to frame the system frequency security requirements, like ROCOF setting, with increment in wind generation share.

5.6 Conclusions

A novel computational framework is proposed for prediction of system inertia condition and PFR adequacy, to improve frequency control capability in low carbon power systems. Demand & wind generation is forecasted and net load is estimated for the proposed day-ahead stochastic scheduling model. First stage in the performed case studies evaluates frequency parameters, like system inertia, PFR, ROCOF & maximum frequency deviation,

following largest infeed loss. System security parameters such as ROCOF and frequency deviation are found to lie within the security limits. Second stage estimates these FR parameters by incrementally adding RES penetration considering network code. Net load is calculated for each penetration level, and is used to estimate maximum RES penetration that system could withstand without violating maximum ROCOF & frequency deviation limits. This analysis further provides forecasted inertia condition and PFR adequacy. This would certainly enhance system's frequency response capability. Moreover, cost analysis performed with incremental wind penetration results in reduced operation cost. Overall cost increases only marginally with a consideration of PFR constraints. Impact of system frequency security parameter variation on wind curtailment & operation cost is analyzed. This analysis would help in selection of suitable ROCOF setting to boost wind generation.

Synthetic inertia contribution from wind generation sources in frequency response constrained UC model is a challenging task. Proposed model could be potentially enhanced to incorporate these challenges.

Chapter – 6

OPTIMAL GENERATION MIX FOR FREQUENCY RESPONSE ADEQUACY IN FUTURE POWER SYSTEM

6.1 Introduction

Over the last decade, amount of electricity generation from carbon-intensive generation sources (*i.e.* coal and oil) has declined, while generation share of renewable energy sources (RES) has increased more than fourfold over the same period [81]-[84]. The European energy targets for 2020-2030 are to accommodate at least 45% generation from RES [83]. Recent study by the National Renewable Energy Laboratory shows that the United States can generate 80% of its electricity from RES by 2050 [84]. As the generation mix on a power system evolves, moving away from traditional generation units, behavior of the power system in response to a power imbalance also changes. Increasing RES share in overall generation mix would pose additional formidable challenges from the technical and economical point of view. Displacement of conventional generation would reduce system's inherent frequency response ability like inertia and PFR, to arrest and stabilize initial frequency deviation in contingent conditions. Reduced system frequency response would make system frequency more sensitive to changes in supply and demand. This would lead to quick frequency deviations, following the loss of generation and/or load.

RES integration could lead to both diversifications of generation sources and increase in overall cost due to the additional resource requirement for flexibility and hence secure system operation [85]. Recent analysis in National Grid, United Kingdom reveals that PFR requirements are expected to increase significantly over the next 15 years. Over the next 5 years this amounts to an increase of 30-40% [75], [108]. This requires efficient generation mix by balancing the profits of generation source variation and cost of security with the PFR provision.

PFR requirement analysis is done for the quantification of variability and uncertainty of the RES [76], [86], [87]. It is observed that the PFR requirements could be partly compensated by the interaction of different type of loads and wind power [77]. Another scenario-based study is performed for different combinations of wind, solar and ocean

wave power generation for computation of PFR requirements caused due to uncertainty. It is concluded that PFR requirements and uncertainty is reduced with RES mix [87]. Diversified RES mix provides smooth generation portfolio. Hence, generation predictability would increase and probability of extremes values would decrease. This would result in reduction in overall system frequency response requirements.

Conventional and RES technology have an idiosyncratic effect on system frequency and there is limited understanding of frequency response adequacy with various generation mix characteristics. A prior understanding of optimal generation mix with secured PFR in future low carbon power system would corroborate system operator to maintain secure and stable power system.

In this context, main contribution of this chapter is to:

(i) Propose a novel exposition of optimal generation mix with the objective of reduced operation cost while maintaining systems' FR ability.

(ii) Assess PFR adequacy with diversified generation mix.

(iii) Model RES uncertainty with pragmatic characterization in the generation mix optimization problem.

(iv) Analyse overall cost for different generation mix cases.

Prior information of system FR with optimal combination of conventional and RES generation could support SO, to efficiently handle inevitable contingencies, like largest infeed loss.

6.2 Problem Formulation

In the proposed model ROCOF and frequency deviation limits, initial generation mix, system data and net load profile is applied as inputs. It considers thermal, hydro, nuclear, uncertain renewable wind & PV units as candidate generators, and provides optimized generation mix and total cost under this mix as outputs. In this work generation from wind & PV is given priority as candidate generators, considering environmental concerns. The formulation follows the way that the candidate generators will be added into the initial generation mix, stage by stage following network security parameters. The selection of the candidate generator at a stage is based on the ROCOF and maximum frequency deviation limit. Wind & PV generation uncertainty is characterized and represented in the proposed model for the pragmatic problem formulation.

6.2.1 RES Uncertainty Characterization

Optimal generation mix would be affected by the availability of RES. Uncertain generation characteristics of wind & PV power would affect generation scheduling and would make it difficult to meet the system demand. Inaccurate scheduling decisions may result in over and under estimation of overall system inertia and PFR requirement. This would create challenges for SO to meet the inevitable contingencies like largest generation outage or loss of large chunk of load. Hence, modeling of wind & PV uncertainty plays an important role in obtaining optimal generation mix. In this work, wind and PV uncertainty is modeled through modified interval forecast method. The algorithms used for wind and PV power uncertainty modeling is provided in Chapter 3.

6.2.2 Modified Interval Unit Commitment

MIUC model proposed in chapter 4 is incorporated to minimize the overall operation cost under uncertain wind & PV generation with the aim to determine optimal generator combination. This model incorporates advantageous features of computationally fast interval UC and economical stochastic UC models to improve day-ahead unit scheduling. In MIUC, PV & wind variability is characterized by ramp up and down scenarios, formulated within the forecasted upper and lower limit. Hourly ramp needs of formulated scenarios depend on net load. Thus, it precisely represents the expected RES output. In MIUC, problem is formulated with mix integer linear programming (MILP) constraints with the aim, to minimize the operating cost of the central forecasted scenario of wind and PV generation *i.e.* n_w and n_{pv}. Objective function shown by Eqn. (6.1) includes start-up cost, no-load cost and running cost of each generating unit. Non-linear cost function is converted to linear segments using piece wise linearization.

$$\min C^o = \sum_{t\in T}\sum_{i\in I}(su_{i,t,j} + Ln_i * \chi_{i,t} + \sum_{b\in B} Cs_{i,b} * g^s_{b,i,t,n1_{w,pv}}) \tag{6.1}$$

Optimization problem is subject to power balance constraints as (6.2)

$$\sum_{i\in I} G_{i,t} = LN_t \quad \forall t \in T \tag{6.2}$$

$$LN_t = LF_t - \sum_{t,w}(W^p * W^{av} * W^{cap}) - \sum_{t,pv}(PV^p * PV^{av} * PV^{cap}) \tag{6.3}$$

In Eqn. (6.3), net load is given as the difference between forecasted demand and load served by RES. Other constraints like generator start-up cost, minimum up/down time and ramping constraints are formulated in same way as proposed in chapter-4.

6.2.3 Frequency Security Limit Based Generation Mix Optimization

In this section, generation mix optimization sub-problem is formulated with frequency response constraints. This formulation would work as a performance evaluator for the main problem. System data and demand profile is used to evaluate the total generation costs and PFR cost for the required time period. Generation mix is restructured with the expansion and contraction of some generation technologies. Hence, investment cost, C^{invest} of generators is considered in the total cost, C^{total}. In this work, wind and PV generation expansion is considered. Large integration of wind and PV would create reliability and system security issues. Hence, this would give rise to loss of load probability or under frequency load shedding issues and in turn incurs societal cost. This cost is considered through increase in PFR requirements. PR represents the Price/MW/ hr., primary response capacity from the conventional generation plants. For simplicity, PFR price is assumed equal for different responsive conventional generation. Now, the optimization problem could be represented as (6.4):

$$\min C^{total} = C^{o} + C^{invest} + PR * \sum_{t \in T} \sum_{i \in I} (P_{i,t}) \tag{6.4}$$

Subject to following frequency security constraints:

Maximum value of ROCOF should satisfy minimum H^{sys} in case of maximum infeed loss, as mentioned in Eqn. (6.5).

$$H^{sys} = \frac{\sum_{i \in I} H_i * Ap_i * \chi_{i,t} - \Delta P * H_i^{L}}{f_0} \geq \left| \frac{\Delta P}{2 * ROCOF_{\max}} \right| \tag{6.5}$$

Constraint (6.6) takes care of available system inertial response, such that $ROCOF_{\max}$ does not violate protection setting and cause instability.

$$\sum_{i \in I} \left\{ \chi_{i,t} * H_i * G_i^{\max} \right\} + H^{eqload} * FL_{t,} \geq H^{req} \quad \forall t \in T \tag{6.6}$$

After deployment of inertial response available with the system, governor PFR is deployed with the maximum ramp rate. Constraint (6.7) ensures PFR adequacy.

$$\sum_{i \in I} P_{i,t} \geq P^{C} - LD * t^{de} * \frac{\Delta f^{\max}}{f_0}, \quad \forall t \in T \tag{6.7}$$

Eqns. (6.8)-(6.14) provides governor droop setting and governor setting for providing PFR. In (6.8) equivalent droop curve is estimated and given in Hz/MW. Eqn. (6.9) ensures PFR adequacy following large frequency variations.

$$D_i^e = \frac{D_i * f_0}{G_i^{\max}}, \qquad \forall i \in I \tag{6.8}$$

$$P_{i,t} \leq \frac{\delta_{i,t}}{D_i^e}(\Delta f^{\max} - G_i^{db}), \quad \forall i \in I, \forall t \in T \tag{6.9}$$

Eqns. (6.10) and (6.11) maintains headroom availability and maintains governor droop. Eqn. (6.12) ensures generator commitment for enabled governor. Eqns. (6.13) & (6.14) assign δ value zero for blocked governor mode and generators with high governor deadband.

$$G_{i,t} + \frac{1}{D_i^e}(\Delta f^{\max} - G_i^{db}) \geq G_i^{\max} * \delta_{i,t} - G_i^{\max} * \gamma_{i,t}, \forall t \in T, \forall i \in I \tag{6.10}$$

$$P_{i,t} \geq \frac{\gamma_{i,t}}{De_i}(\Delta f^{\max} - G_i^{db}) - G_i^{\max}(1 - \delta_{i,t}), \forall i \in I, \forall t \in T \tag{6.11}$$

$$\delta_{i,t} \leq \chi_{i,t} \quad \forall i \in I, \quad \forall t \in T \tag{6.12}$$

$$\delta_{i,t} = 0 \quad \forall i \in G_{ng}, \quad \forall t \in T \tag{6.13}$$

$$G_i^{db} \leq G_i^{db\max} + f_0(1 - \delta_{i,t}), \forall i \in I, \forall t \in T \tag{6.14}$$

Eqn. (6.15) determines the intermediate state frequency value. It depends upon generator PFR capacity, infeed loss value, load damping rate and forecasted demand. Its value should be less than Δf^{nadir}.

$$\Delta f^{ss} = \frac{\Delta P - P_{i,t}}{LD * LF_t} \leq \Delta f^{nadir} \tag{6.15}$$

6.3 Methodology

In this work novel exposition of frequency response constrained generation mix optimization is proposed to uphold the system security criteria considering RES uncertainty and largest infeed loss of the system. Proposed method is complex to solve directly by single optimization. In this work an innovative technique is proposed to handle

the problem using multi-objective optimization. Flow diagram of the proposed approach is shown in Fig. 6.1.

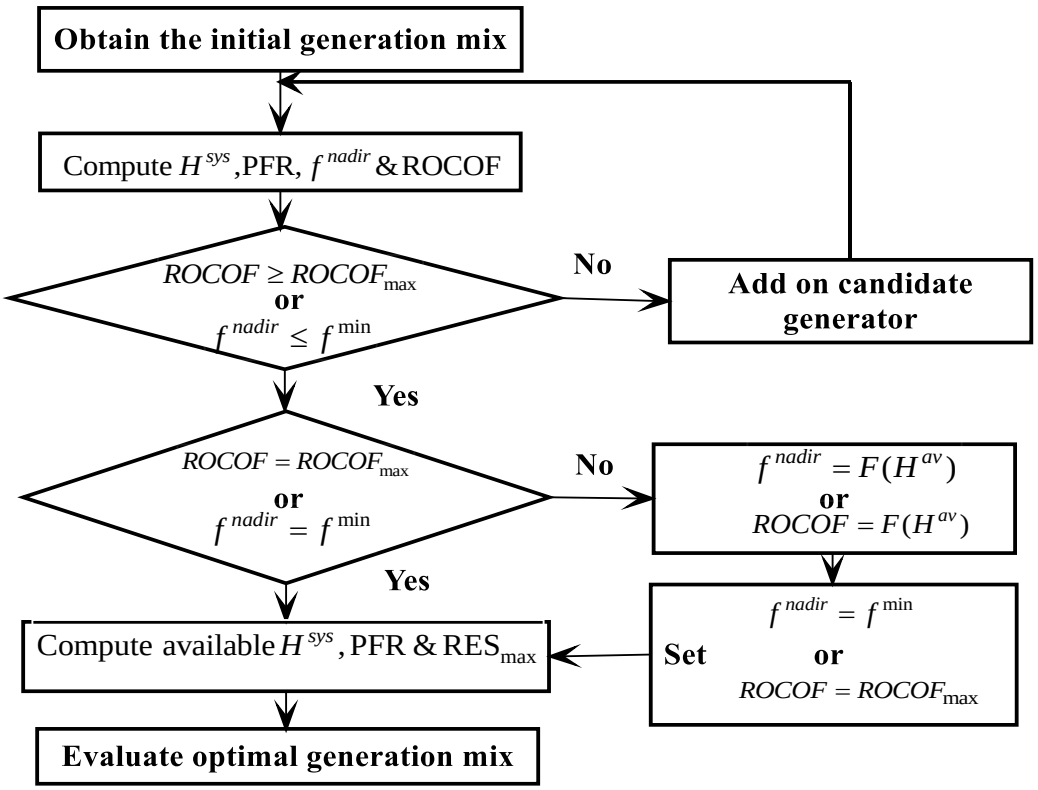

Fig. 6.1: Flow diagram of the frequency response constrained generation mix.

First objective would take care of sub-operational problem with RES uncertainty characterization, while addition of candidate generators from available generation technology and resulting generation mix based on frequency security criteria is evaluated by second objective. At first, initial generation mix is evaluated using MILP based MIUC, and examined whether the frequency security criteria is violated. If it is violated, that shows the generation mix is already at optimal state, otherwise optimization would follow next step.

Based on initial generation mix, assuming U units are added to form the final generation mix without violating system security parameters. The optimization is divided into U cycles. In each cycle, one unit would be added as candidate generator and system security parameter is evaluated. Program is terminated, if security limit reaches. If ROCOF and frequency deviation limit is not violated, another unit would be added into the generation mix for the uth cycle. The $(u+1)$th cycle decisions would be determined

by the optimal generation mix obtained for uth cycle, by repeating the above steps. The program would iterate U times to obtain optimal mix.

6.4 Case Study

6.4.1 Data

This section demonstrates the application of the proposed optimal generation mix model on one area IEEE 24- Bus RTS with installed capacity of 3405 MW [104]. The study considers 11 oil/steam turbine units, 9 coal/steam turbine units, 6 hydro turbine units, 4 oil/combustion units and 2 nuclear units. System peak load is 2850 MW.

Table 6.1: Generator Parameters

Unit Type	G_i^{up} **(MW)**	**Number of units installed**	H_i **(s)**	D_i **(p.u.)**	G_i^{db} **(mHz)**	C^{invest} **($/kW)**
Oil/Steam	12	5	2.6	0.05	15	962
Oil/CT	20	4	2.8	0.05	15	714
Hydro	50	6	3.5	0.05	15	2500
Coal/Steam	76	3	3.0	0.05	15	1610
Oil/Steam	100	3	2.8	0.05	15	962
Coal/Steam	155	3	3.0	0.05	15	962
Oil/Steam	197	3	2.8	0.05	15	962
Coal steam	350	3	3.0	0.05	15	1610
Nuclear	400	2	5.0	0.05	15	1610
Wind	50	1	-	-	-	1240
PV	50	1	-	-	-	1260

Table 6.1 shows each generator parameters. This model considers frequency response parameters of different generation types. Hence, separate model for each generation type is avoided. Actual and forecasted demand for peak load day is shown in Fig. 6.2. Since, wind and PV generation expansion is considered in this work, generator data is modified to include the parameters for these RES. Wind & PV plant of 50 MW each is considered. Nominal frequency (=50 Hz), governor droop (= 5%), dead band (=15 mHz), load damping rate (=1%/Hz) and PFR delivery time (=10 s) are considered as per National Grid standards [106]. Maximum ROCOF of 1.2 Hz/s is considered for the studied test system, to avoid under frequency load shedding after largest infeed loss [113].There are two nuclear generators of 400 MW each, which represent

system's largest capacity units. Out of these 2 units, outage of one is considered. PFR capacity should limit frequency above 49.5 Hz. Maximum PFR requirement is taken as 30% of system's total responsive capacity. Maximum governor dead band should be greater than 100 mHz for all generator units. PFR price is assumed as 10 $/MW/hr. [114].

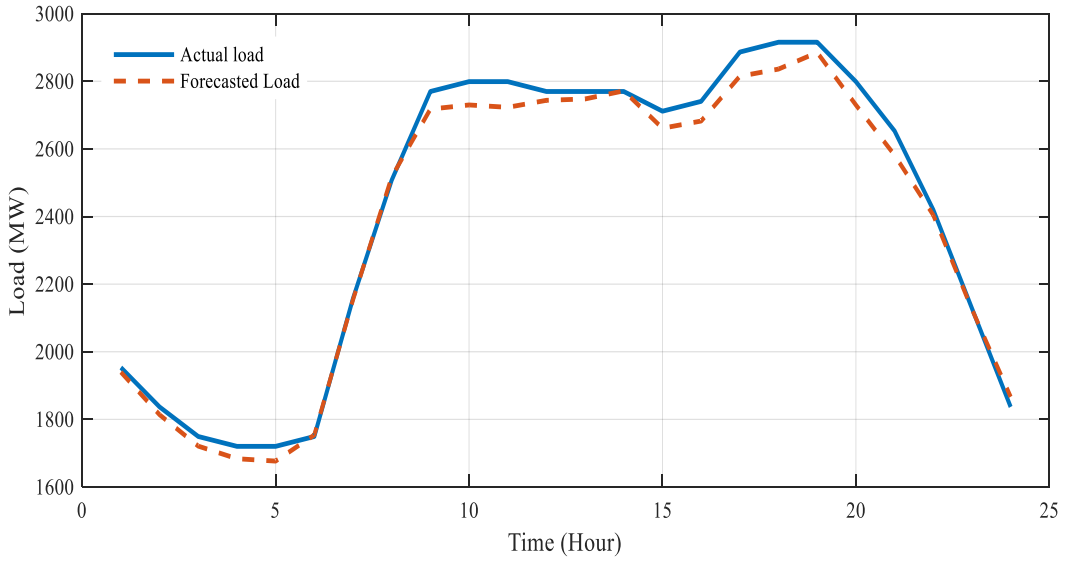

Fig. 6.2: Actual and forecasted load curve for peak load day [104].

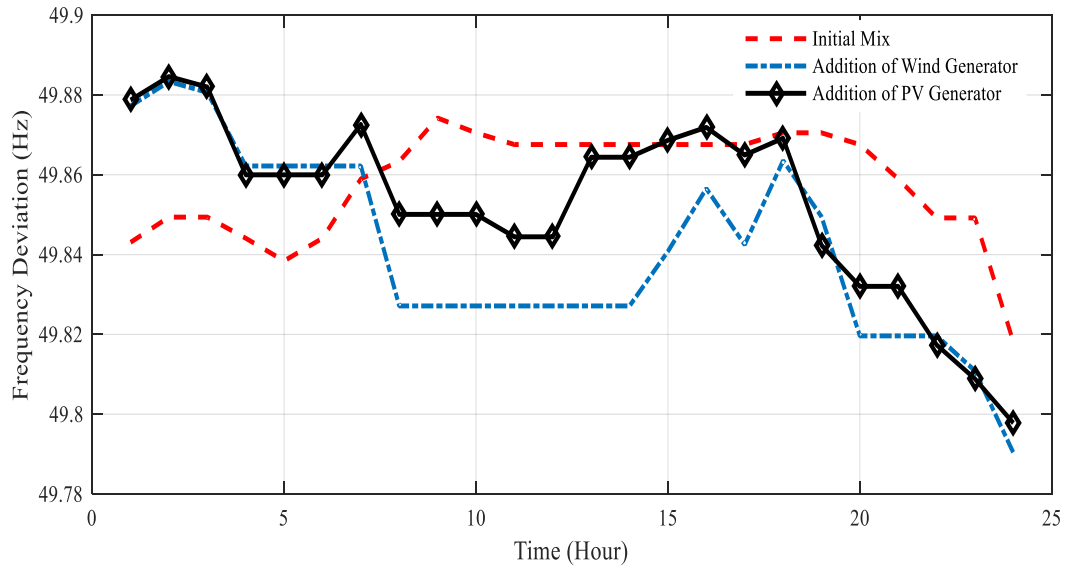

Fig. 6.3: Frequency deviation in all the three cases.

6.4.2 Generation Mix Following Frequency Security Limits

This section analyses the optimal generation mix following frequency security criteria. Effect of largest generation outage on ROCOF and frequency deviation is analyzed and contribution from different generators is obtained. Three cases are considered: (i) Base

Case (without wind & PV) (ii) Wind as candidate generator (iii) PV as candidate generator.

(i) Base Case (without wind & PV)

This case considers initial generation mix available with the test system. It is observed from Figs. 6.3 & 6.4, ROCOF and frequency deviation values are within the limit, *i.e.*, maximum ROCOF is 1.088 Hz/s and maximum frequency deviation is 49.818 Hz. This reflects sufficient inertia and PFR availability with the system. Generation contribution from different generators is shown in Fig. 6.4. As system frequency limit is not violated; candidate generators like wind and PV could be added to the initial generation mix.

(ii) Wind as candidate generator

In this case wind as candidate generator is added to the initial generation mix and system frequency security criteria are assessed. Wind power contribution to feed the demand over the day is shown in Fig. 6.5.

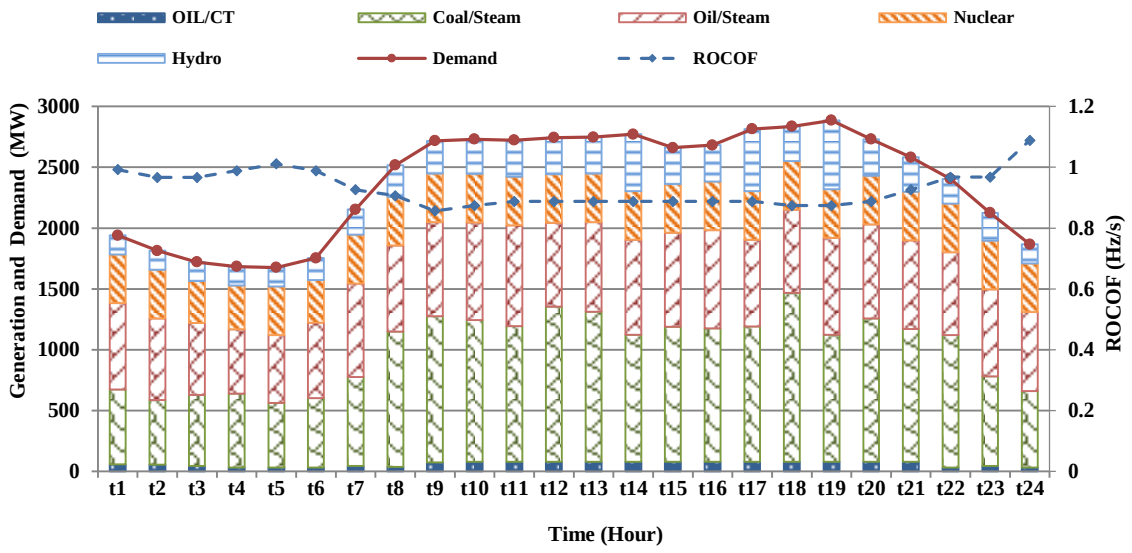

Fig. 6.4: Initial generation mix.

Effect of uncertain wind generation on frequency deviation and ROCOF over a day could be seen from Figs. 6.3 & 6.5. It could be observed that maximum value of ROCOF is 1.183 Hz/s and maximum frequency deviation is 49.79 Hz. This is due to the fact that less number of conventional generators is committed to provide inertial response and PFR. However, these limits are within the prescribed security criteria.

Hence, additional RES generation unit could be added to further assess the system frequency response adequacy.

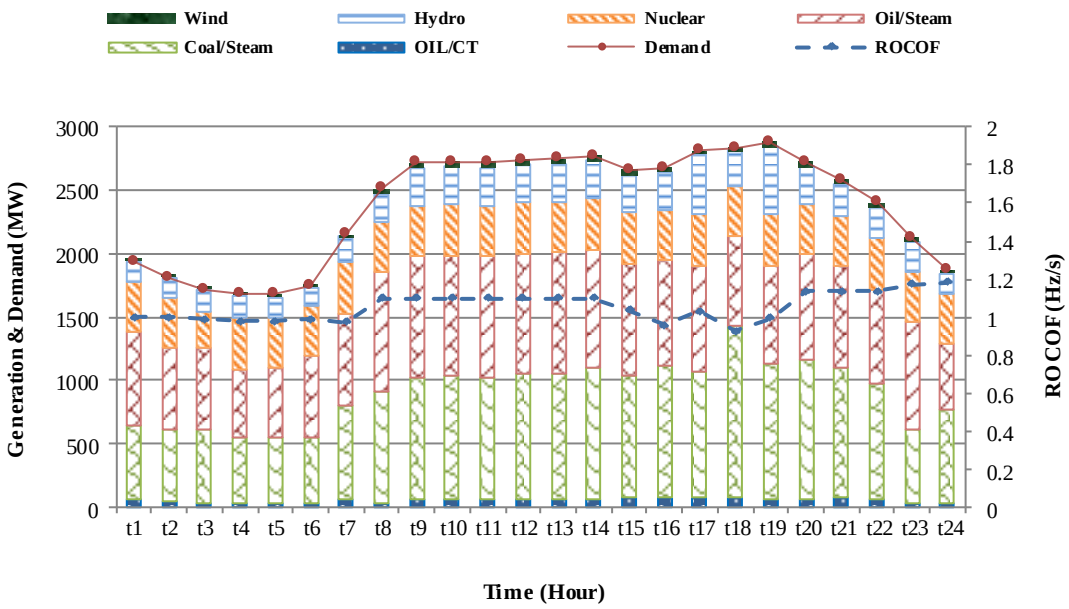

Fig. 6.5: Initial generation mix with wind as candidate generator.

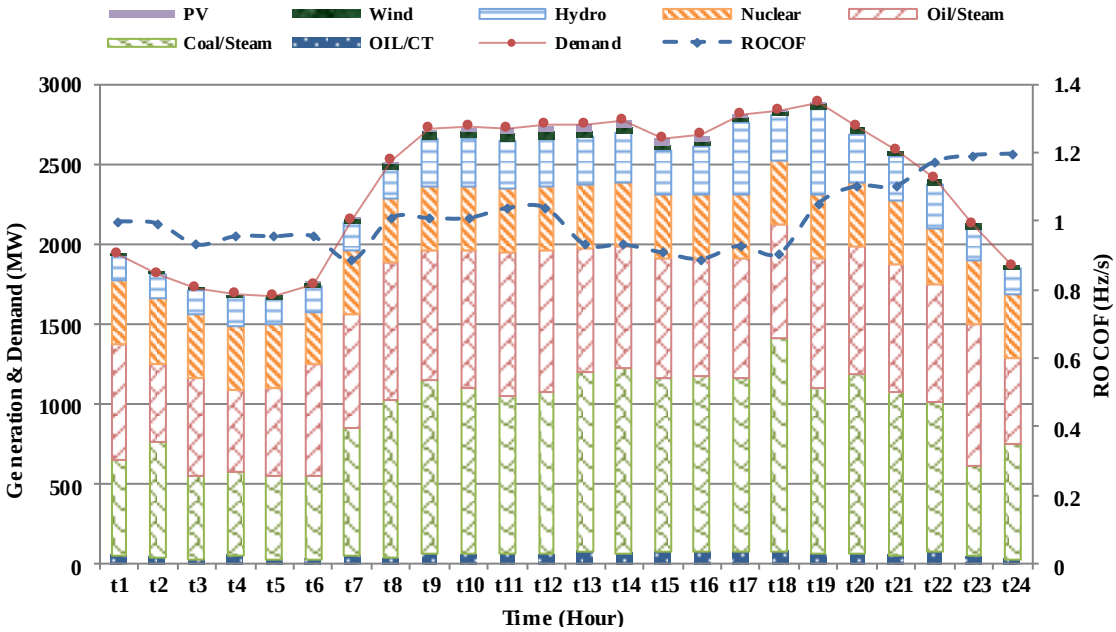

Fig. 6.6: Initial generation mix with PV as candidate generator

(iii) PV as candidate generator

This case considers PV as candidate generator. Addition of PV along with wind generating unit made ROCOF to reach the maximum limit of 1.195 Hz/ s while maximum frequency

deviation reaches to 49.79 Hz/s as shown in Fig. 6.6. Non dispatchable wind and PV generating units jointly feeds MWs of demand, hence commitment of conventional units is lesser. This would result in high ROCOF and frequency deviation. Now, further addition of RES generating unit would lead to violation of considered frequency security criteria. Hence, obtained generation mix is considered as the optimal generation mix for the considered test system.

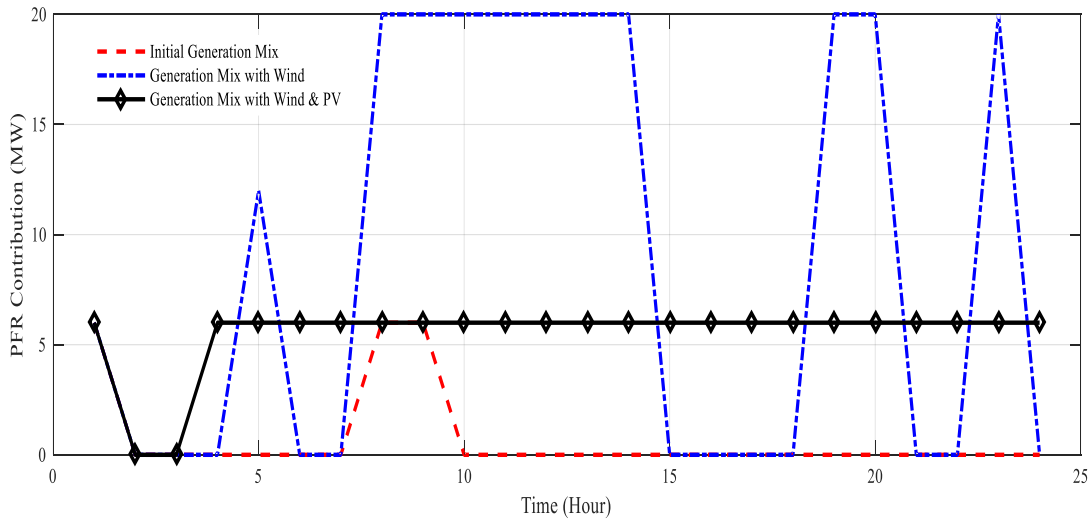

Fig. 6.7: PFR contribution from Oil/CT generating units.

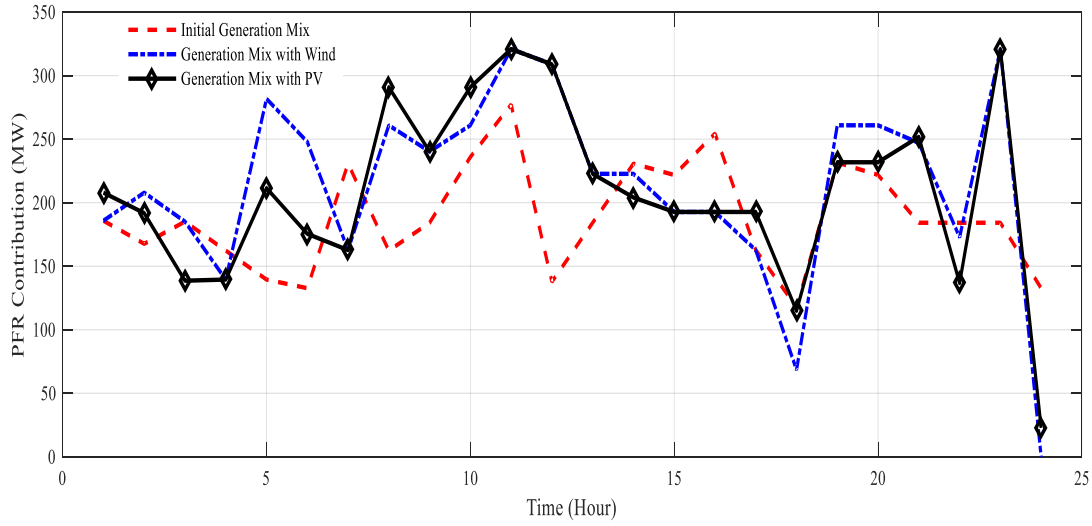

Fig. 6.8: PFR contribution from Coal/Steam generating units.

PFR contributions from generating units like Oil/CT, Coal/Steam, Oil/Steam and Hydro in all the three cases are shown in Figs. 6.7, 6.8, 6.9 & 6.10 respectively. It could be observed from Fig. 6.7 that Oil/CT plant's PFR contribution is for few hours in case of

initial mix, however, in case of addition of wind generation, its magnitude and duration are higher compared to both the cases. In case of addition of PV generation, PFR magnitude is constant for most of the time period.

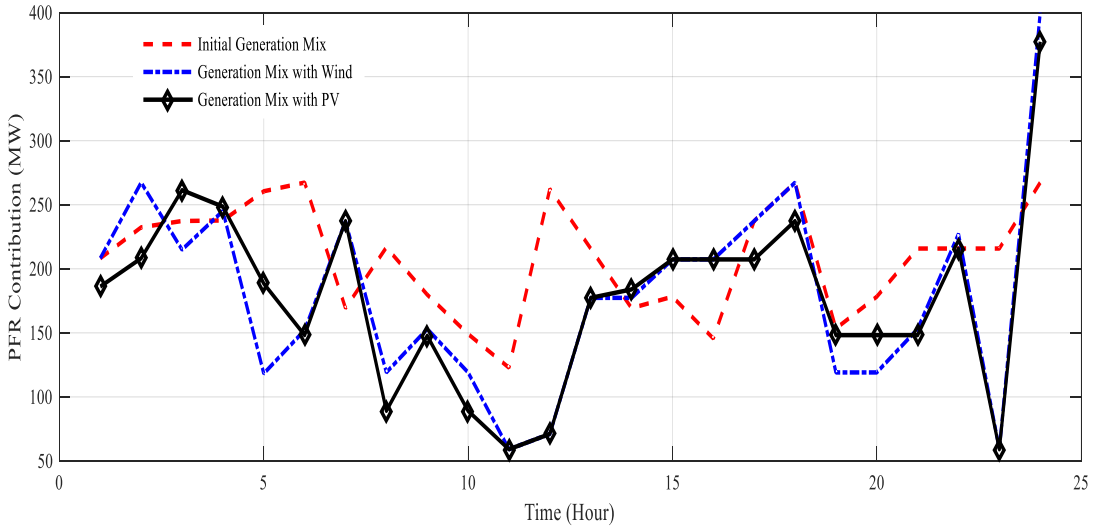

Fig. 6.9: PFR contribution from Oil/Steam generating units.

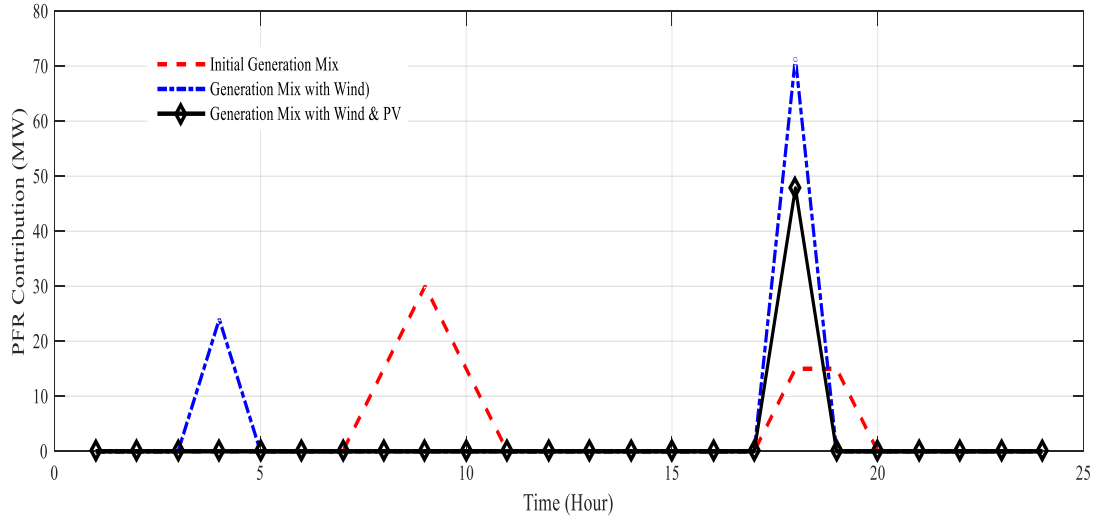

Fig. 6.10: PFR contribution from Hydro generating units.

From Figs. 6.8 & 6.9, it could be observed that Coal/Steam & Oil/Steam plant's PFR contribution is almost similar for the addition of wind and PV cases. In both, the cases magnitude of PFR is higher, because of their higher capacity and number in the overall generation mix. In case of Hydro generator as shown in Fig. 6.10, PFR contribution is almost negligible for most of the time. However, its maximum contribution is for the hour t18. Further, it is observed that in all three cases, nuclear-generating units are weak in

providing PFR and it is zero for the entire time interval. Therefore, its contribution is not shown here.

Fig. 6.11 presents the overall PFR availability for all three cases. It is observed that PFR contribution is higher for initial generation mix. This is due to the fact that number of generators committed per hour is higher. In case of addition of wind and PV unit, net load is reduced. This would lead to displacement of conventional units, hence PFR availability is reduced in both the cases. This PFR reduction would cause higher frequency deviation and further lead to under frequency load shedding if sufficient response is not provided.

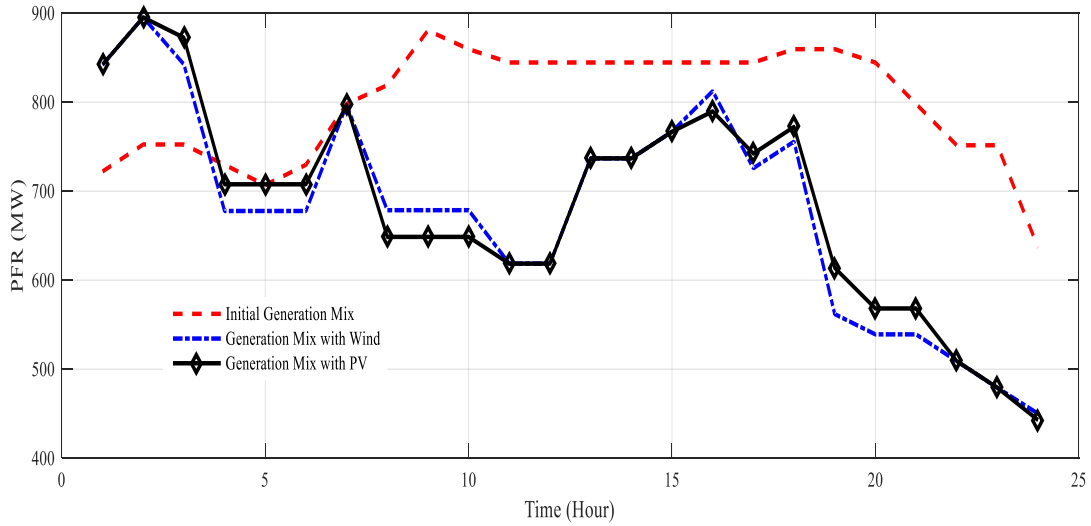

Fig. 6.11: Available PFR in all the three cases.

Table 6.2: Cost Performance

Cases	**Operation Cost ($)**	**Overall Cost ($)**
Initial Generation Mix	499368.5783	44703368.58
Addition of wind	486216.2251	45930216.23
Addition of PV	480444.8847	47184444.88

6.4.3 Overall Cost Performance

This section discusses the cost performance for all the three cases. It could be observed from Table II that operation cost is getting reduced with the addition of wind generation and it reduced more with the addition of PV unit along with the wind. This reduction is because of displacement of conventional units. Wind and PV unit's operation cost is

negligible, as they are free from fuel cost. Hence, these units are not adding any amount in overall operating cost.

Overall cost includes operation cost and investment cost. It could be observed from Table 6.2 that this cost is increasing from initial generation mix case to addition of wind and PV units. As the investment cost of wind & PV unit is higher. This would increase the overall cost. In the proposed work single largest infeed loss is considered to estimate the PFR requirement for worst case contingency. Hence, generator outage probability is not considered.

6.5 Conclusions

This work presents a novel exposition of optimal generation mix formulation for inertial response and PFR adequacy with RES generation expansion. Wind & PV uncertainty is characterized pragmatically using forecasted upper and lower interval and inter hour ramp requirements are considered based on net load scenarios. Hence, wind & PV output is accurately captured. Three cases, *i.e.*, (i) Base case (ii) Wind as candidate generator & (iii) PV as candidate generator are considered and carried out on one area IEEE reliability test system considering network security limits. Rate of change of frequency (ROCOF) setting and frequency deviation is considered as frequency security limit to obtain optimal generation mix. Results obtained provide optimal generation output, PFR contribution and overall cost performance from different generating units. It is analysed that operation cost is reduced with the addition of wind and PV generation. However, the overall cost is increased because of the high investment cost of wind & PV unit. Optimal generation mix is obtained through step by step evaluation of system frequency security criteria.

Proposed framework has potential to assist SO, to enhance system's inertia & PFR adequacy at short-term operations and could be enhanced for achieving economical generation mix considering network security limits in a long-term planning framework.

Chapter – 7

CONCLUSIONS AND RECOMMENDATIONS FOR FUTURE WORK

7.1 General

The electrical power system is a complex, dynamic and interconnected network. The formidable challenge for power engineers is to maintain the system frequency within the specified limits. Dynamic power consumption pattern cause continuous generation-load imbalances. This imbalance should be corrected within the permissible operational time frames, to avoid the system frequency variations. Large frequency variations may cause emergency issues like UFLS and further lead to serious threats to the stability and security of the system. Hence, constant frequency and generation-load balance are identified as the primary challenge for smooth operation of power systems.

Rapid installation of wind/PV farms into the grid would displace the conventional generation at a fast rate. Bulk penetration of these generation sources have significant impact on power system security and reliability, due to uncertain and intermittent generation characteristics. Displacement of conventional generation would reduce the system inherent frequency response capability. Hence, maintaining system frequency response adequacy and the prospect of new generation technologies interfacing with the grid create a range of system operational issues for the SO.

This necessitates a wider understanding of the research challenges arising out of large penetration of RES in the grid and how evolving system technologies and modelling could be used to maintain reliable and secure system operation.

This research attempts to develop a mechanism for frequency response adequacy with the large integration of uncertain wind & PV generation sources. A novel framework for the assessment of role and value of frequency response in the system operation framework mapped with frequency security criteria like ROCOF, Frequency Nadir, and Steady-state frequency is developed. This addresses multiple concerns associated with frequency response adequacy such as comprehensive modeling of dynamic frequency evolution after contingency, uncertainty characterization, and representation in system operation. Developed models and approaches have been illustrated through realistic case studies. A summary of the main findings of the research work carried out in this thesis and future

scope in this area are presented in subsequent sections. Outcomes of this research would be helpful to understand the frequency response challenges with large integration of RES.

7.2 Summary of Significant Findings

Due to RES uncertainty, system operations like scheduling and dispatch becomes challenging decision-making problem. Accurate modeling of involved uncertainties is necessary to solve these decision-making problems. Hence, research work in this thesis begins with modelling of wind and PV generation uncertainty.

This research work considers scenarios & modified interval approach for uncertainty modelling. In the scenario-based framework, uncertainty is treated as a stochastic process and represented through scenarios. Accurate representation of uncertainty generally requires a consideration of a large number of scenarios, thus necessitating the need for scenario-reduction algorithms for fast calculation. In the present work, efficacious algorithms have been proposed for scenario generation and reduction. Scenario generation algorithm is based on time series ARMA model, while the reduction algorithm utilizes the concept of probability distance.

The proposed algorithms have been implemented for wind & PV power scenario generation and reduction located at Illinois Institute of Rural Affairs, USA. Obtained results clearly show the strength of the proposed algorithms for modeling wind & PV power uncertainty.

Scenario-based stochastic approach model RES uncertainty precisely, but requires computationally demanding simulations. In this context, in this work modified interval approach is proposed. Interval forecast already exists in the literature; it is a robust technique, which requires less computational effort than the stochastic approach. In the proposed modified interval model, the advantages of interval and scenario approaches are incorporated. Uncertainty is modeled using upper and lower bounds, as in the interval formulation, but inter-hour ramp requirements are based on net load scenarios and hence accurately capture the expected wind output. Wind & PV uncertainty is characterized by ramping scenarios.

Proposed scenarios and modified interval are used to characterize uncertainty in the frequency response constrained generation and PFR scheduling, prediction of system inertia condition and optimal generation mix for frequency response adequacy framework, as discussed in subsequent paragraphs.

Wind/PV generation uncertainty modelled through scenarios and modified interval approach is extended in frequency response constrained SUC and MIUC computational framework. Large wind/PV generation in existing power system increase the requirement of frequency response services, as the existing wind/PV generators are weak in providing inertia and PFR. This necessitates optimal PFR schedules from UC. Various computational techniques have been proposed to obtain the cost-efficient combination of controllable generation units, which may effectively respond to penetration from intermittent wind/PV generation while maintaining minimal generation cost.

This work contributes by proposing a novel, computationally fast MIUC formulation framework to include system's frequency response constraints. The framework directly aims to contain initial transient frequency behavior within the prescribed system security criteria, following the largest infeed loss. It performs PFR scheduling of committed generators, required to make frequency stable at an intermediate state, following the largest infeed loss. It characterizes wind/PV generation uncertainty pragmatically in the proposed MIUC and SUC problem using ARIMA model, through rigorous scenario analysis. Further, it demonstrates the efficacy of proposed MIUC model through the systematic comparative assessment with SUC, for their PFR scheduling performance; the impact of variation of FR parameters on operation cost and wind curtailment; and for computational and cost performance with varying wind penetration. Computationally fast solutions obtained through the proposed MIUC model, within acceptable time intervals, can strongly benefit system operations with fast FR.

This work is further extended by presenting a notion of inertia and PFR forecast for the low carbon power system. Currently, SOs hardly assess system inertia impact to calculate future PFR requirement, which is planned/procured for an expected worst-case contingency. There is a limited understanding of system behaviour to provide inertia & PFR with high renewable penetration. An understanding of these requirements during such contingencies would provide knowledge about permissible renewable penetration that grids could withstand, following network regulations. Frequency-related issues, such as the operation of frequency controlled reserves, ROCOF protection setting, UFLS, and PFR deployment speed requirement need a proper assessment of available system inertia for secure system operation. As system inertia condition varies over a day's time, fixed PFR estimation based on the worst-case scenario is not efficient. Hence, it is imperative to forecast system inertia for upcoming hours, considering the current operation status of

all generators. Using this information, expected system inertia could be calculated for each hour.

This work contributes by proposing a novel exposition and methodology to predict system inertia condition on one area IEEE RTS with incremental RES generation, following the largest infeed loss. ROCOF and frequency at maximum deviation are considered as a security criterion to obtain maximum RES penetration limit considering network codes. Investigate the impact of variation in frequency security parameters on operation cost and wind & PV curtailment, to obtain suitable ROCOF setting for minimum RES curtailment. Results provide information of forecasted inertia and PFR, along with maximum RES limit, without violating system security criteria. This would corroborate SO in decision making for UC and economic dispatch and pragmatically handle inevitable contingencies, like largest infeed loss. Further, the impact of variation in frequency security criteria on operation cost and RES curtailment is analysed. This helps to identify appropriate ROCOF settings for minimum operation cost and RES curtailment.

Finally, this thesis contributes by proposing a novel exposition of optimal generation mix with the objective of reduced operation cost while maintaining systems' frequency response ability. Assess PFR adequacy with diversified generation mix and analyse overall cost performance for different generation mix cases. Three cases, *i.e.*, (i) Base case (ii) Wind as candidate generator & (iii) PV as candidate generator are considered and carried out on one area IEEE reliability test system considering network security limits. ROCOF setting and frequency deviation are considered as frequency security limit to obtain an optimal generation mix. Results obtained provide optimal generation output, PFR contribution and overall cost performance from different generating units. It is analysed that operation cost is reduced with the addition of wind and PV generation. However, the overall cost is increased because of the high investment cost of wind & PV unit. Optimal generation mix is obtained through step by step evaluation of system frequency security criteria.

The research work presented in this thesis offers an innovative mechanism to mitigate inertial response and PFR challenges through enhanced frequency control capability of power systems. This is an evolving research area for the industry and requires novel mechanisms to handle the same. The area lies at the confluence of multiple streams of knowledge, where electrical engineering, economics, and regulation merge. Such studies

help to develop an understanding of inter-relation between issues arising from different fields of knowledge. The present work provides an understanding of frequency response mechanism and its associated issues such as wind & PV power uncertainty, PFR requirement with variation in system inertia condition and optimal generation mix modeling in a comprehensive framework. The issues handled in this work would continue to attract research interest.

7.3 Recommendations for Future Work

Research and development are a continuous process. Each step of research work opens many avenues for future research. As a consequence of the investigations carried out, a variety of issues pertaining to frequency response adequacy in power system operation has been handled with consideration of wind & PV power uncertainty. Though there are several inter-related issues to be resolved, some require urgent attention due to their wide implications. Following are some of the aspects, identified as a promising area for future research work in the realm of study:

i. The presented scenarios & modified interval algorithms could be further improved by using advanced forecasting models like ECMWF (EU Climate Model) or GFS (NOAA Climate Model) and incorporating information about numerical weather predictions.
ii. Presented scenario reduction algorithm in this thesis is iteratively eliminating the generated scenarios. Such iterative elimination of scenario requires large computational time when the preserved scenarios are small as compared to generated scenarios. Thus, the present scenario reduction process could be accelerated by defining new measures for scenario elimination.
iii. Synthetic inertia provision from wind turbines/PV is believed to play an important role in supporting the frequency response performance in the future low carbon power system. Proposed work could be extended by proposing modelling synthetic inertia contribution from wind & PV
iv. In addition to modelling synthetic inertia contribution from wind & PV plant, it is challenging to incorporate synthetic inertia into a UC model, since there is uncertainty associated with aggregated synthetic inertia from wind turbines/PV.

The proposed research work could be potentially extended to characterize this uncertainty in the generation scheduling framework.

v. Currently, inertia and PFR related ancillary service market mechanism do not have explicit provisions for incentivizing or mandating PFR. This work could be extended to develop a market mechanism for system inertia and PFR provision in low carbon power system.

vi. Enhancement in the energy storage technology with faster response time for active power balance during contingencies proposed work could be improved by investigation of role and value of frequency response support from energy storage technology.

vii. In this work, frequency response assessment is mainly focused from generation side, this work could be extended by considering the response from the demand side. Response from interruptible loads and design of contracts for the same could be the key research area for the extension of the proposed work.

viii. Electric vehicle technology is gaining a wider attention due to its vehicle to grid feature. Proposed work could be extended by the development of the framework for electric vehicles participation in frequency response.

ix. Proposed system inertia prediction model uses RES generation and load forecasting in day-ahead scheduling and estimates PFR requirement. This work could be improved by the development of real-time models for system inertia and PFR requirement prediction.

x. Proposed models and algorithms could be further illustrated by practical case studies based on larger test systems.

xi. Proposed optimal generation mix model for securing frequency response adequacy considers short-term system operation, in addition to this largest generator outage is considered in the proposed work. This work could be extended for a long-term planning framework and consideration of generation outage probability.

Apart from these issues for future research, large-scale wind & PV power integration would pose several unique system operation and planning challenges for system operators. These challenges create ample opportunities for researchers in this area.

REFERENCES

[1] North American Electric Reliability Corporation, "Frequency response initiative report—The reliability role of frequency response," NREC, Washington DC, USA, Tech. Rep., Oct. 2012.

[2] H. Bevrani, "Robust Power System Frequency Control", New York, NY, USA: Springer, 2009.

[3] Global Wind Statistics-2017 [online]. Available: http://gwec.net/global-figures/wind-energy-global-status//.

[4] Global Solar Forecast – A brighter outlook for global PV installations [online]. Available: http://www.mercomcapital.com/global-solar-forecast-a-brighter-outlook-for-global PV installations.

[5] S. Sharma, S. Huang, and N. Sarma, "System inertial frequency response estimation and impact of renewable resources in ERCOT interconnection," *IEEE PES GM*, Detroit, July 2011.

[6] R. Doherty *et al.*, "An assessment of the impact of wind generation on system frequency control," *IEEE Trans. Power Syst.*, vol. 25, no. 1, pp. 452–60, Jan. 2010.

[7] V. Gevorgian, Y. Zhang, and E. Ela, "Investigating the impacts of wind generation participation in interconnection frequency response," *IEEE Trans. Sust. Energy*, vol. 6, no. 3, pp. 1949-3029, July 2015.

[8] L. Ruttledge *et al*, "Frequency response of power systems with variable speed wind turbines*," IEEE Trans. Sust. Energy*, vol. 3, no. 4, pp. 683–91, Aug. 2012.

[9] N.W. Miller *et al.*, "Frequency response of California and WECC under high wind and solar conditions," *IEEE PES GM,* San Diego, July 2012.

[10] National Energy Technology Laboratory (NETL), final report, DOE/NETL-2011/1473, "Frequency Instability Problems in North American Interconnections", May 2011, [online]. Available: https://www.netl.doe.gov.

[11] European Network of Transmission System Operators for Electricity (ENTSOE), initial finding report, "Deterministic frequency deviations," 2nd stage impact analysis, 2012, [online]. Available: https://www.entsoe.eu.

[12] A. J. Conejo, M. Carrión and J. M. Morales, *Decision Making under Uncertainty in Electricity Markets*, Springer, 2010.

[13] A. Sturt and G. Strbac, "Efficient stochastic scheduling for simulation of wind-integrated power systems," *IEEE Trans. Power Syst.*, vol. 27, no. 1, pp. 323–334, Feb. 2012.

[14] J. M. Morales, S. Pineda, A. J. Conejo and M. Carrión, "Scenario reduction for futures market trading in electricity markets," *IEEE Trans. Power Syst.*, vol. 24, no. 2, pp. 878–888, May 2009.

[15] K. C. Sharma, P. Jain and R. Bhakar, "Wind power scenario generation and reduction in stochastic programming framework," *Elect. Power Comp. Syst.*, vol. 41, iss. 3, pp. 271–285, Jan. 2013.

[16] H. Heitsch and W. Romisch, "Scenario reduction algorithms in stochastic programming," *Computat. Optimizat. Appl.*, vol. 24, pp. 187–206, 2003.

[17] M. Kaut and S. W. Wallance, "Evaluation of scenario generation methods for stochastic programming," *Pacific Journal of Optimization*, vol. 3, iss. 2, pp. 257–271, 2007.

[18] Y. Dvorkin, H. Pandžić, M. A. Ortega-vazquez, and D. S. Kirschen, "A hybrid stochastic / interval approach to transmission-constrained unit commitment," *IEEE Trans. Power Syst.*, vol. 30, no. 2, pp. 621–631, Mar. 2015.

[19] H. Pandzic, Y. Dvorkin, T. Qiu, Y. Wang, and D. S. Kirschen, "Toward cost-efficient and reliable unit commitment under uncertainty," *IEEE Trans. Power Syst.*, vol. 31, no. 2, pp. 970–982, Mar. 2016.

[20] J. F. Restrepo and F. Galiana, "Unit commitment with primary frequency regulation constraints," *IEEE Trans. Power Syst.*, vol. 20, no. 4, pp. 1588–1596, Nov. 2005.

[21] P. DU, J. Matevosyan, "Forecast system inertia condition and its impact to integrate more renewables," *IEEE Trans. Smart Grid*, vol. 99, pp. 1-2, Feb. 2017.

[22] M. Dreidy, H. Mokhlis, S. Mekhilef, "Inertia response and frequency control techniques for renewable energy sources: A review," *Renew. Sust. Ener. Reviews*, pp. 144-155, Nov. 2016.

[23] System operability framework, Nov. 2016, [online]. Available: http://www2.nationalgrid.com/ UK/Industry-information/Future-of-Energy/System-Operability-Framework/.

[24] Frequency Task Force of the NERC Resources Subcommittee, *Frequency Response Standard Whitepaper*, Princeton, New Jersey, 2004, [online]. Available: https://www.nerc.com/pa/Stand/Project/Frequency_Response_White_Paper.pdf

[25] EPRI, *Power System Dynamics Tutorial*, Final Report, Palo Alto, California, July 2009, [online]. Available: https://www.epri.com.

[26] P. Kundur, *Power System Stability and Control*. New York, NY, USA: McGraw-Hill, 1994.

[27] O.I. Elgered, *Electric energy system theory: An introduction*, 2nd edn., McGraw- Hill, New York,1982, pp. 55-60.

[28] ENTSO-E, "Network code requirements for grid Connection applicable to all generators," ENTSO-E, Belgium, 2013, [online]. Available: https://www.entsoe.eu.

[29] I. Sotirios *et al*., "A generic model of two-stage grid-connected PV systems with primary frequency response and inertia emulation," *Elec. Pow. Sys. Res.*, vol. 127, pp. 186–196, Oct. 2015.

[30] S.K. Soonee, and S.C. Saxena, "Frequency response characteristics of an interconnected power system – A case study of regional grids in India", *6th Intl. R & D Conf. on Sust. Development of water and energy resources - Needs and Challenges*, Feb. 2007, Lucknow, India.

[31] Energy Networks Association and National Grid, Frequency Changes during Large Disturbances and Their Impact on the Total System, 2013, [online]. Available: https://www.nationalgrid.com.

[32] H. Joseph *et al.*, "Use of frequency response metrics to assess the planning and operating requirements for reliable integration of variable renewable generation", *Ernest Orlando Lawrence Berkeley National Lab.*, Dec. 2010.

[33] I. Bogdan *et al.* ¸ "Frequency Support Functions in Large PV Power Plants With Active Power Reserves", *IEEE Jour. Emerging & Selected Topics in Power Electronics*, Vol. 2, No. 4, Dec. 2014.

[34] X. Ying cheng , and T. Nengling, "Review of contribution to frequency control through variable speed wind turbine," *Renewable Energy*, vol. 36, no. 6, pp. 1671-1677, Aug. 2011.

[35] A.B.T. Attya, and T. Hartkopf, "Control and quantification of kinetic energy released by wind farms during power system frequency drops," *IET Renew. Power Gene*r., vol. 7, no. 3, pp. 210–24, May 2013.

[36] R. G. Almeida and J. A. P. Lopes, "Participation of doubly fed induction wind generators in system frequency regulation," *IEEE Trans. Power Syst.*, vol. 22, no. 3, pp. 944–950, Aug. 2007.

[37] *IEEE Standard for interconnecting distributed resources with electric power systems, IEEE Standard 1547.2, 2008.*

[38] P. Pinson, "Estimation of the uncertainty in wind power forecasting," Ph.D. thesis, Ecole des Mines de Paris, Paris, France, 2006.

[39] M. Yue and X. Wang, "Assessing cloud transient impacts of solar and battery energy systems on grid inertial responses", *Elec. Pow. Comp. and Syst.*, vol. 43, no. 2, pp. 200–211, Jan. 2015.

[40] H. Bevrani, A.Ghosh, and G.Ledwich, "Renewable energy sources and frequency regulation: survey and new perspectives", *IET Renew. Power Gener.* , 2010, vol. 4, no. 5, pp. 438-457.

[41] LIU Xiaoge, XU Zhao, and K. Po WONG, "Recent advancement on technical requirements for grid integration of wind power", *J. Mod. Power Syst. Clean Energy,* vol.1, no. 3, pp. 216–222, Dec. 2013.

[42] R. Yan *et al*., "The combined effects of high penetration of wind and PV on power system frequency response," *Appl. Energy,* vol. 145, pp. 320–330, May 2015.

[43] J. Morren, S.W.H. de Haan, W.L. Kling and J.A. Ferreira, "Wind turbines emulating inertia and supporting primary frequency control," *IEEE Transactions on Power Systems,* vol. 21, no. 1, pp. 433 - 434, Feb. 2006.

[44] J.M. Mauricio *et al.*, "Frequency regulation contribution through variable-speed wind energy conversion systems," *IEEE Trans. Power Sys.,* vol. 24, no. 1, pp. 173-80, Jan. 2009.

[45] J. R. Birge and F. Louveaux, *Introduction to Stochastic Programming*. New York: Springer-Verlag, 1997.

[46] J. Dupacova, G. Consigli and S. W. Wallance, "Scenarios for multistage stochastic programs," *Ann. Operat. Res.,* vol. 100, pp. 25–53, 2000.

[47] A. Salehain, "ARIMA time series modeling for forecasting thermal rating of transmission lines," *in Proc. IEEE PES T & D Distrib. Conf. and Expo.*, Dallas, TX, Sept. 2003.

[48] N. Growe-Kuska, H. Heitsch and W. Romesh, "Scenario reduction and scenario tree construction for power management problems," *in Proc. IEEE Bologna Power Tech. Conf.,* Bologna, Italy, 23–26 Jun. 2003.

[49] N. M. M. Razali and A. H. Hashim, "Backward reduction application for minimizing wind power scenarios in stochastic programming," *in Proc. IEEE Int. Power Eng. Optim. Conf.,* Selangor, Malaysia, 23–24 Jun. 2010.

[50] H. Heitsch and W. Romisch, "A note on scenario reduction for two-stage stochastic programs," *Oper. Res. Lett.,* vol. 35, iss. 6, pp. 731-738, 2007.

[51] D.C. Montgomery, C.L. Jennings, M. Kulahci, "*Introduction to Time Series Analysis and Forecasting,*" New Jersy: John Wiley & Sons, 2008.

[52] L. Wu, M. Shahidehpour, and Z. Li, "Comparison of scenario-based and interval optimization approaches to stochastic SCUC," *IEEE Trans. Power Syst*., vol. 27, no. 2, pp. 913–921, May 2012.

[53] A. Sturt and G. Strbac, "Value of stochastic reserve policies in low-carbon power systems," *Proc. Inst. Mech. Eng. Part O J. Risk Reliab.*, vol. 226, no. 1, pp. 51–64, 2012.

[54] A. Papavasiliou, S. S. Oren, and B. Rountree, "Applying high performance computing to transmission-constrained stochastic unit commitment for renewable energy integration," *IEEE Trans. Power Syst.*, vol. 30, no. 3, pp. 1109–1120, May 2015.

[55] P. Meibom, R. Barth, B. Hasche, H. Brand, C. Weber, and M. O'Malley, "Stochastic optimization model to study the operational impacts of high wind penetrations in Ireland," *IEEE Trans. Power Syst*., vol. 26, no. 3, pp. 1367–1379, Aug. 2011.

[56] J. Dupacova, N. Growe-Kuska, and W. Römisch, "Scenario reduction in stochastic programming: An approach using probability metrics," *Math. Program.*, vol. Ser. A 95, p. 493-511, 2003.

[57] Y. Dvorkin, Y. Wang, H. Pandžić, and D. S. Kirschen, "Comparison of scenario reduction techniques for the stochastic unit commitment," *IEEE PES General Meeting*, Washington, July 2014.

[58] J. Riesz, J. Gilmore and I. Macgill, "Frequency control ancillary service market design: insights from the Australian National Electricity market," *Electr. J.*, vol.28, April, 2015.

[59] Y. G. Rebours, D. S. Kirschen, M. Trotignon, and S. Rossignol, "A survey of frequency and voltage control ancillary services—Part II: economic features," *IEEE Trans. Power Syst.*, vol. 22, no. 1, pp. 358–366, Feb. 2007.

[60] R. Doherty, G. Lalor, and M. O'Malley, "Frequency control in competitive electricity market dispatch," *IEEE Trans. Power Syst.*, vol. 20, no.3, pp. 1588–1596, Aug. 2005.

[61] E. Ela *et al.*, "Market designs for the primary frequency response ancillary service—Part I: Motivation and design," *IEEE Trans. Power Syst.*, vol. 29, no. 1, pp. 421–431, Jan. 2014.

[62] E. Ela, V. Gevorgian, A. Tuohy, B. Kirby, M. Milligan, and M. O'Malley, "Market designs for the primary frequency response ancillary service—Part II: Case Studies," *IEEE Trans. Power Syst.*, vol. 29, no. 1, pp. 432-440, Jan. 2014.

[63] F. Teng and G. Strbac, "Assessment of the role and value of frequency response support from wind plants," *IEEE Trans. on Sust. Energy*, vol. 7, no. 2, pp. 586-595, April 2016.

[64] H. Ahmadi and H. Ghasemi, "Security-constrained unit commitment with linearized system frequency limit constraints," *IEEE Trans. Power Syst.*, vol. 29, no. 4, pp. 1536–1545, July 2014.

[65] F. Teng, V. Trovato, and G. Strbac, "Stochastic scheduling with inertia-dependent fast frequency response requirements," *IEEE Trans. Power Syst.*, vol. 31, no. 2, pp. 1557–1566, Mar. 2016.

[66] P. Tielens , D. V. Hertem , "The relevance of inertia in power systems," *Renew. Sust. Ener. Reviews*, pp. 999-1009, Mar. 2016.

[67] Future ancillary services in ERCOT, Sep. 2013, [Online]. Available: http://www.ercot.com/initial public draft/.

[68] E. Orum *et. al.*, "Future system inertia," *ENTSO-E report*, [Online]. Available:https://www.entsoe.eu/Documents/Publications/SOC/Nordic/Nordic_report_Future_System_Inertia.pdf, pp. 1–58, 2015.

[69] P. Wall, F. González-Longatt, and V. Terzija, "Demonstration of an inertia constant estimation method through simulation," in *Proc. 45th Int. Univ. Power Eng. Conf.*, Aug. 2010.

[70] P. Wall, F. Gonzalez-Longatt, and V. Terzija, "Estimation of generator inertia available during a disturbance," *IEEE PES GM* , San Diego, USA, July 2012.

[71] T. Inoue, H. Taniguchi, Y. Ikeguchi, and K. Yoshida, "Estimation of power system inertia constant and capacity of spinning reserve," *IEEE Trans. Power Syst.*, vol. 12, no. 1, pp. 136–143, Feb. 1997.

[72] D. P. Chassin *et.al.*, "Estimation of WECC system inertia using observed frequency transients", *IEEE Trans. Power Syst.*, vol. 20, no. 2, pp. 1190–1192, May 2005.

[73] P. M. Ashton *et.al.*, "Inertia estimation of the GB power system using Synchro-phasor measurements", *IEEE Trans. Power Syst*., vol. 30, no. 2, pp. 701–709, Mar. 2015.

[74] E. Muljadi, V. Gevorgian, and A. Hoke, "Short-term forecasting of inertial response from a wind power plant," *IEEE Energy Conv. Cong. and Expo.*, Wisconsin, USA, Sep. 2016.

[75] System operability framework, 2015, [online]. Available: http://www2.nationalgrid.com/UK/Industry-information/ Future-of-Energy/ System-Operability-Framework/.

[76] J. Kaboouris and F. D. Kanellos, "Impacts of large-scale wind penetration on designing and operation of electric power systems," *IEEE Trans. Sustainable Energy*, vol. 1, pp. 107-114, Jul. 2010.

[77] H. Holttinen *et.al*., "Currents of change: European experience and perspectives with high wind penetration levels," *IEEE Power and Energy Magazine*, vol. 9, no. 6, pp. 47-59, Nov./Dec. 2011.

[78] J. Sousa, A. Martins, "Optimal renewable generation mix of hydro, wind and photovoltaic for integration into the Portuguese power system," *10th Intl. Conf. on the European Energy Market (EEM)*, May, 2013.

[79] A. Estanqueiro, J. M. Ferreira de Jesus, J. Ricardo, A. Santos, and J. A. Lopes, "Barriers (and Solutions) to very high wind penetration in power systems," *IEEE PES GM*, Tampa, USA June 2007.

[80] H. Lund, "Large-scale integration of wind power into different energy systems," *Energy*, vol. 30, pp. 2402-2412, Oct. 2005.

[81] B.C. Ummels, E. Pelgrum, M. Gibescu, and W. L. Kling, "Comparison of integration solutions for wind power in the Netherlands," *Renew. Power Gen., IET Research Journals*, vol. 3, pp. 279-292, Sep.2009.

[82] M. Keijonen, "What drives Great Britain's electricity generation mix?," Sep. 2016, [Online]. Available: https://www.ofgem.gov.uk/news-blog/our-blog/what-drives-great-britain-s-electricity-generation-mix.

[83] "Viability of the energy mix," 2017, [Online]. Available: http://tyndp.entsoe.eu/insight-reports/energy-mix/.

[84] "NREL report on renewable energy can provide 80 Percent of U.S. electricity by 2050," [Online]. Available: http://www.ucsusa.org/ clean_energy/smart-energy-solutions/increase-renewables/renewable-energy-80-percent-us-electricity.html.

[85] A. Inzunza *et.al*. "CVaR constrained planning of renewable generation with consideration of system inertial response, reserve services and demand participation," *Energy Economics*, pp. 104-117, Aug., 2016.

[86] D. A. Halamay, T. K. A. Brekken, A. Simmons, and S. McArthur, "Reserve requirements impacts of large-scale integration of wind, solar and ocean wave power generation," *IEEE Trans. Sust. Energy*, vol. 2, pp. 321-328, Jul. 2011.

[87] H. Holttinen *et.al.* , "Impacts of large amounts of wind power on design and operation of power systems, results of IEA collaboration," *Wind Energy*, vol. 14, pp. 179–192, Mar. 2011.

[88] [Online]. Available: https://www.renewables.ninja/.

[89] [Online]. Available: https://data.solaranywhere.com/Public/Tutorial.aspx

[90] J. M. M. Gonz´alez, "Impact on system economics and security of a high penetration of wind power," Ph.D. dissertation, Dept. Elect. Eng. Univ. De Castilla-La Mancha, Dec. 2010.

[91] J. P. Hennessey, "Some aspects of wind power statistics," *Int. J. Appl. Meteorol.*, vol. 16, pp. 119–128, Feb. 1977.

[92] A. Garcia, J. L. Torres, E. Prieto and A. De Francisco, "Fitting wind speed distributions: a case study," *Sol. Energy*, vol. 62, no. 2, pp. 139–144, Feb. 1998.

[93] J. A. Carta, P. Ramirez and S. Vela´zquez, "A review of wind speed probability distributions used in wind energy analysis case studies in the Canary Islands," *Renew. Sust. Energ. Rev.*, vol.13, pp. 933–955, June, 2009.

[94] T. Ackermann, *Wind power in power systems.* New York: Wiley, 2005.

[95] S. Pineda and A. J. Conejo, "Scenario reduction for risk-averse electricity trading," *IET Gener. Transm. Distrib*., vol. 4, no. 6, pp. 694–705, June, 2010.

[96] H. Heitsch and W. Romisch, "Scenario reduction algorithms in stochastic programming," *Comput. Optim. Appl.*, vol. 24, pp. 187–206, Feb. 2003.

[97] J. M. Morales, S. Pineda, A. J. Conejo and M. Carrión, "Scenario reduction for futures market trading in electricity markets," *IEEE Trans. Power Syst.,* vol. 24, no. 2, pp. 878–888, May 2009.

[98] Vestas, "A better wind business by design," [Online]. Available: https://www.vestas.com.

[99] *"Matlab and Matlab Simulink,"* ver. R2017a, The Mathworks, 2017.

[100] E. V. Mc Garrigle, J. P. Deane, and P. G. Leahy, "How much wind energy will be curtailed on the 2020 Irish power system?," *Renew. Energy,* vol. 55, pp. 544–553, Feb. 2013.

[101] E. Ela and M. O'Malley, "Studying the variability and uncertainty impacts of variable generation at multiple timescales," *IEEE Trans. Power Syst.,* vol. 27, no. 3, pp. 1324–1333, Aug. 2012.

[102] M. A. Ortega-Vazquez and D. S. Kirschen, "Assessing the impact of wind power generation on operating costs," *IEEE Trans. Smart Grid*, vol. 1, no. 3, pp. 295–301, Dec. 2010.

[103] I. D. Margaris, S. A. Papathanassiou, N. D. Hatziargyriou, A. D. Hansen,and P. Sørensen, "Frequency control in autonomous power systems with high wind power penetration," *IEEE Trans. Sustain. Energy,* vol. 3, no. 2, pp. 189–199, Apr. 2012.

[104] Reliability Test System Task Force, "The IEEE reliability test system—1996," *IEEE Trans. Power Syst.*, vol. 14, no. 3, pp. 1010–1020, Aug. 1999.

[105] "U.S. Energy Information Administration. 'Short-Term Energy Outlook," [Online]. Available: http://www.eia.gov/forecasts/steo.

[106] "National Grid, Security and Quality of Supply Standards." [Online]. Available: http://www2.nationalgrid.com/UK/Industry-information/Electricity-codes/System-Security-and-Quality-of-Supply-Standards/.

[107] *"The SolverManuals,"* ver. 23.7, GAMS, Washington, DC, USA, 2011.

[108] Future energy scenario, July 2016, [Online]. Available: http://www2.nationalgrid.com/UK/Industry-information/.

[109] V. Prakash, K. C. Sharma, R. Bhakar, H. P. Tiwari and F. Li, "Frequency Response Constrained Modified Interval Scheduling Under Wind Uncertainty," *IEEE Trans. Sust. Energy,* vol. 9, no. 1, pp. 302-310, Jan. 2018.

[110] E. Kayacan, U. Baris, and K. Okyay, "Grey system theory based models in time series prediction," *Expert Syst. with Appl.,* vol. 37, pp. 1784–1789, Mar. 2010.

[111] N. A. Masood, R. Yan, and T.K. Saha, "A new tool to estimate maximum wind power penetration level: In perspective of frequency response adequacy," *Appl. Energy*, vol. 154, pp. 209–220, May 2015.

[112] North American Electric Reliability Corporation, "Review of the recent frequency performance of the Eastern, Western and ERCOT Interconnections," Dec. 2010, [Online]. Available: http://www.nerc.com.

[113] "International review of frequency control adaptation," Oct. 2016, [Online]. Available: https://www.aemo.com.au/-/media/Files/Electricity/NEM/Security_and_Reliability/Reports/FPSS-International-Review-of-Frequency-Control.pdf.

[114] C. Yuan *et.al.,* "New problem formulation of emission constrained generation mix," *IEEE Trans. Power Syst*., vol. 28, no. 4, pp. 4064–4070, Nov. 2013.

[115] "Challenges to Grid Integration of Renewable Energy in India," Feb. 2019. [Online]. Available: https://mnre.gov.in/file-manager/akshay-urja/february-2019/Images/34-35.pdf.

[116] "Central Electricity Authority, Large Scale Grid Integration of Renewable Energy Sources-Way Forward," Nov. 2013. [Online]. Available: http://www.cea.nic.in./reports/powersystems/large_scale_integ.pdf.

[117] "Central Electricity Authority, CERC Compendium Final," 2016. [Online]. Available: http://www.cercind.gov.in/2016/regulation/9.pdf .

PUBLICATIONS FROM THE WORK

Based on the research carried out, following papers have been published/submitted for publication in various journals and conferences:

- **International Journals (Published):**

1. V. Prakash, K. C. Sharma, R. Bhakar, H. P. Tiwari and F. Li, "Frequency response with modified interval scheduling under uncertain wind generation," ***IEEE Transactions on Sustainable Energy*, vol. 9, pp. 302-309, Jan. 2018.**
2. V. Prakash, K. C. Sharma, R. Bhakar and H. P. Tiwari, "Modified interval-based generator scheduling for PFR adequacy under uncertain PV generation" ***IET Generation, Transmission & Distribution*, vol. 13, pp. 3723-3733, June 2019.**

- **International Conferences (Published):**

3. V. Prakash, K. C. Sharma, R. Bhakar and H. P. Tiwari, "Primary Frequency Response with Stochastic Scheduling Under Uncertain Photovoltaic Generation," ***IEEE Power Energy Society General Meeting,*** Chicago, USA, Jul. 16-20, 2017**.**
4. V. Prakash, R. Bhakar and H. P. Tiwari, "Stochastic scheduling of primary frequency response for uncertain low carbon power system," ***1st Intl. Conf. on Large-Scale Grid Integration of Renewable Energy in India, organized by minis*try of power & GIZ Germany**, New Delhi, India, Sept. 6-8, 2017.
5. V. Prakash, R. Bhakar, H. P. Tiwari, H. W. Pain, Y. Bian and F. Li, "Primary frequency response in future low carbon scenario: opportunities & challenges," ***IEEE Intl. Conf. on Recent Advances & Innovations in Engg.*** Jaipur, India, Dec. 23-25, 2016.
6. V. Prakash, R. Bhakar, H. P. Tiwari and K. C. Sharma, "Inertia and Primary frequency response assessment under uncertain photovoltaic generation," ***8th IEEE India International Conference on Power Electronics (IICPE-2018)***, Dec. 13-15, 2018, MNIT Jaipur, DOI:10.1109/IICPE.2018.8709539.
7. V. Prakash, R. Bhakar, H. P. Tiwari and K. C. Sharma, "System inertia prediction for primary frequency response adequacy under uncertain wind generation," ***8th IEEE India International Conference on Power Electronics (IICPE-2018)***, Dec. 13-15, 2018, MNIT Jaipur, DOI:10.1109/IICPE.2018.8709539.
8. V. Prakash, P. Kushwaha, K. C. Sharma, R. Bhakar and H. P. Tiwari, "Stochastic security constrained economic dispatch for primary frequency response adequacy under uncertain wind generation, accepted (submission ID: 87) in **2nd *Intl. Conf. on Large-Scale Grid Integration of Renewable Energy in India,*** organized by ministry of power & GIZ Germany, New Delhi, India, Sept. 6-8, 2019.

International Journals (Under Review):

9. V. Prakash, R. Bhakar, H. P. Tiwari and K. C. Sharma, "Optimal generation mix for securing frequency response adequacy in future power system" under review in ***IEEE Transactions on Power Systems.***

APPENDIX A

A.1 One Area IEEE Reliability Test System

The line diagram of one area IEEE RTS has been obtained from [104] and shown in Fig. A1. The relevant line and generating unit data is represented in Tables A1 and A2, respectively.

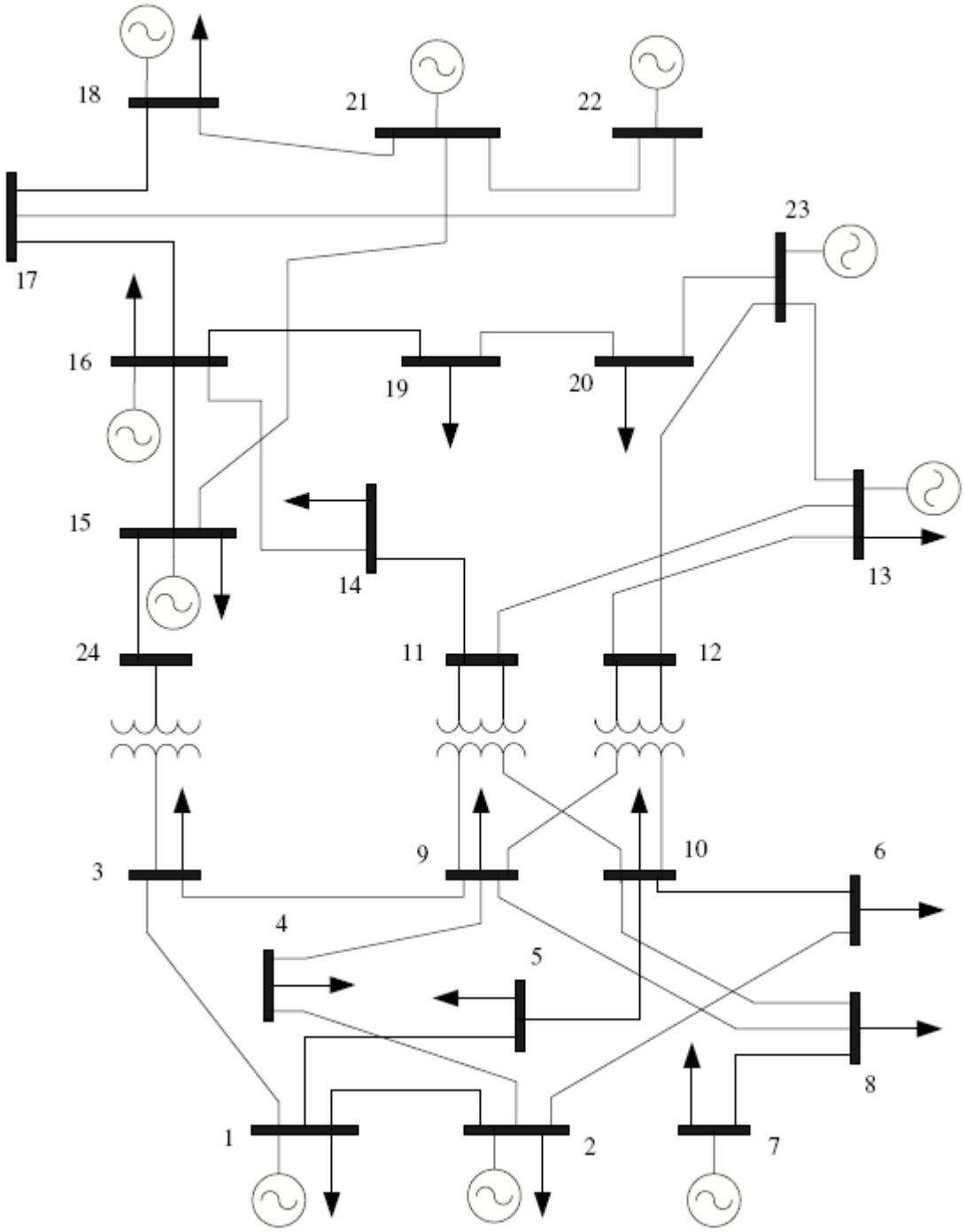

Fig. A1: One area IEEE RTS Configuration.

Table A1: Line Data of One Area IEEE RTS

Line	Reactance (p.u.)	Maximum Power (MVA)
1 -2	0.0146	175
1 -3	0.2253	175
1 -5	0.0907	175
2 -4	0.1356	175
2 -6	0.2050	175
3 -9	0.1271	175
3 -24	0.0840	400
4 -9	0.1110	175
5 -10	0.0940	175
6 -10	0.0642	175
7 -8	0.0652	175
8 -9	0.1762	175
8 -10	0.1762	175
9 -11	0.0840	400
9 -12	0.0840	400
10 -11	0.0840	400
10 -12	0.0840	400
11 -13	0.0488	500
11 -14	0.0426	500
12 -13	0.0488	500
12 -23	0.0985	500
13 -23	0.0884	500
14 -16	0.0594	500
15 -16	0.0172	500
15 -21	0.0249	1000
15 -24	0.0529	500
16 -17	0.0263	500
16 -19	0.0234	500
17 -18	0.0143	500
17 -22	0.1069	500
18 -21	0.0132	1000
19 -20	0.0203	1000
20 -23	0.0112	1000
21 -22	0.0692	500

Table A2: Generating Unit Data of One Area IEEE RTS

Unit Number	Bus Number	Maximum Power (MW)	Unit Group	Unit Type
1	1	20	U20	Oil
2	1	20	U20	Oil
3	1	76	U76	Thermal
4	1	76	U76	Thermal
5	2	20	U20	Oil
6	2	20	U20	Oil
7	2	76	U76	Thermal
8	2	76	U76	Thermal
9	7	100	U100	Oil
10	7	100	U100	Oil
11	7	100	U100	Oil
12	13	197	U197	Oil
13	13	197	U197	Oil
14	13	197	U197	Oil
15	12	12	U12	Oil
16	12	12	U12	Oil
17	12	12	U12	Oil
18	12	12	U12	Oil
19	12	12	U12	Oil
20	12	155	U155	Thermal
21	16	155	U155	Thermal
22	18	400	U400	Nuclear
23	21	400	U400	Nuclear
24	22	50	U50	Hydro
25	22	50	U50	Hydro
26	22	50	U50	Hydro
27	22	50	U50	Hydro
28	22	50	U50	Hydro
29	22	50	U50	Hydro
30	23	155	U155	Thermal
31	23	155	U155	Thermal
32	23	350	U350	Thermal